

AUS Repository

Thermodynamic Analysis of Integrated Fuel Cell and Solar Energy Systems

Item Type	Thesis
Authors	Ratlamwala, Tahir Abdul Hussain
Download date	2026-04-16 11:42:53
Link to Item	http://hdl.handle.net/11073/2731



THERMODYNAMIC ANALYSIS OF INTEGRATED FUEL CELL AND
SOLAR ENERGY SYSTEMS

A THESIS IN MECHANICAL ENGINEERING

Presented to the faculty of the American University of Sharjah
College of Engineering
In partial fulfilment of
the requirements for the degree

MASTER OF SCIENCE

by
TAHIR ABDUL HUSSAIN RATLAMWALA
BSc. 2009

Sharjah, U.A.E
June 2011

©

Tahir Abdul Hussain Ratlamwala

2011

We approve the thesis of Tahir Abdul Hussain Ratlamwala

Date of signature

Dr. Mohamed Gadalla
Associate Professor,
Mechanical Engineering Department
Thesis Advisor

Dr. Ibrahim Dincer
Professor, Engineering and Applied Science
University of Ontario Institute of Technology
Thesis Co-Advisor

Dr. Saad Ahmed
Professor
Mechanical Engineering Department
Graduate Committee

Dr. Naif Darwish
Professor
Chemical Engineering Department
Graduate Committee

Dr. Essam M. Wahba
Assistant Professor
Mechanical Engineering Department
Graduate Committee

Dr. Mohammad Ameen Al-Jarrah
Department Head
Mechanical Engineering Department

Dr. Hany El Kadi
Associate Dean
College of Engineering

Dr. Yousef Al-Assaf
Dean
College of Engineering

Dr. Gautam Sen,
Vice Provost
Research and Graduate Studies

Thermodynamic Analysis of Integrated Fuel Cell and Solar Energy Systems

Tahir Abdul Hussain Ratlamwala

Master of Science in Mechanical Engineering

American University of Sharjah

ABSTRACT

In the last few decades, world has seen an exponential increase in energy demand. This high increase in demand brought with it the issue of global warming. In this research, we will be studying alternative energy sources integrated with absorption cooling system for better and sustainable future. This thesis sheds light on results obtained by modelling Proton Exchange Membrane Fuel Cell (PEMFC) and Solar Photo Voltaic Thermal (PV/T) integrated with Triple Effect Absorption Cooling System (TEACS) and Quadruple Effect Absorption Cooling System (QEACS). Energy and Exergy analyses using Engineering Equation Solver (EES) are carried out for integrated systems and results are presented in this thesis. The results presented in this thesis are for the specific operating conditions and cannot be generalized to all systems. The detailed energy and exergy analyses of integrated systems show that energy and exergy efficiencies of the PEMFC decrease from 69.7 % to 35 % and 56.4 % to 34 %, respectively, when the current density and the temperature of the PEMFC are increased. However, energetic and exergetic COPs increase from 1.53 to 2.66 and 0.6 to 1.1, respectively, with increase in the temperature of the PEMFC. On the other hand, when the pressure, and the current density of the PEMFC are

increased, the energetic and exergetic COP decrease from 2.8 to 1.6 and 1.3 to 0.6, respectively. Increase in PEMFC current density results in the decrease of the overall energetic and exergetic efficiencies from 66.9% to 33.4%, and 25.9% to 12.9%, respectively. For the Solar PV/T integrated with TEACS, it is found that the overall energy and exergy efficiency varies greatly from month to month because of the variation in the solar radiation and the time for which it is available. The highest energy and exergy efficiencies are obtained for the month of March and their value is 15.6% and 7.9%, respectively. However, the hydrogen production is maximum for the month of August and its value is 9.7 kg because in august, the solar radiation is high and is available for almost 13 hrs daily. The maximum energetic and exergetic COPs are calculated to be 2.28 and 2.145, respectively and they are obtained in the month of June when solar radiation is high for the specified cooling load of 15 kW. This research is intended to help researchers and governments around the world to design the integrated systems for better environmentally friendly, efficient and sustainable future.

Table of Contents

ABSTRACT	III
LIST OF FIGURES	VII
LIST OF TABLES7	IX
NOMENCLATURE	X
ACKNOWLEDGEMENTS.....	XIV
CHAPTER 1 INTRODUCTION.....	1
1.1 Background and Motivation.....	1
1.1.1 Fuel Cell.....	1
1.1.2 Solar PV/T	2
1.1.3 Absorption System.....	3
1.1.4 Problem statement.....	3
1.1.5 Objectives	4
1.1.6 Scope.....	4
1.1.7 Methodology.....	5
1.2 Literature Survey	5
1.2.1 Fuel Cell.....	5
1.2.1.1 Tubular solid oxide fuel cell	6
1.2.1.2 Direct Methanol Fuel Cell.....	7
1.2.1.3 Alkaline Fuel Cell	8
1.2.1.4 Direct Formic Acid Fuel Cell.....	9
1.2.1.5 Proton Exchange Membrane Fuel Cell	10
1.2.2 Solar PV/T	11
1.2.2.1 Flat Plate Collectors	12
1.2.2.2 Parabolic trough	12
1.2.3 Absorption Systems	13
1.2.4 Exergy Analysis	14
1.2.5 Homogeneous Mixture.....	14
1.2.6 Heterogeneous Mixture.....	15
1.2.7 PEMFC Integrated with TEACS for Cooling and Power Production	15
1.2.8 Solar PV/T Integrated with TEACS for Cooling and Hydrogen Production	17
1.2.9 PEMFC Integrated with QEACS for Cooling Production	18
1.2.10 Research Results and Summary of Key Findings	20
1.2.11 Thesis Organization	21
CHAPTER 2 SYSTEM DESCRIPTION AND ENVIRONMENTAL IMPACT	22

2.1	Operational Principle of PEMFC Integrated with TEACS for Cooling and Power Production.....	22
2.2	Operational Principle of Solar PV/T Integrated with TEACS for Cooling and Hydrogen Production	24
2.3	Operational Principle of PEMFC Integrated with QEACS for Cooling Production ..	28
2.4	Environmental Impact	30
CHAPTER 3	THERMODYNAMIC ANALYSIS.....	33
3.1	Energy and Exergy Analyses of PEMFC integrated with TEACS for Cooling and Power Production	33
3.2	Energy and Exergy Analyses of Solar PV/T integrated with TEACS for Cooling and Hydrogen Production	38
3.3	Thermodynamic Analysis of PEMFC integrated with QEACS for Cooling Production	42
CHAPTER 4	RESULTS AND DISCUSSION.....	47
4.1	PEMFC Integrated with TEACS for Cooling and Power Production	47
4.2	Solar PV/T Integrated with TEACS for Cooling and Hydrogen Production	57
4.3	PEMFC Integrated with QEACS for Cooling Production.....	68
CHAPTER 5	CONCLUSIONS AND RECOMMENDATIONS.....	74
5.1	Conclusions	74
5.2	Recommendations	75
REFERENCES	76
VITA.....	84

LIST OF FIGURES

FIG. 1. 1 SCHEMATIC DIAGRAM OF THE TSOFC [4].....	6
FIG. 1. 2 SCHEMATIC DIAGRAM OF THE DIRECT METHANOL FUEL CELL [6]	7
FIG. 1. 3 SCHEMATIC DIAGRAM OF THE ALKALINE FUEL CELL [8].....	8
FIG. 1. 4 SCHEMATIC DIAGRAM OF THE DIRECT FORMIC ACID FUEL CELL. [9].....	9
FIG. 1. 5 SCHEMATIC OF PEMFC	10
FIG. 1. 6 SCHEMATIC DIAGRAM OF SOLAR PV/T	11
FIG. 2. 1 SCHEMATIC DIAGRAM OF PEMFC INTEGRATED WITH TEACS	24
FIG. 2. 2 SCHEMATIC DIAGRAM OF SOLAR PV/T INTEGRATED WITH TEACS.....	27
FIG. 2. 3 SCHEMATIC DIAGRAM OF QEACS INTEGRATED WITH PEMFC.....	30
FIG. 4. 1 VALIDATION OF THE MODEL WITH MERT ET AL. [69]	48
FIG. 4. 2 EFFECT OF TEMPERATURE OF THE FUEL CELL ON THE POWER AND IRREVERSIBILITY RATE OF FUEL CELL.....	50
FIG. 4. 3 EFFECT OF TEMPERATURE OF THE FUEL CELL ON THE ENERGY AND EXERGY EFFICIENCIES OF THE FUEL CELL	50
FIG. 4. 4 EFFECT OF TEMPERATURE OF THE FUEL CELL ON THE ENERGETIC AND EXERGETIC COP OF THE ABSORPTION SYSTEM.....	51
FIG. 4. 5 EFFECT OF PRESSURE OF THE FUEL CELL ON THE POWER AND IRREVERSIBILITY RATE OF FUEL CELL	52
FIG. 4. 6 EFFECT OF PRESSURE OF THE FUEL CELL ON THE ENERGY AND EXERGY EFFICIENCIES OF THE FUEL CELL.....	53
FIG. 4. 7 EFFECT OF PRESSURE OF THE FUEL CELL ON THE ENERGETIC AND EXERGETIC COP OF THE ABSORPTION SYSTEM.....	54
FIG. 4. 8 EFFECT OF CURRENT DENSITY OF THE FUEL CELL ON THE POWER AND IRREVERSIBILITY RATE OF FUEL CELL	55
FIG. 4. 9 EFFECT OF CURRENT DENSITY OF THE FUEL CELL ON THE ENERGY AND EXERGY EFFICIENCIES OF THE FUEL CELL	55
FIG. 4. 10 EFFECT OF CURRENT DENSITY OF THE FUEL CELL ON THE ENERGETIC AND EXERGETIC COP OF THE ABSORPTION SYSTEM.....	56
FIG. 4. 11 EFFECT OF CURRENT DENSITY ON THE ENERGETIC AND EXERGETIC EFFICIENCIES OF THE INTEGRATED SYSTEM	57
FIG. 4. 12 EFFECT OF CURRENT DENSITY ON THE RATE OF EXERGY DESTRUCTION OF THE INTEGRATED SYSTEM	57
FIG. 4. 13 MONTHLY AVERAGE SOLAR RADIATION OF 2009 IN U.A.E	59
FIG. 4. 14 MONTHLY AVERAGE AIR INLET TEMPERATURE FOR 2009 IN U.A.E	60
FIG. 4. 15 THE RATE OF MONTHLY ENERGY PRODUCTION OF PV/T SYSTEM	60
FIG. 4. 16 MONTHLY THERMAL AND ELECTRICAL EFFICIENCY OF PV/T FOR EVERY MONTH	62
FIG. 4. 17 MONTHLY COP VARIATION OF ABSORPTION COOLING SYSTEM	62

FIG. 4. 18 AMOUNT OF MONTHLY HYDROGEN PRODUCTION	64
FIG. 4. 19 OVERALL MONTHLY ENERGY AND EXERGY EFFICIENCIES	64
FIG. 4. 20 OVERALL ENERGY AND EXERGY EFFICIENCIES FOR DIFFERENT SOLAR RADIATION INTENSITIES	65
FIG. 4. 21 POWER OUTPUT OF PV/T AND MASS OF HYDROGEN PRODUCTION V/S AREA OF THE PV/T	66
FIG. 4. 22 RATE OF HEAT PRODUCTION AND THERMAL EFFICIENCY OF THE PV/T V/S AIR INLET TEMPERATURE	67
FIG. 4. 23 ENERGETIC AND EXERGETIC COPS OF THE ABSORPTION COOLING SYSTEM V/S AIR INLET TEMPERATURE OF PV/T	68
FIG. 4. 24 VARIATION OF BOTH ENERGETIC AND EXERGETIC COPS WITH T_{FC}	69
FIG. 4. 25 VARIATION OF BOTH OVERALL ENERGETIC AND EXERGETIC EFFICIENCIES WITH T_{FC}	70
FIG. 4. 26 VARIATION OF BOTH ENERGETIC AND EXERGETIC EFFICIENCIES OF PEMFC WITH T_{FC}	70
FIG. 4. 27 VARIATION OF BOTH ENERGETIC AND EXERGETIC COPS WITH P_{FC}	71
FIG. 4. 28 VARIATION OF BOTH OVERALL ENERGETIC AND EXERGETIC EFFICIENCIES WITH P_{FC}	72
FIG. 4. 29 VARIATION OF BOTH ENERGETIC AND EXERGETIC EFFICIENCIES OF PEMFC WITH P_{FC}	72
FIG. 4. 30 VARIATION OF POWER OF THE FUEL CELL, RATE OF HEAT OUTPUT OF THE FUEL CELL, AND COOLING LOAD OF THE QEACS WITH AREA OF THE PEMFC	73

LIST OF TABLES

TABLE 4. 1 PEM FUEL CELL CONSTANTS.....	49
TABLE 4. 2 SOLAR PV/T CONSTANTS.....	58

NOMENCLATURE

A	area, m^2
<i>b</i>	breadth of PV module, m
COP	Coefficient of performance
ex	specific exergy, $kJ\ kg^{-1}K^{-1}$
\dot{E}_x	rate of exergy kW
\dot{E}	rate of energy, kW
F	Faraday's constant, $Col\ mol^{-1}$
h	specific enthalpy, $kJ\ kg^{-1}$
HHV	higher heating value
h_{ba}	heat transfer coefficient from black surface to air, $W\ m^{-2}\ K^{-1}$
h_t	heat transfer coefficient from black surface to air through glass, $W\ m^{-2}\ K^{-1}$
h_{p1G}	penalty factor due to the presence of solar cell material, glass and EVA for glass to glass PV/T system, $W\ m^{-2}\ K^{-1}$
h_{p2G}	penalty factor due to presence of interface between glass and working fluid through absorber plate for glass to glass PV/T system, $W\ m^{-2}\ K^{-1}$
\dot{i}	irreversibility rate, kW
<i>i</i>	current density, $A\ cm^{-2}$
i_0	exchange current density, $A\ cm^{-2}$
i_{max}	limiting current density, $A\ cm^{-2}$
<i>L</i>	length of the PV module, m
MW	molecular weight, $kg\ kmol^{-1}$
\dot{m}	mass flow rate, $kg\ s^{-1}$
\dot{n}	molar flow rate, $mol\ s^{-1}$
<i>n</i>	number of electrons involved
P	PEM fuel cell pressure
\dot{Q}	heat transfer rate, kW
<i>r</i>	ratio

R	universal gas constant , $J mol^{-1} K^{-1}$
s	specific entropy, $kJ kg^{-1}K^{-1}$
\dot{S}_{gen}	rate of entropy generation, $kW K^{-1}$
t_{mem}	membrane thickness, cm
T	temperature, K
U_b	overall heat transfer coefficient from bottom to ambient, $W m^{-2} K^{-1}$
U_L	overall heat transfer coefficient from solar cell to ambient through top and back surface of insulation, $W m^{-2} K^{-1}$
U_t	overall heat transfer coefficient from solar cell to ambient through glass cover, $Wm^{-2} K^{-1}$
U_{tb}	overall heat transfer coefficient from glass to black surface through solar cell, $W m^{-2} K^{-1}$
\dot{W}	work rate, kW
x_A	anode dry gas mole fraction
x_C	cathode dry gas mole fraction
x_{H_2}	hydrogen mole fraction
x_{O_2}	oxygen mole fraction
Greek letters	
α_A	anode transfer coefficient
α_C	cathode transfer coefficient for fuel cell
α_c	absorptivity of solar cell
β_1, β_2	concentration of overvoltage constants
β_c	packing factor of solar cell
ϵ	utilization factor
η	efficiency
η_c	solar cell efficiency
η_{el}	electrical efficiency
η_{ov}	overall thermal efficiency
η_{th}	thermal efficiency
$\eta_{electrolyzer}$	electrolyzer efficiency

τ_g	transitivity of glass
ξ_A	anode stoichiometry
ξ_C	cathode stoichiometry
Subscripts	
a	air
ai	air inlet
abs	absorber
bs	back surface of PV/T
c	solar cell
CHX	condenser heat exchanger
con	condenser
G	subscript for glass to glass PV/T system
EN	energy
Ex	exergy
eva	evaporator
FC	fuel cell
H ₂	Hydrogen
HTG	high temperature generator
HHX	high temperature heat exchanger
HL	heat loss
LHX	low temperature heat exchanger
LTG	low temperature generator
MTG	medium temperature generator
MHX	medium temperature heat exchanger
V.HTG	very high temperature generator
V.HHX	very high temperature heat exchanger
1...41	state numbers
0	ambient or reference condition
o	fuel cell condition
req	required
Superscript	

PH physical
CH chemical

ACKNOWLEDGEMENTS

I would like to express my utmost gratitude to my thesis advisors, Dr. Mohamed Gadalla and Dr. Ibrahim Dincer for allowing me to join their team, for their expertise, kindness, and most of all, for their patience. I am very thankful to them for supporting me and encouraging me during the course of my study.

My thanks and appreciation goes to my thesis committee members, Dr. Saad Ahmed, Dr. Naif Darwish, and Dr. Essam M. Wahba for reading my thesis and providing me with useful feedbacks.

I am also very thankful to my parents and sisters for their love, encouragement, and sacrifices. Without their support I wouldn't have been able to carry out my work.

In the end, I will like to thank my fiancé, Zahrah, for her love and continuous support.

Chapter 1 Introduction

Energy plays a vital role in our life. We utilize energy in almost everything we do, from health equipments to transportation to human comfort. Last few decades have seen an unexpected growth in energy demand. This demand for energy is increasing at such a high rate that even major countries in the world are finding it hard to keep up with the demand. Especially countries in Gulf Region, where more than 60% of energy is utilized to run conventional vapour-compression air-conditioning systems, the demand of energy is increasing at an unprecedented rate. As the demand increases, the emission of CO₂, NO_x and other green house gases also increases due to the use of fossil fuel as major energy provider. Many environmental issues are caused by or relate to the production, transformation and use of fossil fuel energy, for example, acid rain, stratospheric ozone depletion and global climate change [1]. Humankind has now realized that emissions of these gasses are deteriorating our environment at high pace in shape of change in climate and increase in water levels due to the melting of ice. Also, the conventional systems which run on fossil fuels have low efficiency and high amount of emission of green house gases. These dis-benefits of using conventional system made researchers to think about a new source of energy which is eco-friendly and efficient also. Proton Exchange Membrane Fuel cell (PEMFC) and Solar PV/T systems provide an attractive alternative to conventional fossil fuel systems for power production. Also, research has been carried out in the field of absorption system, in order to replace conventional vapour-compression systems. PEMFC and Solar PV/T system integrated with absorption system provide an excellent alternative to the energy crisis for the gulf region, as these integrated systems are eco-friendly, and sustainable at the same time.

1.1 Background and Motivation

This section provides a brief background of the PEMFC, Solar PV/T, and absorption refrigeration system.

1.1.1 Fuel Cell

A fuel cell is a power and heat producing device which converts chemical energy directly into electrical energy and heat with the use of membrane. The membrane is used to separate fuel molecules into proton and electron. Protons are allowed to pass through the membrane where as electrons go through the circuit giving power. These electrons and protons combine with an oxidizing agent on the cathode side to produce heat and water. The idea of fuel cell was first introduced by Christian Friedrich Schönbein in 1839 and was later used by Welsh scientist Sir William Robert Grove to further advance the fuel cell technology. This new technology got its first boost when General Electric Company (G.E.) employed two chemists W. Thomas Grubb and Leonard Niedrach to work in the field of fuel cell and take it from theory and place it in physical world. The modified cell used sulphonated polystyrene ion-exchange membrane as the electrolyte; with platinum deposited on the membrane. Platinum serves as catalyst that speeds up the hydrogen oxidation and oxygen reduction. The resulting fuel cell was called 'Grubb-Niedrach fuel cell'. G.E. along with NASA and Douglas pursued the development of fuel cells to make this technology as user friendly as possible.

United Technology Corporations (UTC) was the first company to commercially manufacture stationary fuel cell systems. The commercial application was wide spread; it was used in co-generation power plant in hospitals, universities and large office buildings. UTC Power still sells 200 kW systems in the market; UTC also is the sole supplier of fuel cells to NASA for use in space vehicles [2].

1.1.2 Solar PV/T

Solar energy is the free energy which is available to us in the universe. Practices of harnessing solar energy date back to the ancient time when it was used to cook food and boil water. Solar Photovoltaic Thermal systems utilize the free solar energy to produce power and heat. Photovoltaic system converts solar radiation into direct power using semiconductors which are placed together in the photovoltaic cell. On the other hand, solar thermal system uses a fluid which runs through the duct on which solar radiations are falling, hence, gaining heat from

the solar radiation and leaving the duct at higher temperature than inlet of the duct. Solar PV systems combined with solar thermal system are known as Solar PV/T system. Solar PV/T systems harness solar energy to produce both power and heat at the same time. The use of solar PV/T system has increased in last decade due to the demand of environmental friendly and cheap energy source.

1.1.3 Absorption System

Absorption systems were widely used in the early years of the twentieth century, but were replaced by vapour-compression due to the high Coefficient of Performance (COP). On average absorption system has one fifth of the COP of vapour-compression cycle. As the issue of depletion of environment started taking toll in the last decade, absorption systems again came into existence. Unlike the vapour-compression refrigeration, the absorption refrigeration system is considered a “heat driven” system that eliminates the need of compressor which is energy eating device. It replaces the energy-intensive compression in a vapour compression system with a heat activated thermal system [3].

1.1.4 Problem statement

As the demand of energy is increasing at an unprecedented rate, it has become very important to come up with a system which is energy efficient, eco-friendly and sustainable at the same time. In the gulf region, more than 60% of energy produced is utilized to run the refrigeration systems. In this region where there is an ample amount of fossil fuel, majority of power plants are run on the basis of fossil fuels. As the demand is increasing the installation of new fossil fuel power plants are also increasing. These fossil fuel power plants emit loads of green house gasses such a CO₂, NO_x, SO₂ and so on, which are harming the environment. Moreover, the refrigeration systems which are used untill date are vapour-compression systems which consume loads of energy in order to compress working refrigerant from one state to another. Due to all these drawbacks of fossil fuel and vapour-compression systems, it has become eminent to introduce new power and cooling production technologies which are environmental friendly, efficient, and sustainable. This research is focussed towards providing hybrid systems for better future. Systems studied in this research are combination of

PEMFC, Solar PV/T, TEACS, and QEACS. The absorption system studied runs on ammonia-water solution. These systems were selected based on their overall performance and their effect on environment. Sustainability also played a major role in selection of these systems as the purpose of this research is to provide hybrid systems which are effective, environmental friendly, and sustainable for building operations.

1.1.5 Objectives

The objective of this research is to carry out thermodynamic analysis of alternative energy and cooling production systems separately, and then integrate them with each other to attain a combination of systems which are renewable, environmental friendly and sustainable. In this research different alternative energy systems integrated with novel absorption systems will be studied from thermodynamics point of view to see the effect of different parameters on the end result of the system. The objective of this research is to propose different integrated renewable/alternative energy systems which can cater the problem of high energy demand and emission of green house gases. The specific objectives of this study are:

1. Examine the operating principles of PEMFC integrated with TEACS, Solar PV/T integrated with TEACS, and PEMFC integrated with QEACS.
2. Conduct energy and exergy analyses of PEMFC integrated with TEACS, Solar PV/T integrated with TEACS, and PEMFC integrated with QEACS.
3. See the effect of pressure, temperature, current density, and condenser load on performance of PEMFC integrated with TEACS, and PEMFC integrated with QEACS.
4. Observe the effect of monthly weather data, solar radiation, air temperature, and condenser load on the performance of Solar PV/T integrated with TEACS

1.1.6 Scope

The scope of the research involves studying different types of alternative energy systems and absorption cooling systems. Later coming up with a novel absorption system integrated with alternative energy source for the better future. The new system should be sufficient enough to provide power and cooling to the

building without relying on the government grid to make the system sustainable on its own.

1.1.7 Methodology

At first PEMFC, Solar PV/T, and single and multiple effect absorption systems will be modelled thermodynamically and their thermodynamic properties such as enthalpy, entropy etc. will be obtained from Engineering Equation Solver (EES). Once above mentioned systems are modelled individually and satisfactory results are obtained then different combinations of PEMFC, Solar PV/T, and absorption systems integrated with each other will be modelled thermodynamically. Both energy and exergy analyses will be conducted to see the effect of different operating parameters on the efficiency and effectiveness of the overall system. EES will be used to obtain thermodynamic relations and Microsoft Visio will be utilized to make the schematics of the systems studied.

1.2 Literature Survey

There are different types of renewable/alternative energy sources available. In this thesis, PEMFC, Solar PV/T, and absorption systems integrated with each other will be investigated.

1.2.1 Fuel Cell

There are several types of fuel cells available to work on, yet all of them are not feasible for several reasons. Details for these different fuel cells and the reasons they were not feasible will follow below:

1.2.1.1 Tubular solid oxide fuel cell

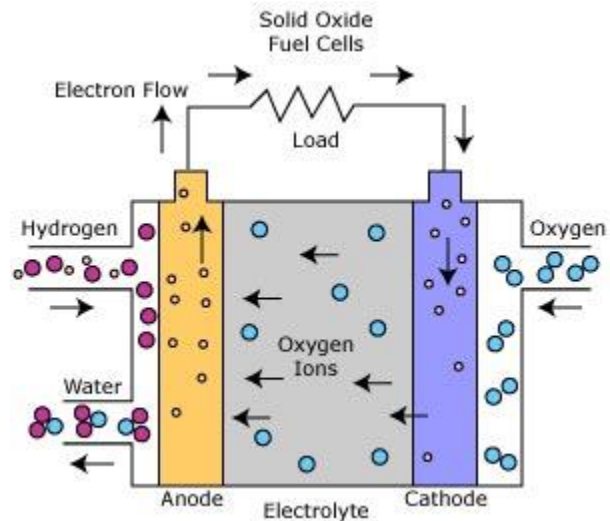


Fig. 1. 1 Schematic diagram of the TSOFC [4]

This is a solid oxide fuel cell that differs greatly from most common fuel cells in terms of the technologies it employs. First of all the whole cell is in the solid state, including the electrolyte, anode and cathode. All of them are composed of ceramics and the cells are arranged in a tubular fashion. This type of fuel cell operates at temperatures up to 1000 °C. The waste heat that is produced as a result of the operation is often used in a combined cycle to generate further energy [5].

Oxygen from air is passed through the cathode side in the tubular cell and hydrogen is passed over the anode side of the tubular cell and electrons are generated at the anode side, where they are collected to flow through a circuit to create electricity. Fig. 1.1 shows the schematic for the cell. The efficiency of this fuel cell is around 50%; however, in the cases where waste heat is recovered, the efficiency of this fuel cell reaches the range of 80 - 85%. [5]

The drawback of this fuel cell is that it requires the maintenance of a very high temperature, which is not practical and easy to maintain on a small scale residential building.

1.2.1.2 Direct Methanol Fuel Cell

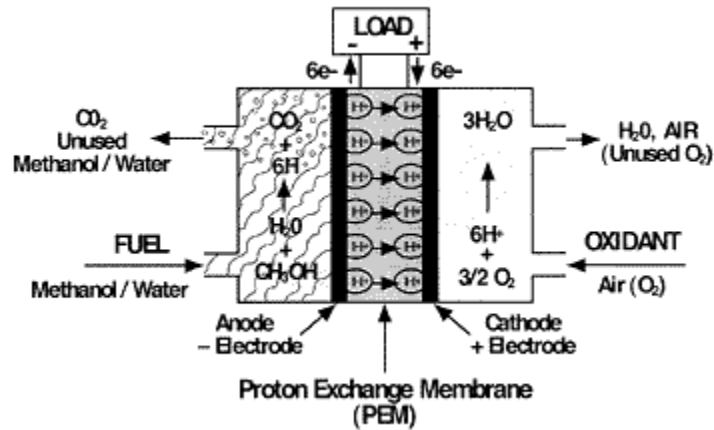


Fig. 1. 2 Schematic diagram of the Direct Methanol Fuel Cell [6]

This is a proton exchange fuel cell which is most similar to the PEMFC in the sense that the charge carrier is the proton from a hydrogen atom and the electrolyte is a polymer as shown in Fig. 1.2. At the anode side, methanol and water combine and react to produce carbon dioxide, hydrogen ions, and the protons that cross the membrane. At the cathode, the oxygen, hydrogen ions and protons combine to produce water. [7]

This fuel cell has been successfully used to power a number of small electronic appliances such as cell phones and laptops; however its use has not entirely become commercial [7].

The drawbacks with this type of cell are its low efficiency, making it necessary to employ the use of greater quantities of expensive platinum catalyst, and the fact that methanol is a toxic substance. The toxicity of the methanol used in particular, makes it impractical to implement it in a residential building due to safety issues.

1.2.1.3 Alkaline Fuel Cell

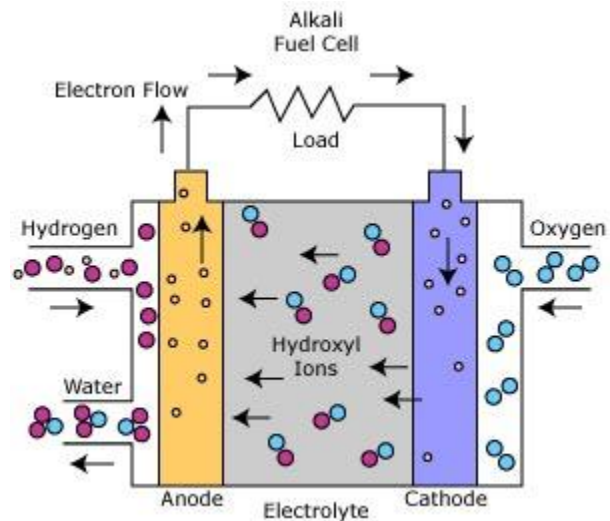


Fig. 1. 3 Schematic diagram of the alkaline fuel cell [8]

Being one of the best developed types of fuel cell, the alkaline fuel cell has been successfully used in many space and underwater operations.

Oxygen is supplied to the cathode of this cell and hydrogen is supplied to the anode. Using aqueous potassium hydroxide in a stable and porous matrix as an electrolyte, and a hydroxyl ion as a charge carrier, the products of this reaction are water and electrons. A schematic showing the operation is shown in Fig. 1.3. This fuel cell operates on a range of 80 – 220 °C. The problem with this fuel cell is the sensitivity of its electrolyte. When exposed to carbon dioxide, water and methane, the electrolyte is poisoned, damaging it and reducing its performance. [8]

This type of fuel cell is one of the most efficient ever produced and the components used to manufacture it are also relatively inexpensive as the catalyst used is abundant and inexpensive when compared to other fuel cells; however, its use is restricted to underwater applications and areas with vacuum, such as spacecraft, where the presence of carbon dioxide or other compounds detrimental to its electrolyte are not present and may not hamper its operational abilities [8]. The issue of electrolyte sensitivity thus makes it a non-feasible choice for the object of this thesis.

1.2.1.4 Direct Formic Acid Fuel Cell

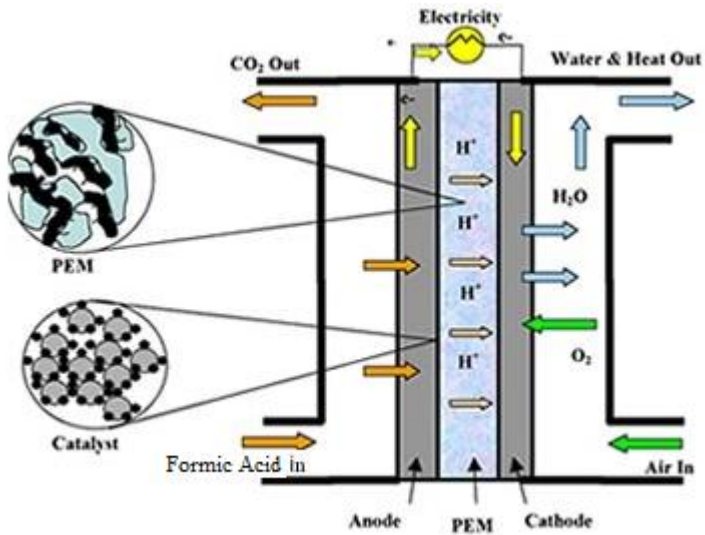


Fig. 1. 4 Schematic diagram of the Direct Formic Acid Fuel Cell. [9]

Similar to the methanol fuel cell, the direct formic acid fuel cell involves a direct feed of formic acid to the cell without the need of catalytic reforming. Formic acid and oxygen are converted into carbon dioxide and water and electrons that are released in the reaction generate the electric output. Similar to the PEMFC, a polymer membrane is used whereby only ions are allowed to pass through [10]. The flow of charges is from the anode to the cathode. The schematic of this cell is shown in Fig. 1.4.

The storage of formic acid is much easier than the storage of hydrogen, making it more advantageous than the PEMFC in this respect. Furthermore, formic acid is not toxic like methanol, and it does not cross the membrane as in the methanol fuel cell, raising the maximum possible efficiency of the cell [10]. The drawback of this cell is the low power density, and the low power output, making this type of cell suitable only for smaller electronic devices. This is why this cell was impractical to work on as a source of alternative energy; hence, it was not selected for use in the thesis.

1.2.1.5 Proton Exchange Membrane Fuel Cell

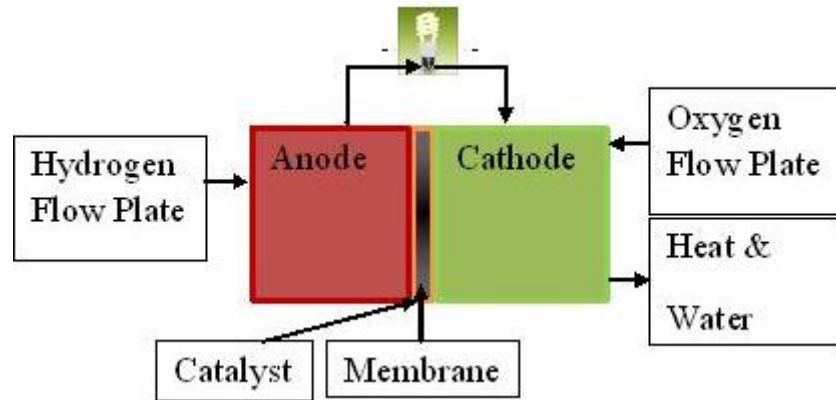


Fig. 1. 5 Schematic of PEMFC

PEMFC involves direct feed of hydrogen to the anode side of the plate and oxygen to the cathode side of the plate. Hydrogen molecules are split into protons and electrons and only protons are allowed to pass through the membrane. Electrons travel through the circuit giving out power. Electrons, protons, and oxygen combine with each other on the cathode side giving out heat, and water as shown in Fig. 1.5.

PEM fuel cells have appeared as a promising source of energy which can cater our problem related to efficient, effective, sustainable, and eco-friendly system. Hydrogen energy system is considered to be one of the most effective solutions, and can play a significant role in providing better environment and sustainability. It is an energy-efficient, low-polluting fuel [1]. Other advantage of using PEM fuel cells for sustainable operation is that they work at lower temperature and are easy to operate. PEM fuel cells are one of the most promising fuel cells because of its advantages such as simplicity, low operating temperature, and easy maintenance [11, 12]. Hydrogen is expected to play a key role in the near future as an energy carrier for sustainable development [13-23]. The use of hydrogen as an energy provider by using fuel cell holds a great potential due to higher efficiency, and eco-friendliness. Also, use of hydrogen as a fuel makes the energy generation process eco-friendly, because, the by-product of this process is water. The use of hydrogen in fuel cells to generate electricity is efficient and clean with water as the only by-product [14-19]. In the future, the role of hydrogen may become more important, as some researchers suggest that the

world's energy systems may undergo a transition to an era in which the main energy carriers will be hydrogen [21-24].

1.2.2 Solar PV/T

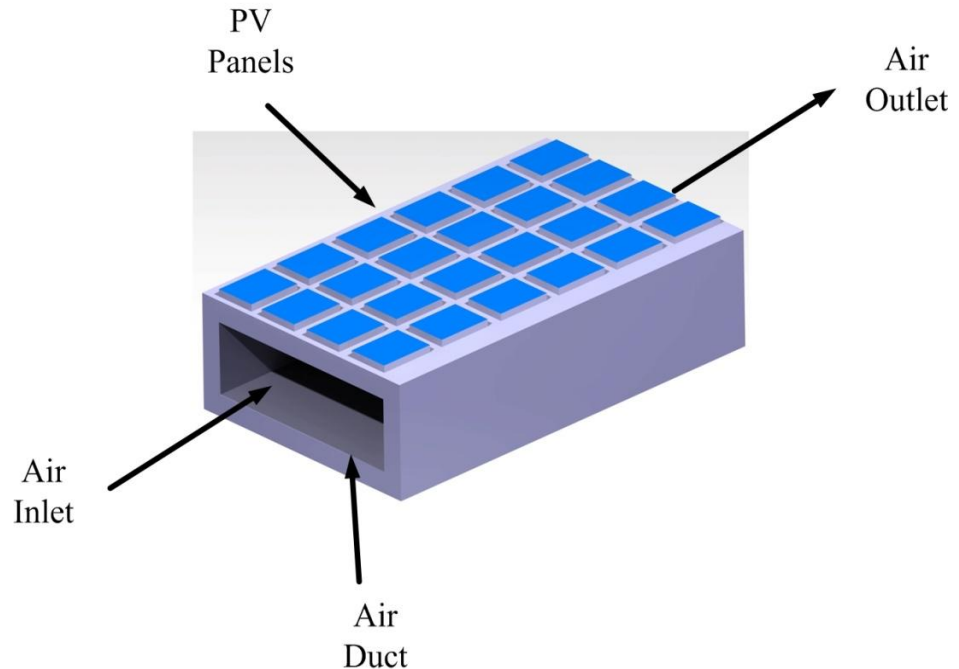


Fig. 1. 6 Schematic diagram of Solar PV/T

Solar PV/T systems are the systems which harness solar energy to produce power and heat as shown in Fig. 1.6. These systems directly convert solar radiation in to power and heat using semiconductors embedded in the PV panel. A photovoltaic/thermal hybrid solar system (PV/T) is a combination of photovoltaic (PV) and solar thermal components/systems that produce electricity and heat from one integrated component or system [25]. The PV/T collector produces thermal and electrical energy simultaneously. In addition, it is one of the cheapest ways of producing power and heat as solar energy is a gift to us from the nature. Though solar PV systems on their own have low efficiency but when they are integrated with thermal system to make PV/T system, the overall efficiency of the system enhances. Besides the higher overall energy performance, the advantage of the PV/T system lies in the reduction of the demands on physical space and the equipment cost through the use of common frames and brackets as compared to the separated PV and solar thermal systems placed side-by-side [26]. There are different types of solar systems available which are explained below.

1.2.2.1 Flat Plate Collectors

These are the most common types of collectors used at present. They consist of a transparent cover which allows solar radiation to pass through. These solar radiations are then absorbed by the semiconductors which are laid together to make a module with a black base to produce electricity. The black base absorbs the solar radiation. These solar modules are placed on top of a duct. As the solar radiations are absorbed the black bottom of the module gets heated up and then this heat is transferred to the fluid flowing through the duct in order to give heat. Water flows into a lower corner of the collector and becomes heated before exiting through a higher corner [27].

1.2.2.2 Parabolic trough

This type of collector is generally used in solar power plants. A trough-shaped parabolic reflector is used to concentrate sunlight on an insulated tube or heat pipe, placed at the focal point, containing coolant which transfers heat from the collectors to the boilers in the power station. These types of solar panel have higher efficiency than flat plate solar panels as the trough shape concentrates solar radiation on the focal point, hence reducing the amount of rays reflected and enhancing the efficiency. Measured results under typical operating conditions show thermal efficiency around 58% and electrical efficiency around 11%, therefore a combined efficiency of 69% [28].

1.2.3 Absorption Systems

Maximum amount of energy available in the grid of the Gulf countries is used to provide cooling. Most of the cooling systems used at present are conventional vapor-compression cooling system. These systems utilize huge amount of energy to run the compressor to achieve the required high pressure of the system. This high energy consumption leads to usage of more fossil fuel for the production of power which results in higher greenhouse gases emissions. In order to reduce the load on the grid and to make the cooling system more eco-friendly, researchers have worked on absorption systems. The absorption cooling technology is one of the best alternatives to the compression cooling in the aspects of energy diversification and environmental protection. Absorption systems use heat as an input to the system unlike conventional system. This use of heat instead of electrical power results in significant reduction in the power requirement of the system and hence, reducing the use of fossil fuels. Since the absorption technology was extensively used for practical application, a number of high-performance absorption cycles have been introduced for both residential and industrial applications. The performance of a cooling cycle is represented by the COP which is the ratio of cooling capacity to energy input. Most amount of work is being done on single and double effect absorption systems by researchers [e.g., 29-32]. The COP of a conventional double-effect LiBr/H₂O absorption cooling cycle is approximately 1.2. Here the “effect” implies the number of actual use of energy input to produce cold, thus the multiple-effect cycles have higher COP values. Recently, the triple-effect absorption cycle has attracted much interest to replace the conventional machine as the more efficient one. The expected COP value of the triple-effect cycle is known to be about 30% higher than that of the double-effect cycle. A basic type of triple-effect cycle might be simply composed by adding one more generator into the existing series-or parallel-flow double-effect cycle. Some types of advanced triple-effect cycles have been also suggested to improve the energy efficiency of the basic triple-effect cycle. However, the construction of a triple-effect absorption cooling machine using the efficient lithium bromide-based working fluid has been greatly hindered by the corrosion

problem caused by the high generator temperature above 473.15 K. The conventional LiBr/H₂O solution is known to cause a serious problem of corrosion [33]. Hence, in order to increase the COP of the system and to cater the problem of corrosion, a triple effect parallel flow absorption system using ammonia-water solution is analyzed. Earth metal salt is a well known inhibitor used for systems operating with Ammonia-water solution. Therefore, the problem of corrosion which arises in LiBr/H₂O system can be taken care of in a cheap and an efficient way. In addition, use of triple effect absorption systems can help getting COP above 1.6 [12]. In case of triple effect absorption system, rare amount of research work is being published and the papers which are being published such as [33-36] use LiBr/H₂O solution, which has a drawback of corrosion at high temperature.

1.2.4 Exergy Analysis

Exergy analysis is a powerful tool for the design, optimization, and performance evaluation of energy systems. The general principles and methodology of exergy analysis can be found in various sources [37-44]. An exergy analysis usually aims to determine the actual and maximum efficiencies of a system and the sites of exergy destruction. An exergy analysis of a complex system can be performed by analyzing the components of the system separately. Identifying the main sites of exergy destruction provides the direction for potential improvements. An important object of exergy analysis for systems is to find the real efficiency or COP of the system. In terms of COP it is the ratio of exergy destructed by the evaporator to the exergy destructed by the HTG. In general exergetic efficiency is defined as exergetic content of the output divided by exergetic content of input.

1.2.5 Homogeneous Mixture

A homogenous mixture is uniform in composition no matter what is the molecule size of a substance. The various properties such as density, temperature, pressure, and volume etc. of a homogenous mixture are uniform throughout. A homogeneous mixture cannot be separated into its molecules just by mechanical means such as centrifuging. In nature all gasses are homogenous due to their property of diffusing into each other when brought in contact. Example of a

homogenous mixture is moist air which is a mixture of dry air and water vapour [45].

1.2.6 Heterogeneous Mixture

A heterogeneous mixture is non-uniform mixture. Substances of heterogeneous mixture display different volume, temperature, pressure, and density etc. at a given state. A heterogeneous mixture substance can be separated using ordinary mechanical means such as settling or centrifuging. An example of a heterogeneous mixture is a fog which is a mixture of water liquid and saturated air [45].

After discussion each elements of the research individually, in the later sub-sections discussion on three integrated systems will be carried out. The aim of this research is to provide reader with different systems which can act in an efficient, effective, and sustainable manner. These three systems were developed by integrating PEMFC, Solar PV/T and multiple-effect absorption system together.

1.2.7 PEMFC Integrated with TEACS for Cooling and Power Production

First integrated system studied utilizes PEMFC and absorption system to provide efficient, effective, and sustainable power and cooling. There are works being carried out to integrate renewable energy sources with the refrigeration systems in order to make them efficient, eco-friendly and sustainable. The achievement of sustainability in the building sector necessitates a tremendous effort to reduce energy demand, boost energy efficiency and increase the share of renewable energy sources [46]. Most of this work has concentrated on integrating solar energy with absorption system. Solar or waste heat driven absorption cooling plants can provide summer comfort conditions in buildings at low primary energy consumption [47]. However, solar energy on its own cannot be looked at as the sustainable source because of its low efficiency and dependence on the sun. Besides the grid-connected photovoltaic (PV) system, another timely example of the distributed residential energy supply technology is small-scale combined heat and power (micro CHP) generation, with a maximum electrical output capacity between roughly 1 kW and 10 kW [48]. This issue of

sustainability makes PEM fuel cells more reliable and advisable. In recent years, hybrid photovoltaic-hydrogen/fuel cell energy systems have been popular as energy production systems that are clean, environmental-friendly, modular, and independent from fossil fuels [49]. Integration of PEMFC with TEACS makes the system tri-generation, as this system produced power, heat, and cold at the same time. The benefit of integrating PEM fuel cell with the absorption system is that it produces nearly the same amount of heat as power and this heat and power can be used to cater the energy demand of the house; hence, making it sustainable. A PEMFC produces nearly a similar amount of waste heat as its electrical power output so as to render its energy-conversion efficiency of roughly 80%. For an automotive fuel cell engine rated at 100kW, this means 100kW heat dissipation rate. This thermal energy dissipated can be used for powering absorption refrigeration cycle [50]. Moreover, PEM fuel cells have shown better performance than its competitors when they are running physically. Operational fuel cell systems have demonstrated superior performance to combustion-based generation technologies at scales from 5kW to 2MW, a range that includes the electrical requirements of most buildings [51]. PEM fuel cell integrated with TEACS can be considered as a trigeneration system, because trigeneration systems include those processes of production and simultaneous use of electricity, heat and cold, from a single fuel source [52]. In addition, integration of PEM fuel cell with absorption systems has also attracted the attention of many researchers [e.g., 50, 52-55]. These researchers have tried to study the feasibility of integrating PEM fuel cell with air-conditioning systems. The results showed the feasibility of using PEM fuel cell for cooling, increasing the total efficiency of the fuel cell system [50]. There are very limited studies related to the investigation of the performance of an absorption system integrated with a PEM fuel cell available in the literature. Also, the most amounts of studies which are being done are on the integration of PEM fuel cell with the single effect systems or integration of solar system with absorption system. This is a motivation behind conducting research in this field, the main goal of this part of overall research is to develop a relationship for an

integrated PEM fuel cell with TEACS and evaluate the performance of the system based on efficiency, COPs, cooling load and utilization factor.

1.2.8 Solar PV/T Integrated with TEACS for Cooling and Hydrogen Production

Another alternative to achieving effective, efficient and sustainable cooling and power is the use of solar energy as an energy provider for cooling and hydrogen production. Water electrolysis currently provides an attractive solution to the problem of hydrogen production. One of the major benefits which water electrolysis has over other technologies for production of hydrogen is that it is compatible with both recent technologies and future technologies such as solar, wind, wave, geothermal, etc. This benefit makes it an ideal choice to be used even during transition period from fossil fuels to renewable. Other benefit of using water electrolysis is that it can provide onsite hydrogen which can be handy for sustainable buildings. Provision of on-site, on-demand hydrogen generation at homes, service stations and other end-user sites lead to a reduction in transport/storage costs of hydrogen [56, and 57]. Most of the water electrolysis technologies to date have used an acidic or alkaline electrolyte systems and PEM electrolysis system for hydrogen generation [58-62]. Typical system efficiencies quoted are in the 55–75% range with most commercial systems having efficiencies below 65% [56].

In order to run the water electrolysis equipment to produce hydrogen in an environmental friendly manner we need to use an environmentally benign energy source. Solar PV/T holds a great potential to be the power source for the electrolysis system and at the same time providing energy to run the absorption system. There are many researchers who have studied the integrated system, which uses renewable energy technologies to produce hydrogen. The idea of using solar as a power source for the water electrolysis is widely supported by researchers because solar can provide a cheap source of energy which is environmentally benign. Majority of the work is done on the usage of solar energy for production of hydrogen such as by researchers [63-70]. In this part of research we will be using solar energy integrated with absorption cooling technology and water electrolysis system for the production of cooling and hydrogen.

1.2.9 PEMFC Integrated with QEACS for Cooling Production

The third system studied in this paper makes use of hydrogen energy to provide cooling using more effective and efficient quadruple effect absorption system. Majority of the power plants working in the countries situated in gulf region use fossil fuel. Such a high usage of fossil fuels brings with it high amount of green house gasses emission. It also causes problems to the environment, such as global warming, air pollution, ozone depletion, forest destruction and emission of the harmful gasses. It has become more significant than ever to design an air-conditioning system that is energy efficient and eco-friendly. The PEM fuel cells appear to be a promising power source for the air conditioning system because of its numerous potential and application opportunities and with a benefit of being energy efficient and eco-friendly. Hydrogen as a fuel holds in itself all the capabilities of working as an alternative fuel which is environmentally friendly and sustainable at the same time. Hydrogen is expected to play a key role in the near future as an energy carrier for sustainable development [13, 16, 20, and 23]. The use of hydrogen as an energy provider by using fuel cell holds a great potential due to higher efficiency, and eco-friendliness. Also, use of hydrogen as a fuel makes the energy generation process eco-friendly, because, the by-product of this process is water. The use of hydrogen in fuel cells to generate electricity is efficient and clean with water as the only by-product [16 and 20]. In the future, the role of hydrogen may become more important, as some researchers suggest that the world's energy systems may undergo a transition to an era in which the main energy carriers will be hydrogen [23, and 71-74]. All these benefits associated with PEMFC make it an attractive solution to the energy and environment crisis. These benefits also make it a good contender for the combine power and cooling production systems.

There are many alternatives available to the conventional air conditioning systems, but two prominent ones are adsorption system, and absorption system. Reasonable amount of work has been done on adsorption systems [75]. The energy need especially for food refrigeration applications is huge and requires potential solutions through renewable such as solar. Absorption refrigeration

systems appear to be a key solution to meet the energy requirement [29]. The common applications are single-effect and double-effect absorption refrigeration system rarely. Of course, increasing the effect will increase the efficiency or coefficient of performance of the system. Therefore, in this part of the study we propose a QEACS integrated with PEM fuel cell as a potential solution to these problems. This system uses least amount of energy input to the system in order to cool the space. Moreover, the source of energy for this system is hydrogen which is considered as green fuel. Therefore, the by-products of the PEM fuel cell are steam and water. In addition, quadruple effect absorption system recovers the near maximum amount of heat from the system with the help of three heat-exchangers and three generators.

Absorption systems have always received some attention in the past by many researchers [e.g., 30-32, and 76-77] who tried/to analyze and evaluate the system with different working fluid combinations (more commonly with water-LiBr and ammonia-water). Recently, due to global warming problem and other issues, the attention has been renewed with a greater interest to study these with renewables. At present, work on integration of sustainable energy sources to triple effect absorption cooling system (TEACS) is being carried out in order to make the system more efficient and eco-friendly as compared to single and double effect absorption systems. At present solar energy and fuel cell is attached to the TEACS due to its eco-friendliness nature as it is discussed in detail elsewhere [50, 53, 78, and 79-82].

The absorption cooling technology is one of the best alternatives to the compression cooling in the aspects of energy diversification and environmental protection. Since the absorption technology was extensively used for practical application, a number of high-performance absorption cycles have been introduced for both residential and industrial applications. The performance of a cooling cycle is represented by the COP which is the ratio of cooling capacity to energy input. The COP of a conventional double-effect LiBr/H₂O absorption cooling cycle is approximately 1.2. Here the “effect” implies the number of actual use of energy input to produce cold, thus the multiple-effect cycles have

higher COP values. Recently, the triple-effect absorption cycle has attracted much interest to replace the conventional machine as the more efficient one. The expected COP value of the triple-effect cycle is known to be about 30% higher than that of the double-effect cycle. In this paper we study a novel QEACS using ammonia-water solution. We use ammonia-water solution because of the ease of controlling corrosion which can hinder the function of the system greatly. The construction absorption cooling machine using the efficient lithium bromide-based working fluid has been greatly hindered by the corrosion problem caused by the high generator temperature above 473.15 K. The conventional LiBr/H₂O solution is known to cause a serious of corrosion problem. [33]

In the open literature, there are no studies undertaken to investigate the performance of quadruple effect refrigeration systems integrated with PEM fuel cell through COPs, and overall efficiency. This has been the motivation behind this novel work. In this regard, the main goal of this part of the thesis is to develop and analyze a quadruple effect absorption refrigeration system integrated with PEM fuel cell through energy and exergy. Evaluate its performance through energy and exergy based COPs for various operating conditions. In addition, conduct parametric studies to investigate the effects of varying temperature of the PEMFC, pressure of the PEMFC, and area of the PEMFC on the overall system performance.

1.2.10 Research Results and Summary of Key Findings

The motivation behind conducting this research was to propose and design a system which can cater the problem of global warming in the best way possible. In this research, three integrated systems were studied. These three integrated systems consisted of PEMFC, Solar PV/T, and absorption cooling technologies. These three systems were selected on the basis of their environmental friendliness and advantage of providing cheap, effective, efficient, and sustainable outputs. All three integrated system studied in this research were thermodynamically modeled in EES. The results of parametric studies showed that these systems can be looked at as reliable systems to meet future energy demands and to cater the problem of global warming. It was found that increasing T_{FC} results in lower efficiency of the

fuel cell but it results in higher COPs of the absorption system. Moreover, increase in pressure, current density and area of the fuel cell results has positive effect on the efficiency of the fuel cell and negative effect on the performance of the absorption system. The solar system performed best in the months when solar radiations were high and maximum COPs of absorptions system were obtained for the same months. In addition, maximum hydrogen output using electrolysis is obtained for the month when solar radiation was high and was available for relatively longer time. These results show that the systems studied are capable of providing us with sustainable and global warming free future.

1.2.11 Thesis Organization

In this chapter, the background of the individual systems and integrated systems, the problem statement, the objectives of the research, its scopes, method of approach as well as the summary of key findings have been outlined. The remaining chapters will be organized as follows.

The description of all three integrated systems is provided in details in chapter two. Also, the impact of this research on environment is discussed in second chapter. However, in chapter three thermodynamic modeling of each integrated system is provided. This chapter helps reader understand how each integrated system is formulated and which equations and properties are being used to carry out the energy and exergy analysis of the integrated systems studied in this thesis. Chapter four comprises of the results obtained by carrying out thermodynamic analysis of all three integrated systems studied in this thesis. In this chapter, very comprehensive discussion is done on how system behaves when its operating parameters are changed. Finally, conclusion of this work, and recommendations for future work are stated in chapter five.

Chapter 2 System Description and Environmental Impact

2.1 Operational Principle of PEMFC Integrated with TEACS for Cooling and Power Production

The integrated system, which is analyzed in this section, can be seen in Fig. 2.1. Hydrogen is being fed into the PEM fuel cell using cylinders filled with pure hydrogen. This hydrogen is supplied to the hydrogen flow plate, which is in contact with the Membrane Electrode Assembly (MEA). When hydrogen molecules come in contact with MEA, they break into protons and electrons owing to the characteristic of MEA of accepting only protons. Electrons are then taken away from the anode side with the help of an electric connection and are then fed into the electrical system to give out energy. After giving out energy, electrons are brought back to the cathode-side flow plate where protons are already available. The air is supplied on the cathode-side flow plate. The air, protons and electrons combine together to give out steam and water as by-products. The power and heat generated by the fuel cell are then fed into the TEACS. Small amount of power is fed into the pump of TEACS. All of the heat and the remaining amount of power are being fed into the High Temperature Generator (HTG) where strong solution coming from the absorber at state 21 is being heated to leave as a weak solution at state 22 and ammonia-water vapor mixture at state 8. Weak solution coming out of state 22 then gives out heat in the High temperature Heat Exchange (HHX) and combines with weak solution coming from state 19 and leaves at state 24. This weak solution from state 24 then gives out heat in the Medium temperature Heat Exchanger (MHX) and combines with weak solution from state 16 to leave at state 26. This weak solution then enters the Low temperature Heat Exchanger (LHX) where it heats the strong solution coming from state 11c. After giving heat, weak solution at state 27 enters expansion valve where it loses temperature and enters the absorber at state 28. The ammonia-water vapor mixture from state 8 then enters the Medium Temperature Generator (MTG) where it heats the strong solution coming from state 18 and leaves as ammonia-water vapour mixture at state 5 and 7. These two ammonia-water vapor mixtures then combine to leave at state 7a. Ammonia-water

vapor mixture at state 7a enters the Low Temperature Generator (LTG) and heats the strong solution coming from state 15 and leaves as ammonia-water vapor mixture at state 6 and 4. State 6 goes directly into the condenser while state 4 goes into the Condenser Heat Exchanger (CHX) to lose heat to the liquid coming from state 11b and leave at state 13. Ammonia-water vapor mixture leaving CHX at state 3 enters the condenser and gives out heat and then leaves at state 2, which passes through the expansion valve and leaves at state 2a to enter the evaporator. In the evaporator, heat is being gained by the system and the heated mixture leaves at state 1 to enter the absorber where it gives out heat and mixes with the weak solution coming from state 28. This mixed solution then leaves at state 11 in the form of strong solution to enter the pump and the process starts again.

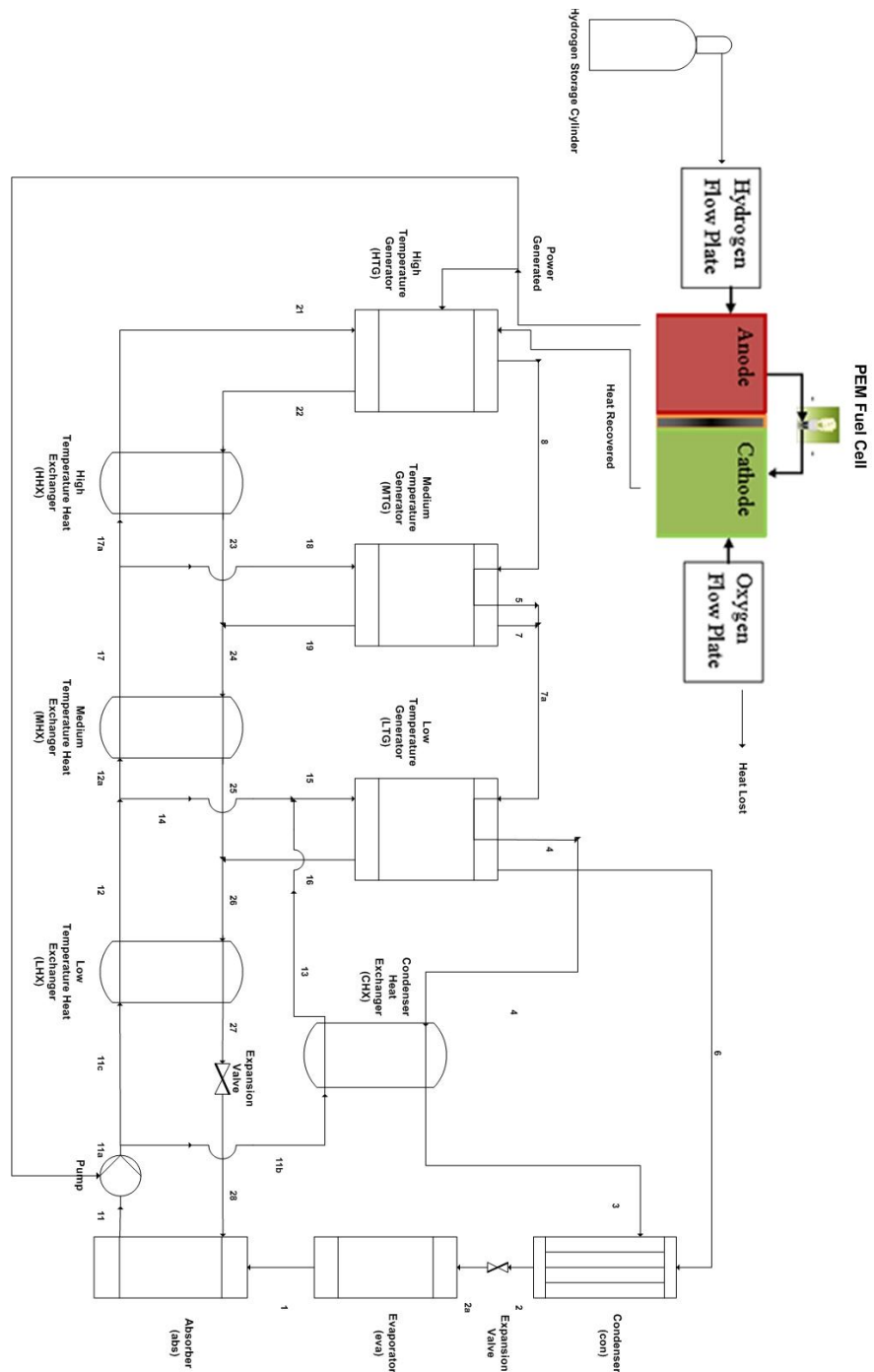


Fig. 2. 1 Schematic diagram of PEMFC integrated with TEACS

2.2 Operational Principle of Solar PV/T Integrated with TEACS for Cooling and Hydrogen Production

In this part of the thesis, we have studied an integrated solar PV/T absorption cooling system for the cooling and hydrogen production as shown in

Fig. 2.2. Solar PV/T system considered in this paper is glass to glass thermal system. Solar radiations fall on top of the PV modules which are placed on top of tunnel (duct) through which air is passed. These PV modules take in solar radiation and use it to break the bond inside the module to produce protons and electrons. The electrons are then taken out to give power. Power produced is supplied to the electrolyzer and the pump in the cooling cycle. The electrolyser is utilized to break the water molecule bond. As the water molecule breaks, it splits in to hydrogen and oxygen. The hydrogen molecules are then taken out of the electrolyser and are stored in a tank. The hydrogen molecules which are obtained through electrolysis can later be used as an energy source to HTG by burning hydrogen in HTG or using it as a power generating source by supplying it to PEMFC depending on the end user. On the other hand, air enters the tunnel which is placed beneath the PV module. This air then comes in contact with the down surface of the PV module which is heated up by the solar radiation and therefore transfer of heat takes place. As the air passes through the tunnel it gets heated up. This hot air is then fed into the HTG of the absorption cooling system and is used as an energy source for the absorption cooling system. Moreover, small amount of power produced by PV panels is fed into the pump of TEACS and the rest of the power is fed into the electrolyser to produce hydrogen. All of the heat is being fed into the high temperature generator (HTG) where strong solution coming from absorber at state 21 is being heated to leave as a weak solution at state 22 and ammonia-water vapour mixture with concentration of 0.999 at state 8. Weak solution coming out of state 22 then gives out heat in the high temperature heat exchange (HHX) and combines with weak solution coming from state 19 and leaves at state 24. The weak solution from state 24 then gives out heat in the medium temperature heat exchanger (MHX) and combines with weak solution from state 16 to leave at state 26. This weak solution then enters the low temperature heat exchanger (LHX) where it pre-heats the strong solution coming from state 11c. After giving heat, weak solution at state 27 enters expansion valve where drop in pressure and temperature takes place before entering the absorber at state 28. The ammonia-water vapour mixture from state 8 then enters the medium

temperature generator (MTG) where it heats the strong solution coming from state 18 and leaves as ammonia-water vapour mixture at state 5 and state 7. These ammonia-water vapour mixtures combine together to leave at state 7a as an ammonia-water vapour mixture. Vapour at state 7a enters the low temperature generator (LTG) and heats the strong solution coming from state 15 and leaves as ammonia-water vapour mixture at state 6 and state 4. State 6 goes directly into the condenser while state 4 goes into the condenser heat exchanger (CHX) to lose heat to the liquid coming from state 11b and leaves at state 13. Ammonia-water vapour mixture leaving CHX at state 3 enters the condenser, where gives out heat and then leaves at state 2. This pre-cooled ammonia-water mixture then passes through the expansion valve and leaves at state 2a after losing pressure and temperature to enter the evaporator. In the evaporator heat is being gained by the system and the heated mixture leaves at state 1 to enter the absorber, where it gives out heat to the surrounding and leaves at state 11 to enter the pump and the cycle repeats.

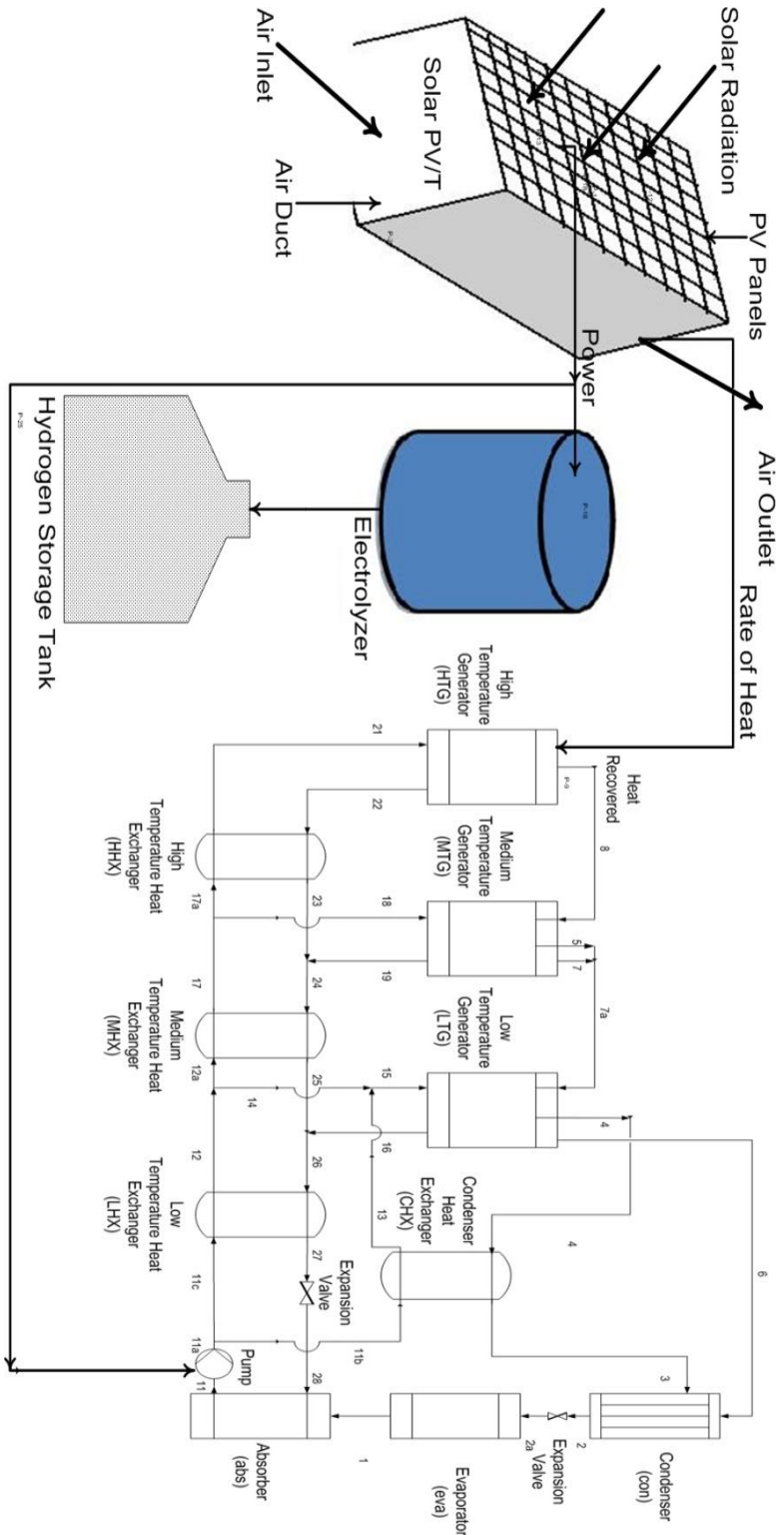


Fig. 2. 2 Schematic diagram of Solar PV/T integrated with TEACS

2.3 Operational Principle of PEMFC Integrated with QEACS for Cooling Production

Several multiple effect absorption systems are being used to enhance the COP of the system. Here, we consider a parallel flow quadruple effect absorption system using ammonia-water solution integrated with PEM fuel cell, which is shown schematically in Fig. 2.3. This system consists of four generators which are, v. high temperature generator, high temperature generator, medium temperature generator, and low temperature generator. In addition, it has five heat exchangers, which are called, v. high temperature heat exchanger, high temperature heat exchanger, medium temperature heat exchanger, low temperature heat exchanger, and a condenser heat exchanger. Moreover, the system consists of two expansion valves, one condenser, one evaporator, one absorber, one pump, and a fuel cell. The process starts at the V.HTG side, where strong solution coming from the absorber (state 36) is heated up, so that the vaporized ammonia-water can be extracted from the solution (state 37) and the remaining solution known as weak solution (state 38) is returned to the absorber. The strong solution leaves the absorber at state 1 and passes through the pump to exit at state 2 where it is divided into state 17 and state 19. State 19 then goes through the LHX and leaves at state 3. Then it divides into two streams state 21 and state 20. State 20 goes through MHX and leaves at state 24 where it divides into state 25 and state 26. State 25 goes to HHX and leaves at state 29. This stream is again divided in to two streams namely state 34 and state 35. State 35 then goes into the V.HHX and leaves at state 36 to enter the V.HTG. Same way, before reaching the absorber (state 16) weak solution passes through V.HHX (state 40) where it mixes with state 30 and leaves at state 41 to enter HHX. This weak solution then passed through MHX and LHX giving out heat to strong solution to reach an expansion valve (state 16) before entering the absorber again. Meanwhile the vaporized ammonia-water from state 37 enters HTG where it boils up the strong solution coming from HHX (state 34). The weak solution then leaves the HTG at state 30 to mix with the stream coming from V.HHX before reaching absorber. However the vaporized ammonia-water leaves the HTG at state 31 and mixes with state 28 before entering MTG. The same process

continues till the vaporized ammonia-water reaches CHX at state 6. This vaporized ammonia-water then gives out heat to stream coming from pump before entering condenser. Another vaporized ammonia-water stream leaving LTG at state 7 also enters condenser. In the condenser these streams from state 6 and state 7 give out heat to the air and leave the condenser at state 9. Stream at state 9 enters an expansion valve where it expands before entering evaporator at state 10. In the evaporator ammonia-water mixture absorbs heat from the cooling place and leave at state 11 to enter the absorber. In this system fuel cell is being used as an energy source. The fuel is being supplies to the cell using cylinders. The necessary values and equations for the performance of fuel cell were taken from ref. [80].

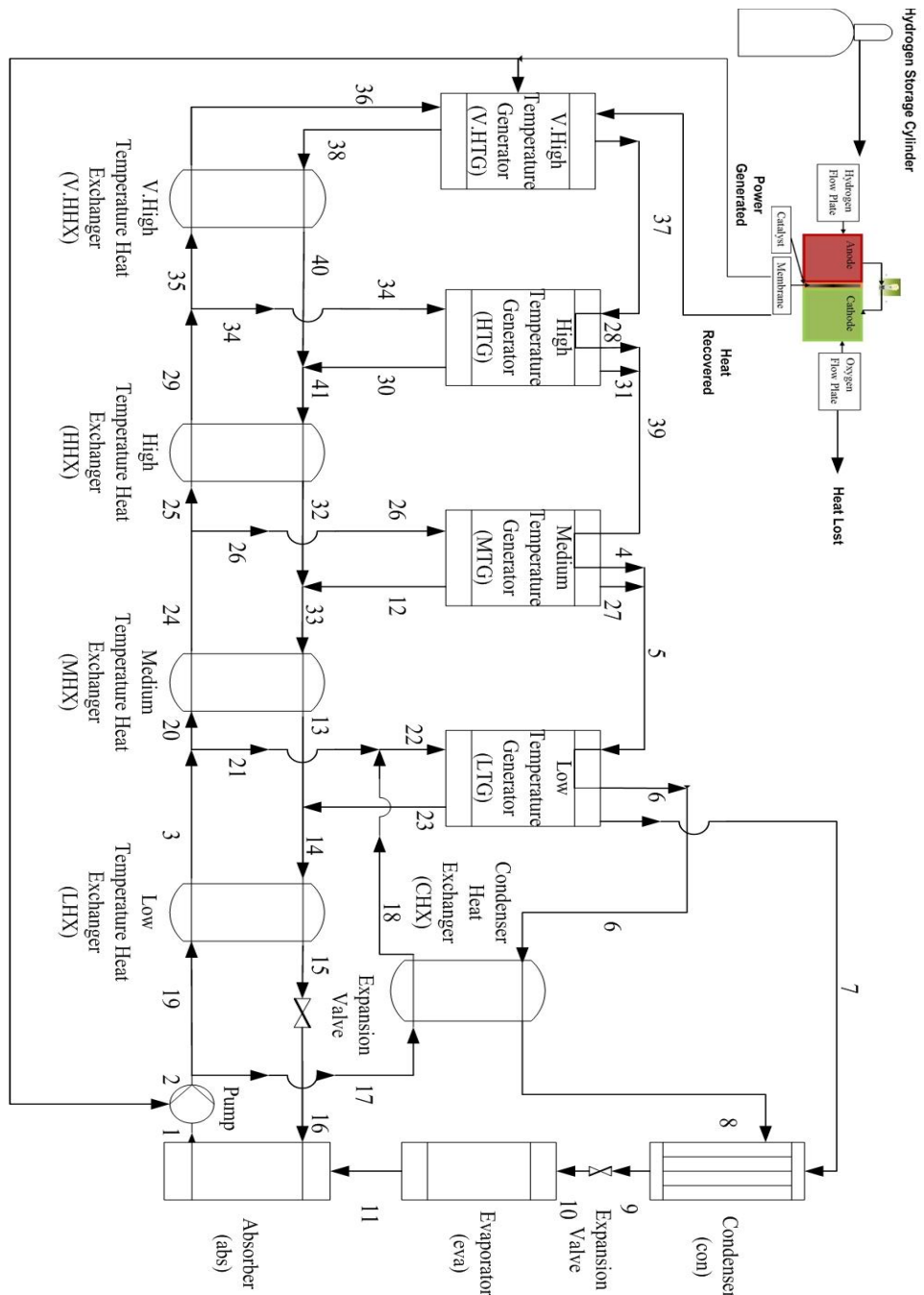


Fig. 2. 3 Schematic diagram of QEACS integrated with PEMFC

2.4 Environmental Impact

In recent time's world has seen an exponential increase in the demand of energy. Such an unexpected rise in energy demand has become a point of concern for both developed and developing countries. In this research, we try to provide different solutions for sustainable building operations in order to make research globally implacable. The PEMFC is expected to play a major role in the

alleviation of global warming since the end products of the internal chemical reactions are clean water and steam. The greenhouse effect is the phenomenon due to which solar radiation reflected back from the surfaces of bodies on the Earth's surface is not transmitted back into space. Due to the increased content of gases such as carbon dioxide and carbon monoxide, a result of the internal combustion engine for example, this radiation remains trapped within the Earth's atmosphere, thereby increasing the overall temperature of the Earth's surface. By making use of the abundant supply of hydrogen and oxygen available in the atmosphere, it is easy to obtain clean and safe energy without the harmful effects of combustion. Moreover, combustible fluids only offer marginal efficiency compared to the most efficient of PEMFCs with an efficiency of 79%. Furthermore, in light of the worldwide water crisis, the output of the PEMFC is an additional source of clean water fit for human consumption. As they are made of virtually harmless components whose disposal is not a problem, they pose no threat to the environment at the end of their life cycle. Moreover, use of Solar PV/T provides an attractive alternative for power and heating production. Solar PV/T systems are considered free of running cost systems as they use solar radiation for heating and power production which is freely available to human kind. In addition, absorption cooling systems require very less amount of energy input as compared to conventional vapour-compression refrigeration systems. The use of absorption systems reduces the load on the national grid and therefore reduces the load on governments. This reduction in energy consumption results in reduction in green house gasses as now governments will have to produce lesser amount of power to meet the demand.

Addition of PEMFC and Solar PV/T system with Absorption cooling system is one of the most attractive alternatives for environmental friendly future. All the systems used in this research are environmentally friendly and do not emit green house gasses. Use of these integrated systems also help making a sustainable building as PEMFC and Solar PV/T integrated with absorption system can cater the need of heating, cooling, and power. These systems use environmentally benign fuel to provide heating, cooling, and power.

One thing that has to be noted though is the effect of global warming and how these systems play their roles in alleviating the problems caused by the greenhouse effect. The PEM fuel cell gives 99.9% pure water as a byproduct. As previously mentioned, this water can be consumed as drinkable water after specific water treatments. The water which passes through the Solar PV/T system can be obtained through geothermal water source, hence making system sustainable. In conclusion, the systems analysed in this research will be helpful to researchers and governments throughout the world while choosing an integrated system for sustainable building operations.

Chapter 3 Thermodynamic Analysis

3.1 Energy and Exergy Analyses of PEMFC integrated with TEACS for Cooling and Power Production

In order to run the system, mass, energy, and exergy balance equations are written for the PEM fuel cell, and the components of TEACS. Also, equations to calculate efficiency of the cell, and utilization factor of the system are written.

3.1.1 PEM Fuel Cell Unit

In order to analyze we need to start with the fuel cell by writing the molar fraction for hydrogen and oxygen as given below [64]

$$x_{H_2} = \frac{1 - x_{H_2O,A}}{1 + (x_A/2)(1 + [\zeta_A/(\zeta_A - 1)])} \quad (3.1a)$$

$$x_{O_2} = \frac{1 - x_{H_2O,C}}{1 + (x_C/2)(1 + [\zeta_C/(\zeta_C - 1)])} \quad (3.1b)$$

After calculating the mole fraction of hydrogen and oxygen, the saturation pressure of the water based on the temperature of the cell is obtained by [64]

$$\log_{10} P_{sat} = -2.1794 + 0.02953 \times T - 9.1837 \times 10^{-5} \times T^2 + 1.4454 \times 10^{-7} \times T^3 \quad (3.2)$$

Hence, the saturation pressure is then used to find the mole fraction of water at anode and cathode side using equation given below:

$$x_{H_2O,A} = \frac{P_{sat}}{P_A} \quad (3.3a)$$

$$x_{H_2O,C} = \frac{P_{sat}}{P_C} \quad (3.3b)$$

The power output per unit specific area of the fuel cell is given by

$$\dot{W}_{FC} = i \times [V_{rev} - v_{act} - v_{ohm} - v_{conc}] \quad (3.5)$$

where the reversible voltage is

$$V_{rev} = 1.229 - 8.5 \times 10^{-4}(T_{FC} - 298.15) + 4.3085 \times 10^{-5} \times T_{FC} \left[\ln(p_{H_2}) + \frac{1}{2} \ln(p_{O_2}) \right] \quad (3.5a)$$

The activation voltage at anode and cathode are given as

$$v_{actAnode} = \frac{RT_{FC}}{\alpha_A n F} \ln \left(\frac{i}{i_0} \right) \quad (3.5b)$$

$$v_{actcathode} = \frac{RT_{FC}}{\alpha_C n F} \ln \left(\frac{i}{i_0} \right) \quad (3.5c)$$

The ohmic voltage is

$$v_{ohmic} = iR_{ohmic} \quad (3.5d)$$

Where

$$R_{ohmic} = \frac{t_{mem}}{\sigma_{mem}}$$

$$\sigma_{mem} = (0.005139\lambda_{mem} - 0.00326)\exp\left[1268\left(\frac{1}{303} - \frac{1}{T_{FC}}\right)\right]$$

The membrane water content is calculated by [64]:

$$\lambda_{mem} = 0.043 + 17.81 a_1 - 39.85 a_1^2 - 39.85 a_1^3$$

where a_1 represents water activity in the membrane and is expressed as follows

$$a_1 = x_{H_2O} \left(\frac{P}{P_{sat}}\right)$$

And the concentration overvoltage is defined as

$$v_{conc} = i \left(\beta_1 \frac{i}{i_{max}}\right) \quad (3.5e)$$

The concentration of overvoltage constants depends on the inlet pressure and the saturation pressure and is calculated as follows [64]

For $\frac{P_i}{0.1173} + P_{sat} < 2.0 \text{ atm}$, the value of β_1 becomes

$$\beta_1 = (7.16 \times 10^{-4} T - 0.622) \left(\frac{P_i}{0.1173} + P_{sat}\right) + (-1.45 \times 10^{-3} T + 1.68)$$

When $\frac{P_i}{0.1173} + P_{sat} > 2.0 \text{ atm}$, the value of β_1 becomes

$$\beta_1 = (8.66 \times 10^{-5} T - 0.068) \left(\frac{P_i}{0.1173} + P_{sat}\right) + (-1.6 \times 10^{-4} T + 0.54)$$

and

$$\beta_2 = 2.0$$

The rate of heat output of the cell which is fed into the HTG is calculated based on exergy balance and is given by

$$\begin{aligned} \dot{Q}_{FC} = & \{T_0[\sum(\dot{n} \times s)_{out} - \sum(\dot{n} \times s)_{in}] + \dot{W}_{FC} + (\dot{n} \times ex)_{H_2out} + \\ & (\dot{n} \times ex)_{H_2O,out} - (\dot{n} \times ex)_{H_2in} - (\dot{n} \times ex)_{O_2in}\} \times \left(r_{HL} + (1 - \right. \\ & \left. r_{HL}) \frac{T_0}{T_{FC}}\right)^{-1} \end{aligned} \quad (3.6)$$

The molar flow rate of hydrogen, oxygen, and water at inlet and outlet are obtained by

$$\dot{n}_{H_2,reacted} = 2\dot{n}_{O_2,reacted} = \dot{n}_{H_2O,pro} = \frac{i}{2F} \quad (3.7a)$$

$$\dot{n}_{H_2,in} = \dot{n}_{H_2,reacted} + \dot{n}_{H_2,out} \quad (3.7b)$$

$$\dot{n}_{O_2,in} = \dot{n}_{O_2,reacted} + \dot{n}_{O_2,out} \quad (3.7c)$$

The irreversibility rate is found using the formula given below

$$\dot{I}_{FC} = - \left(1 - \frac{T_0}{T_{FC}}\right) \times r_{HL} \times \dot{Q}_{FC} - \dot{W}_{FC} + \dot{E}x_{H_2,i} + \dot{E}x_{O_2,i} - \dot{E}x_{H_2,o} - \dot{E}x_{O_2,o} - \dot{E}x_{H_2O,o} \quad (3.8)$$

where

$$\dot{E}_x = \dot{n} \times ex$$

$$ex = ex^{PH} + ex^{CH}$$

$$ex^{PH} = (h - h_0) - T_0 \times (s - s_0)$$

$$ex^{CH} = (h - h_0) - T_0 \times (s - s_0) - \frac{R \times T_0 \times \ln\left(\frac{P_i}{P_0}\right)}{MW}$$

Here, P_i represent inlet pressure of the gas and P_0 represents ambient pressure.

For further details on the PEM fuel cell, see refs. [63-64].

3.1.2 TEACS Unit

- For High Temperature Generator

After getting the heat and power output from the PEM fuel cell, the equations for HTG were written in order to run the TEACS to achieve the cooling load and to provide hot water. The amount of energy given to HTG is shown below

$$\dot{Q}_{HTG} = \dot{W}_{FC} + \dot{Q}_{FC} - \dot{W}_{PUMP} \quad (3.9)$$

The relationship for calculating enthalpy of a homogeneous mixture using concentrations is shown by the following equation

$$h_{21} = x_{21} h_{21,ammonia} + (1-x_{21}) h_{21,water} \quad (3.10)$$

This equation shows the relationship for one state, and the same relationship is used for other states as well.

The mass balance equations are given as follows

$$\dot{m}_{21} x_{21} = \dot{m}_{22} x_{22} + \dot{m}_8 x_8 \quad (3.11)$$

$$\dot{m}_{21} = \dot{m}_{22} + \dot{m}_8 \quad (3.12)$$

In order to obtain the outlet conditions of the HTG, the following equation is used

$$\dot{m}_{21} h_{21} + \dot{Q}_{HTG} = \dot{m}_{22} h_{22} + \dot{m}_8 h_8 \quad (3.13)$$

The entropy balance becomes

$$\dot{m}_{21} s_{21} + \frac{\dot{Q}_{HTG}}{T_{HTG}} + \dot{S}_{gen} = \dot{m}_{22} s_{22} + \dot{m}_8 s_8 \quad (3.14)$$

The exergy destruction in HTG is

$$\dot{E}_{x_{dest}} = T_0 \times \dot{S}_{gen} \quad (3.15)$$

and same relationship is used for other generators also.

- For High Temperature Heat Exchanger

The mass and energy balance equation for HHX are given below

$$\dot{m}_{22} = \dot{m}_{23} \quad (3.16a)$$

$$\dot{m}_{17a} = \dot{m}_{21} \quad (3.16b)$$

$$\dot{m}_{17a} h_{17a} + \dot{Q}_{HHX} = \dot{m}_{21} h_{21} \quad (3.17)$$

$$\dot{m}_{22} h_{22} = \dot{Q}_{HHX} + \dot{m}_{23} h_{23} \quad (3.18)$$

- For Condenser

The mass and energy balance equations for the condenser are given below

$$\dot{m}_2 = \dot{m}_6 + \dot{m}_3 \quad (3.19)$$

$$\dot{Q}_{con} = \dot{m}_w (h_{w,o} - h_{w,i}) \quad (3.20)$$

$$\dot{m}_2 h_2 + \dot{Q}_{con} = \dot{m}_6 h_6 + \dot{m}_3 h_3 \quad (3.21)$$

The entropy balance equation can be written as

$$\dot{m}_{21} s_{21} + \dot{S}_{gen} = \dot{m}_{22} s_{22} + \dot{m}_8 s_8 + \frac{\dot{Q}_{con}}{T_{con}} \quad (3.22)$$

The exergy destruction in condenser is calculate using

$$\dot{E}_{x_{dest}} = T_0 \times \dot{S}_{gen} \quad (3.23)$$

- For Evaporator

Below mentioned equations are for mass and energy balance of evaporator

$$\dot{m}_{2a} = \dot{m}_1 \quad (3.24)$$

$$\dot{m}_{2a} h_{2a} + \dot{Q}_{eva} = \dot{m}_1 h_1 \quad (3.25)$$

The entropy balance equation is written as

$$\dot{m}_{2a} s_{2a} + \frac{\dot{Q}_{eva}}{T_{eva}} + \dot{S}_{gen} = \dot{m}_1 s_1 \quad (3.26)$$

The exergy destruction in evaporator is calculates using

$$\dot{E}_{x_{dest}} = T_0 \times \dot{S}_{gen} \quad (3.27)$$

- For Absorber

The following energy balance equation is used to calculate the heat rejected from the absorber

$$\dot{m}_{11} h_{11} + \dot{Q}_{abs} = \dot{m}_1 h_1 + \dot{m}_{28} h_{28} \quad (3.28)$$

The entropy balance is calculated using

$$\dot{m}_{11} s_{11} + \frac{\dot{Q}_{abs}}{T_{abs}} + \dot{S}_{gen} = \dot{m}_1 s_1 + \dot{m}_{28} s_{28} \quad (3.29)$$

The exergy destruction in absorber is given by

$$\dot{E}_{x_{dest}} = T_0 \times \dot{S}_{gen} \quad (3.30)$$

- For Pump

The work done by the pump is calculated using the equation given below

$$\dot{m}_{11} = \frac{\dot{W}_p}{h_{11a} - h_{11}} \quad (3.31)$$

Energy and exergy efficiencies of the cell are calculated by

$$\eta_{FC,Energy} = 0.95 \frac{\dot{W}_{FC}}{i \times (1.25)} \quad (3.32a)$$

Where 1.25 V represents the electromotive force relative to the lower heating value of hydrogen and 0.95 is the fuel utilization coefficient. This coefficient represents the ratio of the mass of fuel reacted in cell to the mass of fuel input to the cell. Therefore, equation (32a) is derived for the lower heating value of hydrogen and can be found in literature [12].

$$\eta_{FC,Exergy} = \frac{\dot{W}_{FC} + (1 - \frac{T_0}{T_{FC}}) \times \dot{Q}_{HTG}}{(\dot{E}_x)_{H_2} + (\dot{E}_x)_{O_2}} \quad (3.32b)$$

The thermal exergy of evaporator and HTG are given by

$$\dot{E}_{x_{eva,th}} = (1 - \frac{T_0}{T_{eva}}) \times \dot{Q}_{eva} \quad (3.33a)$$

$$\dot{E}_{x_{HTG,th}} = (1 - \frac{T_0}{T_{HTG}}) \times \dot{Q}_{HTG} \quad (3.33b)$$

The energetic and exergetic COPs are calculate based on

$$\text{COP}_{\text{EN}} = \frac{\dot{Q}_{\text{eva}}}{\dot{Q}_{\text{HTG}} + \dot{W}_{\text{Pump}}} \quad (3.34a)$$

$$\text{COP}_{\text{Ex}} = \frac{\dot{E}x_{\text{eva,th}}}{\dot{E}x_{\text{HTG,th}} + \dot{W}_{\text{Pump}}} \quad (3.34b)$$

Overall exergy destruction becomes

$$\dot{I}_{\text{overall}} = T_0 \times \left[\left(\frac{\dot{Q}_{\text{con}}}{T_{\text{con}}} \right) + \left(\frac{\dot{Q}_{\text{abs}}}{T_{\text{abs}}} \right) + \left(\frac{\dot{Q}_{\text{eva}}}{T_{\text{eva}}} \right) - (\dot{m}_{\text{H}_2} \times s_{\text{H}_2}) - (\dot{m}_{\text{O}_2} \times s_{\text{O}_2}) \right] \quad (3.35)$$

Overall energy and exergy efficiencies are defined as

$$\eta_{\text{ovEN}} = \frac{\dot{Q}_{\text{eva}}}{\dot{m}_{\text{H}_2} \times \text{HHV}_{\text{H}_2}} \quad (3.36a)$$

$$\eta_{\text{ovEx}} = \frac{\dot{E}x_{\text{eva}}}{\dot{m}_{\text{H}_2} \times \text{Ex}_{\text{H}_2}} \quad (3.36b)$$

3.2 Energy and Exergy Analyses of Solar PV/T integrated with TEACS for Cooling and Hydrogen Production

3.2.1 Solar PV/T System

The equations which are used to solve the mathematical model of PV/T system are derived from Joshi et al. [54]. Moreover, the assumptions and constants of solar PV/T system are listed in table 4.2.

The equation to calculate power produced by PV module is given as

$$\dot{W}_{\text{solar}} = \eta_c \times \dot{I} \times \beta_c \times \tau_g \times A \quad (3.37)$$

The rate of heat transfer is given by

$$\dot{Q}_{\text{solar}} = \frac{\dot{m}_a \times c_{p_a}}{U_L} \times \left((h_{p2G} \times z \times \dot{I}) - U_L \times (T_{\text{ai}} - T_0) \right) \times \left[1 - \exp \left(\frac{-b \times U_L \times L}{\dot{m}_a \times c_{p_a}} \right) \right] \quad (3.38)$$

where

$$z = \alpha_b \times \tau_g^2 \times (1 - \beta_c) + h_{p1G} \times \tau_g \times \beta_c \times (\alpha_c - \eta_c) \quad (3.39)$$

The rate of exergy of solar energy is calculated by

$$\dot{E}x_{\text{solar}} = \left[1 - \left(\frac{T_0 + 273.15}{T_{\text{sun}}} \right) \right] \times \dot{I} \times A \quad (3.40)$$

Electrical and thermal efficiencies are defined as

$$\eta_{\text{el}} = \eta_c \times (1 - 0.0045 \times (T_c - 25)) \quad (3.41)$$

where

$$T_c = \frac{\tau_g \times \beta_c \times i \times (\alpha_c - \eta_c) + U_t \times T_0 + h_t \times T_{bs}}{U_t + h_t} \quad (3.41a)$$

$$T_{bs} = \frac{z \times i + (U_t + U_{tb}) \times T_0 + h_{ba} \times T_{air}}{U_b + h_{ba} + U_{tb}} \quad (3.41b)$$

$$T_{air} = \left[T_0 + \frac{h_{p2G} \times z \times i}{U_L} \right] \times \left[1 - \frac{1 - \exp\left(\frac{-b \times U_L \times L}{\dot{m}_a \times c_{pa}}\right)}{\frac{b \times U_L \times L}{\dot{m}_a \times c_{pa}}} \right] + T_{ai} \times \left[\frac{1 - \exp\left(\frac{-b \times U_L \times L}{\dot{m}_a \times c_{pa}}\right)}{\frac{b \times U_L \times L}{\dot{m}_a \times c_{pa}}} \right] \quad (3.41c)$$

$$\eta_{th} = \frac{\dot{Q}_{solar}}{i \times b \times L} \quad (3.42)$$

3.2.2 Electrolyzer

The electrolyzer is used to split water molecule into hydrogen and oxygen molecule, where hydrogen molecule is stored in the tank for later usage as an energy provider to the HTG or as a fuel to produce power using PEMFC. The amount of hydrogen produced depends on the efficiency of the electrolyzer, higher heating value of the hydrogen and power input to the electrolyzer.

$$\eta_{electrolyzer} = \frac{\dot{m}_{H_2} \times HHV}{\dot{W}_{solar} - \dot{W}_{pump}} \quad (3.43)$$

3.2.3 Absorption Cooling System

- For High Temperature Generator

After getting the heat and power output from the PEM fuel cell, equations for HTG were written in order to run the TEACS to achieve the cooling load and to provide hot water. The amount of energy given to HTG is shown below

$$\dot{Q}_{HTG} = \dot{Q}_{solar} \quad (3.44)$$

The relationship for calculating enthalpy of homogenous a mixture using concentrations is shown by the following equation

$$h_{21} = x_{21} h_{21, ammonia} + (1 - x_{21}) h_{21, water} \quad (3.45)$$

Which shows the relationship for one state, and the same relationship is used for other states.

The mass balance equations are given as follows

$$\dot{m}_{21} x_{21} = \dot{m}_{22} x_{22} + \dot{m}_8 x_8 \quad (3.46)$$

$$\dot{m}_{21} = \dot{m}_{22} + \dot{m}_8 \quad (3.47)$$

In order to obtain the outlet conditions of the HTG, the following equation is used

$$\dot{m}_{21} h_{21} + \dot{Q}_{HTG} = \dot{m}_{22} h_{22} + \dot{m}_8 h_8 \quad (3.48)$$

The entropy balance is

$$\dot{m}_{21} s_{21} + \frac{\dot{Q}_{HTG}}{T_{HTG}} + \dot{S}_{gen} = \dot{m}_{22} s_{22} + \dot{m}_8 s_8 \quad (3.49)$$

The exergy destruction in HTG is

$$\dot{E}x_{dest} = T_0 \times \dot{S}_{gen} \quad (3.50)$$

And same relationship is used for other generators also.

- For High Temperature Heat Exchanger

The energy balance equation for HHX is given below.

$$\dot{m}_{17a} h_{17a} + \dot{Q}_{HHX} = \dot{m}_{21} h_{21} \quad (3.51)$$

$$\dot{m}_{22} h_{22} = \dot{Q}_{HHX} + \dot{m}_{23} h_{23} \quad (3.52)$$

- For Condenser

The mass, and energy balance equations for the condenser are give below

$$\dot{m}_2 = \dot{m}_6 + \dot{m}_3 \quad (3.53)$$

$$\dot{Q}_{con} = \dot{m}_w (h_{w,o} - h_{w,i}) \quad (3.54)$$

$$\dot{m}_2 h_2 + \dot{Q}_{con} = \dot{m}_6 h_6 + \dot{m}_3 h_3 \quad (3.55)$$

The entropy balance is

$$\dot{m}_6 s_6 + \dot{m}_3 s_3 + \dot{S}_{gen} = \dot{m}_2 s_2 + \frac{\dot{Q}_{con}}{T_{con}} \quad (3.56)$$

The exergy destruction in condenser is

$$\dot{E}x_{dest} = T_0 \times \dot{S}_{gen} \quad (3.57)$$

- For Evaporator

Below mentioned equations are for mass and energy balance of evaporator

$$\dot{m}_{2a} = \dot{m}_1 \quad (3.58)$$

$$\dot{m}_{2a} h_{2a} + \dot{Q}_{eva} = \dot{m}_1 h_1 \quad (3.59)$$

The entropy balance is

$$\dot{m}_{2a} s_{2a} + \frac{\dot{Q}_{eva}}{T_{eva}} + \dot{S}_{gen} = \dot{m}_1 s_1 \quad (3.60)$$

The exergy destruction in evaporator is

$$\dot{E}x_{dest} = T_0 \times \dot{S}_{gen} \quad (3.61)$$

- For Absorber

The following energy balance equation is used to calculate the heat rejected from the absorber.

$$\dot{m}_{11} h_{11} + \dot{Q}_{abs} = \dot{m}_1 h_1 + \dot{m}_{28} h_{28} \quad (3.62)$$

The entropy balance is

$$\dot{m}_{11} s_{11} + \frac{\dot{Q}_{abs}}{T_{abs}} = \dot{m}_1 s_1 + \dot{m}_{28} s_{28} + \dot{S}_{gen} \quad (3.63)$$

Exergy destruction in absorber is

$$\dot{E}x_{dest} = T_0 \times \dot{S}_{gen} \quad (3.64)$$

- For Pump

The work done/ by the pump is calculated using the equation given below.

$$\dot{m}_{11} = \frac{W_{Pump}}{h_{11a} - h_{11}} \quad (3.65)$$

The thermal exergy of evaporator and HTG are given by

$$\dot{E}x_{eva,th} = \left(1 - \frac{T_0}{T_{eva}}\right) \times \dot{Q}_{eva} \quad (3.66a)$$

$$\dot{E}x_{HTG,th} = \left(1 - \frac{T_0}{T_{HTG}}\right) \times \dot{Q}_{HTG} \quad (3.66b)$$

The energetic and exergetic COPs are as

$$COP_{EN} = \frac{\dot{Q}_{eva}}{\dot{Q}_{HTG} + \dot{W}_{Pump}} \quad (3.67a)$$

$$COP_{Ex} = \frac{\dot{E}x_{eva,th}}{\dot{E}x_{HTG,th} + \dot{W}_{Pump}} \quad (3.67b)$$

- Overall efficiencies

Overall energy and exergy efficiencies are defined as

$$\eta_{ov,EN} = \frac{\dot{m}_{H_2} \times HHV + \dot{Q}_{eva}}{i \times b \times L} \quad (3.68a)$$

$$\eta_{ov,Ex} = \frac{\dot{E}x_{H_2} \times \dot{E}x_{eva,th}}{\dot{E}x_{solar}} \quad (3.68b)$$

3.3 Thermodynamic Analysis of PEMFC integrated with QEACS for Cooling Production

3.3.1 PEM Fuel Cell Unit

In order to analyze we need to start with the fuel cell by writing the molar fraction for hydrogen and oxygen as given below:

$$X_{H_2} = \frac{1 - x_{H_2O,A}}{1 + (x_A/2)(1 + \zeta_A/\zeta_A - 1)} \quad (3.69a)$$

$$X_{O_2} = \frac{1 - x_{H_2O,C}}{1 + (x_C/2)(1 + \zeta_C/\zeta_C - 1)} \quad (3.69b)$$

After calculating the mole fraction of hydrogen and oxygen, the saturation pressure of the water based on the temperature of the cell is obtained by:

$$\log_{10} P_{sat} = -2.1794 + 0.02953 \times T - 9.1837 \times 10^{-5} \times T^2 + 1.4454 \times 10^{-7} \times T^3 \quad (3.70)$$

Hence, the saturation pressure is then used to find the mole fraction of water at anode and cathode side using equation given below:

$$X_{H_2O_A} = \frac{P_{sat}}{P_A} \quad (3.71a)$$

$$X_{H_2O_C} = \frac{P_{sat}}{P_C} \quad (3.71b)$$

The power output per unit specific area of the fuel cell is given by

$$\dot{W}_{FC} = i \times [V_{rev} - v_{act} - v_{ohm} - v_{conc}] \quad (3.72)$$

Where the reversible voltage is

$$V_{rev} = 1.229 - 8.5 \times 10^{-4}(T_{FC} - 298.15) + 4.3085 \times 10^{-5} \times T_{FC} \left[\ln(p_{H_2}) + \frac{1}{2} \ln(p_{O_2}) \right] \quad (3.73a)$$

The activation voltage at anode and cathode are given as

$$v_{actAnode} = \frac{RT_{FC}}{\alpha_A n F} \ln \left(\frac{i}{i_0} \right) \quad (3.73b)$$

$$v_{actcathode} = \frac{RT_{FC}}{\alpha_C n F} \ln \left(\frac{i}{i_0} \right) \quad (3.73c)$$

The ohmic voltage is

$$v_{ohmic} = i R_{ohmic} \quad (3.73d)$$

Where

$$R_{ohmic} = \frac{t_{mem}}{\sigma_{mem}}$$

$$\sigma_{mem} = (0.005139\lambda_{mem} - 0.00326)\exp\left[1268\left(\frac{1}{303} - \frac{1}{T_{FC}}\right)\right]$$

The membrane water content is calculated by [30]:

$$\lambda_{mem} = 0.043 + 17.81 a_1 - 39.85 a_1^2 - 39.85 a_1^3$$

Where a_1 represents water activity in the membrane and is expressed as follows:

$$a_1 = x_{H_2O}\left(\frac{P}{P_{sat}}\right)$$

And the concentration overvoltage is defined as

$$v_{conc} = i\left(\beta_1 \frac{i}{i_{max}}\right) \quad (3.73e)$$

The concentration of overvoltage constant depends on the inlet pressure and the saturation pressure and is calculated as follows [39]:

For $\frac{P_i}{0.1173} + P_{sat} < 2.0 \text{ atm}$, the value of β_1 becomes

$$\beta_1 = (7.16 \times 10^{-4} T - 0.622) \left(\frac{P_i}{0.1173} + P_{sat}\right) + (-1.45 \times 10^{-3} T + 1.68)$$

When $\frac{P_i}{0.1173} + P_{sat} > 2.0 \text{ atm}$, the value of β_1 becomes

$$\beta_1 = (8.66 \times 10^{-5} T - 0.068) \left(\frac{P_i}{0.1173} + P_{sat}\right) + (-1.6 \times 10^{-4} T + 0.54)$$

And

$$\beta_2 = 2.0$$

The heat output of the cell which is fed into the HTG is calculated based on exergy balance and is given by

$$\begin{aligned} \dot{Q}_{FC} = & \{T_0[\sum(\dot{n} \times s)_{out} - \sum(\dot{n} \times s)_{in}] + \dot{W}_{FC} + (\dot{n} \times ex)_{H_2out} + \\ & (\dot{n} \times ex)_{H_2O,out} - (\dot{n} \times ex)_{H_2in} - (\dot{n} \times ex)_{O_2in}\} \times \left(r_{HL} + \right. \\ & \left. (1 - r_{HL}) \frac{T_0}{T_{FC}}\right)^{-1} \end{aligned} \quad (3.74)$$

The molar flow rate of hydrogen, oxygen, and water at inlet and outlet are obtained by

$$\dot{n}_{H_2,reacted} = 2\dot{n}_{O_2,reacted} = \dot{n}_{H_2O,pro} = \frac{i}{2F} \quad (3.74a)$$

$$\dot{n}_{H_2,in} = \dot{n}_{H_2,reacted} + \dot{n}_{H_2,out} \quad (3.74b)$$

$$\dot{n}_{O_2,in} = \dot{n}_{O_2,reacted} + \dot{n}_{O_2,out} \quad (3.74c)$$

The irreversibility rate is found using the formula given below:

$$\dot{I}_{FC} = - \left(1 - \frac{T_0}{T_{FC}} \right) \times r_{HL} \times \dot{Q}_{FC} - \dot{W}_{FC} + \dot{E}x_{H_2,i} + \dot{E}x_{O_2,i} - \dot{E}x_{H_2,o} - \dot{E}x_{O_2,o} - \dot{E}x_{H_2O,o} \quad (3.75)$$

Where

$$\dot{E}_x = \dot{n} \times ex$$

$$ex = ex^{PH} + ex^{CH}$$

$$ex^{PH} = (h - h_0) - T_0 \times (s - s_0)$$

$$ex^{CH} = (h - h_0) - T_0 \times (s - s_0) - \frac{R \times T_0 \times \ln \left(\frac{P_i}{P_0} \right)}{MW}$$

Here, P_i represent pressure of the gas and P_0 represents ambient pressure.

For further details on the PEM fuel cell, see ref. [39].

3.3.2 QEACS Unit

- For Very High Temperature Generator

After getting the heat and power output from the PEM fuel cell, the equations for V.HTG were written in order to run the QEACS to achieve the cooling load and to provide hot water. The amount of energy given to V.HTG is shown below

$$\dot{Q}_{V,HTG} = \dot{W}_{FC} + \dot{Q}_{FC} - \dot{W}_{PUMP} \quad (3.76)$$

The mass balance equations are given as follows

$$\dot{m}_{36} x_{36} = \dot{m}_{37} x_{37} + \dot{m}_{38} x_{38} \quad (3.77)$$

$$\dot{m}_{36} = \dot{m}_{37} + \dot{m}_{38} \quad (3.78)$$

In order to obtain the outlet conditions of the V.HTG, the following equation is used

$$\dot{m}_{36} h_{36} + \dot{Q}_{V,HTG} = \dot{m}_{37} h_{37} + \dot{m}_{38} h_{38} \quad (3.79)$$

The exergy destruction in HTG is

$$\dot{E}x_{V,HTG} = \dot{E}x_{37} - \dot{E}x_{38} - \dot{E}x_{36} \quad (3.80)$$

Where,

$$\dot{E}x_{37} = \dot{m}_{37}((h_{37} - h_0) - T_0(s_{37} - s_0))$$

And same relationship is used for other states.

- For Very High Temperature Heat Exchanger

The energy balance equation for V.HHX is given below.

$$\dot{m}_{35} h_{35} + \dot{Q}_{V.HHX} = \dot{m}_{36} h_{36} \quad (3.81)$$

$$\dot{m}_{38} h_{38} = \dot{Q}_{V.HHX} + \dot{m}_{40} h_{40} \quad (3.82)$$

- For Condenser

The mass and energy balance equations for the condenser are given below

$$\dot{m}_9 = \dot{m}_7 + \dot{m}_8 \quad (3.83)$$

$$\dot{m}_9 h_9 = \dot{m}_7 h_7 + \dot{m}_8 h_8 + \dot{Q}_{con} \quad (3.84)$$

- For Evaporator

Below mentioned equations are for mass and energy balance of evaporator

$$\dot{m}_{10} = \dot{m}_{11} \quad (3.85)$$

$$\dot{m}_{10} h_{10} + \dot{Q}_{eva} = \dot{m}_{11} h_{11} \quad (3.86)$$

- For Absorber

The following energy balance equation is used to calculate the heat rejected from the absorber.

$$\dot{m}_{11} h_{11} + \dot{m}_{16} h_{16} = \dot{m}_1 h_1 + \dot{Q}_{abs} \quad (3.87)$$

- For Pump

The work done by the pump is calculated using the equation given below.

$$\dot{W}_p = \dot{m}_1(h_2 - h_1) \quad (3.88)$$

Energy and exergy efficiencies of the cell are calculated by

$$\eta_{FC,Energy} = 0.95 \frac{\dot{W}_{FC}}{i \times (1.25)} \quad (3.89a)$$

Where 1.25 V represents the electromotive force relative to the lower heating value of hydrogen and 0.95 is the fuel utilization coefficient. This coefficient represents the ratio of the mass of fuel reacted in cell to the mass of fuel input to the cell. Therefore, equation (32a) is derived for the lower heating value of hydrogen and can be found in literature [18].

$$\eta_{FC,Exergy} = \frac{W_{FC} + \left(1 - \frac{T_0}{T_{FC}}\right) \times \dot{Q}_{FC} + \dot{I}_{FC}}{\dot{m}_{H_2} Ex_{H_2}} \quad (3.89b)$$

The energetic and exergetic COPs are as

$$COP_{EN} = \frac{\dot{Q}_{eva}}{\dot{Q}_{V,HTG} + \dot{W}_P} \quad (3.90a)$$

$$COP_{Ex} = \frac{\dot{Ex}_{eva}}{\dot{Ex}_{V,HTG} + \dot{W}_P} \quad (3.90b)$$

Overall exergy destruction becomes

$$\dot{I}_{overall} = T_0 \times \left[\left(\frac{\dot{Q}_{con}}{T_{con}} \right) + \left(\frac{\dot{Q}_{abs}}{T_{abs}} \right) + \left(\frac{\dot{Q}_{eva}}{T_{eva}} \right) - (\dot{m}_{H_2} \times s_{H_2}) - (\dot{m}_{O_2} \times s_{O_2}) \right] \quad (3.91)$$

Overall energy and exergy efficiencies are defined as

$$\eta_{EN_{overall}} = \frac{\dot{Q}_{eva}}{\dot{m}_{H_2} \times h_{H_2}} \quad (3.92a)$$

$$\eta_{ovEx} = \frac{\dot{Ex}_{eva}}{\dot{m}_{H_2} \times Ex_{H_2}} \quad (3.92b)$$

Chapter 4 Results and Discussion

4.1 PEMFC Integrated with TEACS for Cooling and Power Production

In this section, results of first integrated systems studied are discussed in details. The effects of fuel cell parameters and TEACS parameters on the performance of the overall system are studied. We have carried out energy and exergy analyses of the PEM fuel cell integrated with triple-effect absorption cooling system to see the effect of temperature, pressure, membrane thickness, and current density of the fuel cell on the power output of the cell, efficiency of the cell and the COPs of the absorption cooling system. In this section homogenous mixture of ammonia-water is used to run TEACS. Exergy analysis is carried out as they take in consideration the irreversibility available in the system. This irreversibility is the major source of vast difference between theoretical and practical results when only energy analysis is carried out. Before carrying out the extensive parametric study of the PEM fuel cell integrated to TEACS, it is decided to conduct some validation to ensure that the model developed is correct and acceptable. The PEM fuel cell model is compared with the study done earlier by Mert et al. [17]. This comparison can be seen in Fig. 4.1. It is found that the efficiency behaves in the similar manner when current density is increased with little difference in the values. This confirms the accuracy of the present model and encourages proceeding with the analysis. All the assumptions which are studied in this section are listed in table 4.1.

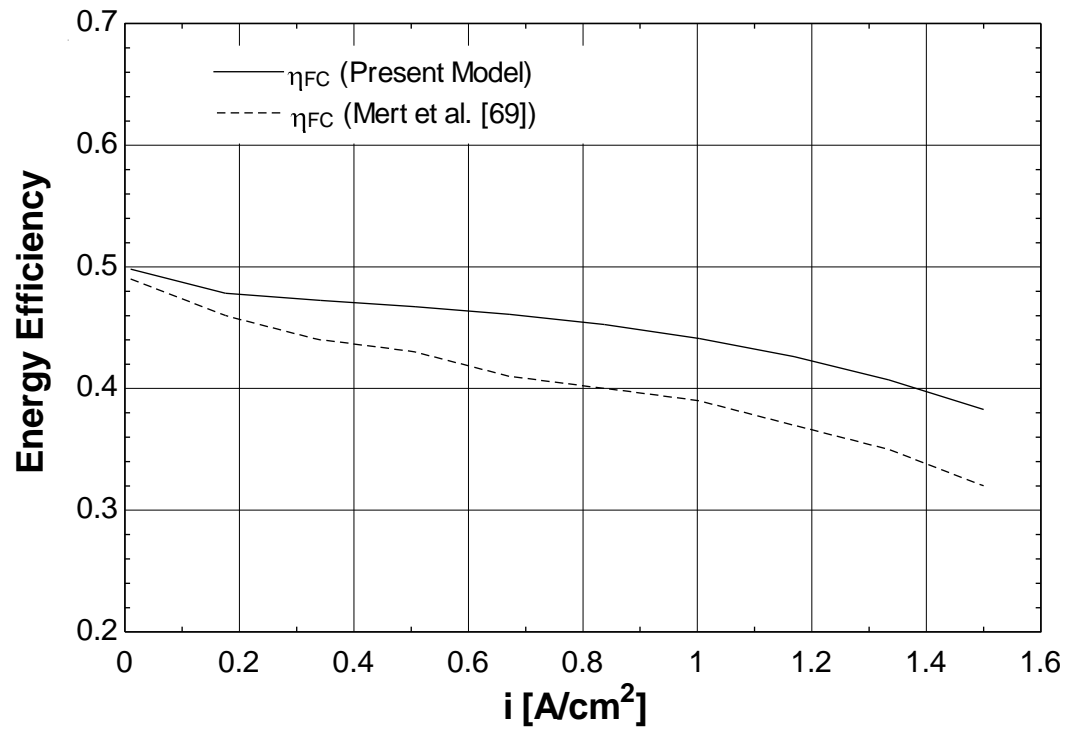


Fig. 4. 1 Validation of the model with Mert et al. [69]

Table 4. 1 PEM fuel cell constants

Parameters	Symbol and values
Anode stoichiometry	ξ_A (1.5) [11]
Cathode stoichiometry	ξ_C (3)
Anode transfer coefficient	α_A (0.5) [11]
Cathode transfer coefficient	α_C (1) [11]
Universal gas constant (J/mole K)	R (8.314)
Faraday's constant (Col/mole)	F (96,485)
Higher heating value of H ₂ (J/mole)	HHV_{H_2} (286,000)
Dead state pressure (atm)	P_0 (1.0)
Dead state temperature (K)	T_0 (298)
Heat loss ration	r_{HL} (0.2) [11]
Number of electrons involved	n (2.0) [11]
Anode dry gas mole fraction	x_A (0.0) [11]
Cathode dry gas mole fraction	x_C (3.76) [11]
Fuel Cell specific area	A (0.45)

When the temperature of the cell is varied from 300 K to 360 K, the power output and irreversibility rate of the cell is found to be decreasing from 5.9 kW to 4.9 kW and 5.87 kW to 4.7 kW, respectively. This behavior can be seen in Fig. 4.2. This behavior is noticed because as the temperature of the cell increases the heat transfer from the cell increases. As the temperature increases, the difference between the temperature of the cell and the surrounding temperature increases. As we know that the heat transfer of any system is calculated based on the temperature difference, rise in temperature increases the heat transfer from the fuel cell. This results in less power production and higher heat production. As the heat transfer rate increases and the power produced by the fuel cell decreases, the

overall irreversibility rate of the fuel cell decreases. This decrease in the power and irreversibility rate, results in the decrease in the energy and exergy efficiency of the cell, which vary from 49.6% to 41.2% and 37.8% to 33.8%, respectively. This decrease in the efficiency can be seen in Fig. 4.3.

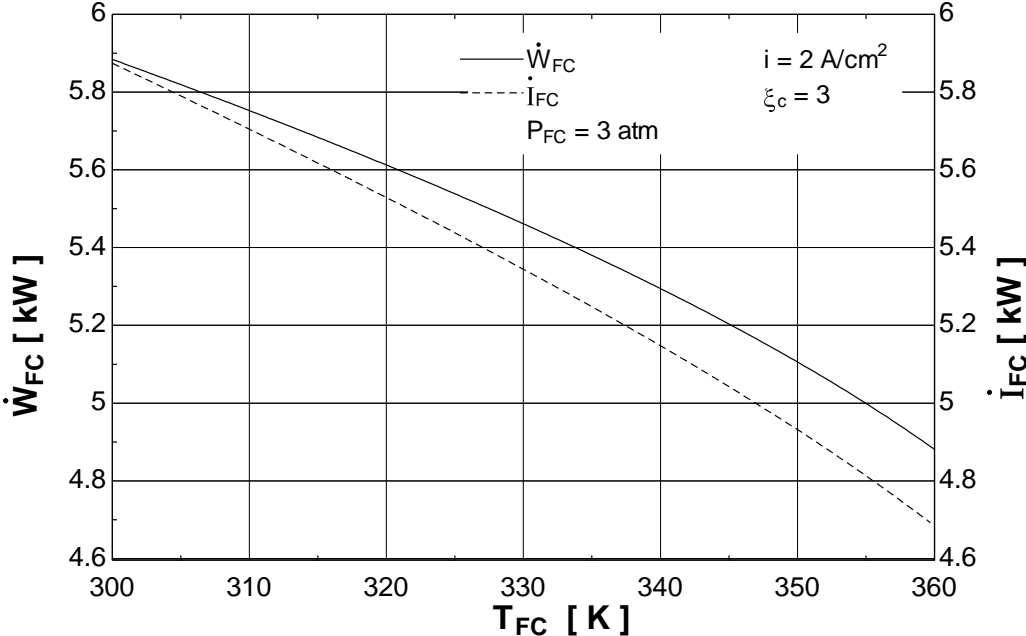


Fig. 4. 2 Effect of temperature of the fuel cell on the power and irreversibility rate of fuel cell

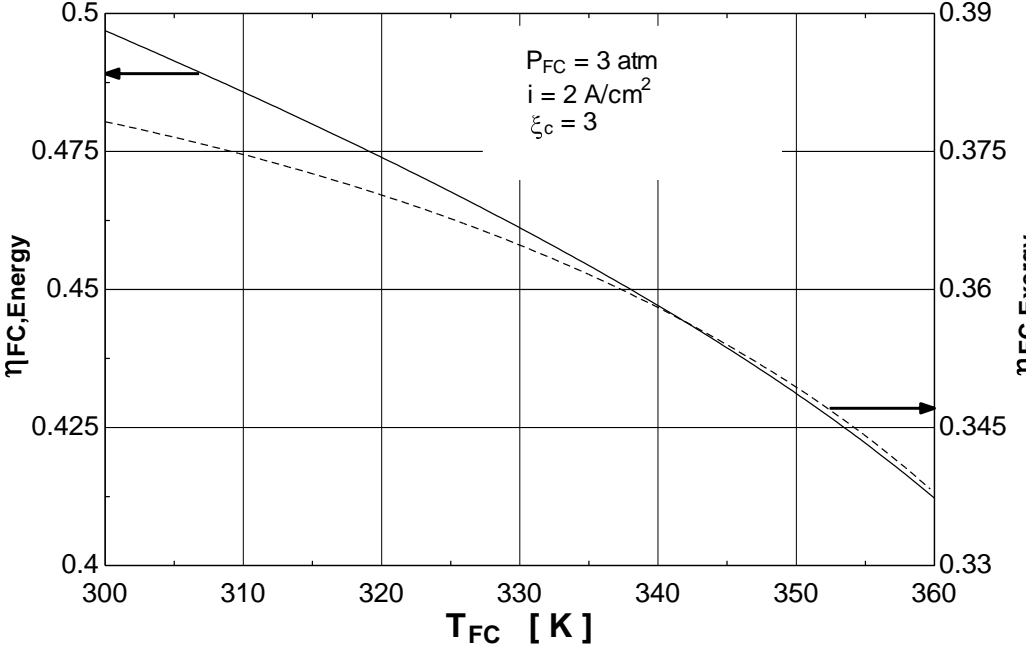


Fig. 4. 3 Effect of temperature of the fuel cell on the energy and exergy efficiencies of the fuel cell

Fig. 4.4 allows us to see the effect of increase in the temperature of the cell from 300 K to 360 K on the energetic and exergetic COPs of the absorption system. With the increase in the temperature of the cell, the energetic and exergetic COPs are found to be increasing from 2.12 to 2.37 and 0.91 to 1.04, respectively. When the temperature of the cell is increased, the power generated by the fuel cell decreases, which results in the less input to the absorption system in terms of energy to obtain the desired cooling load. Now, as the energy supplied to the absorption system to achieve the desired cooling load decreases, the COP of the system increases because lesser amount of energy is being consumed by the absorption system to provide the required amount of cooling.

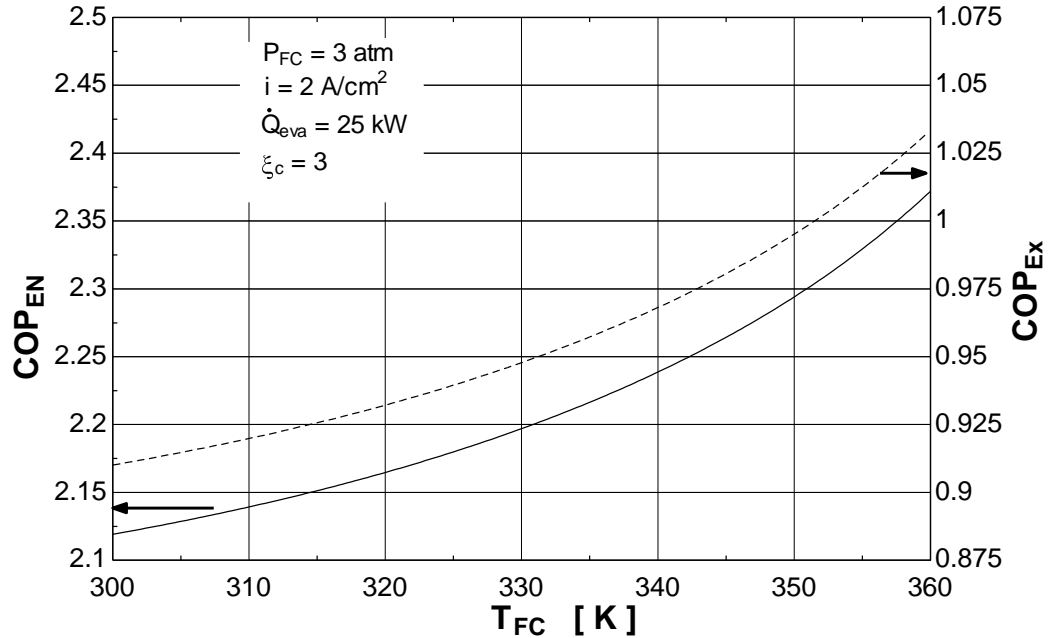


Fig. 4. 4 Effect of temperature of the fuel cell on the energetic and exergetic COP of the absorption system

The effect of increase in pressure of the cell from 300 kPa to 500 kPa on the power and irreversibility rate of the fuel cell is shown in Fig. 4.5. As the pressure increases, the power and the irreversibility rate are found to be increasing. They increase from 5.04 kW to 5.15 kW, and 4.8 kW to 5.0 kW, respectively for different membrane thicknesses. As the pressure increases, the energy and exergy value of the hydrogen increases because enthalpy and entropy are directly related to the pressure and temperature. Also, increase in pressure on the anode side while keeping pressure constant at cathode side increases the

pressure difference between two sides of membrane electrode assembly (MEA), which allows more suction of protons owing to the higher-pressure drop. As the power and irreversibility rate increase, the energy and exergy efficiency also increase. These efficiencies increase from 42.5% to 43.5%, and 34.6% to 35.2%, respectively, which can be seen in Fig. 4.6. This increase in efficiency is seen because at higher pressure the fuel cell produces higher power and therefore more amount of energy coming from the inlet hydrogen is being utilized. This results in the higher energy and exergy efficiency of the fuel cell. In addition, the thickness of the membrane barely affects the performance of the system as can be seen in Fig. 4.5 and Fig. 4.6. This behavior is observed because the power output of the PEMFC is very small and the stack consists of very few MEAs. However, in case of high energy production, huge numbers of MEAs are stacked together. The increase in MEAs results in increase in the overall thickness of the PEMFC and this is where effect of membrane becomes prominent. The purpose of studying membrane thickness is to show that membrane thickness plays a role in the output of the PEMFC.

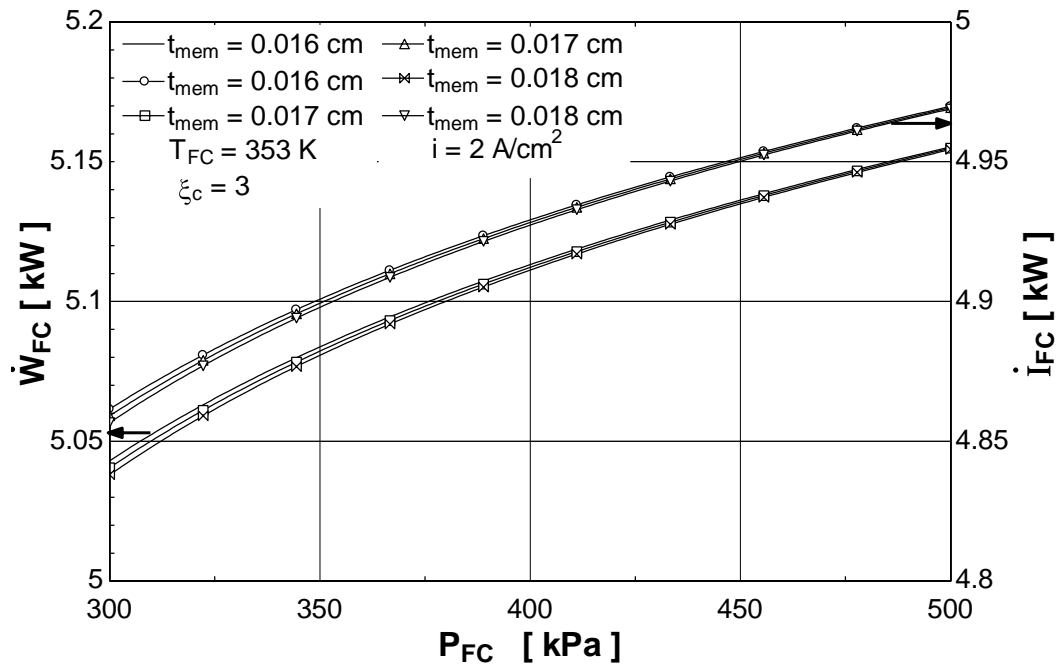


Fig. 4. 5 Effect of pressure of the fuel cell on the power and irreversibility rate of fuel cell

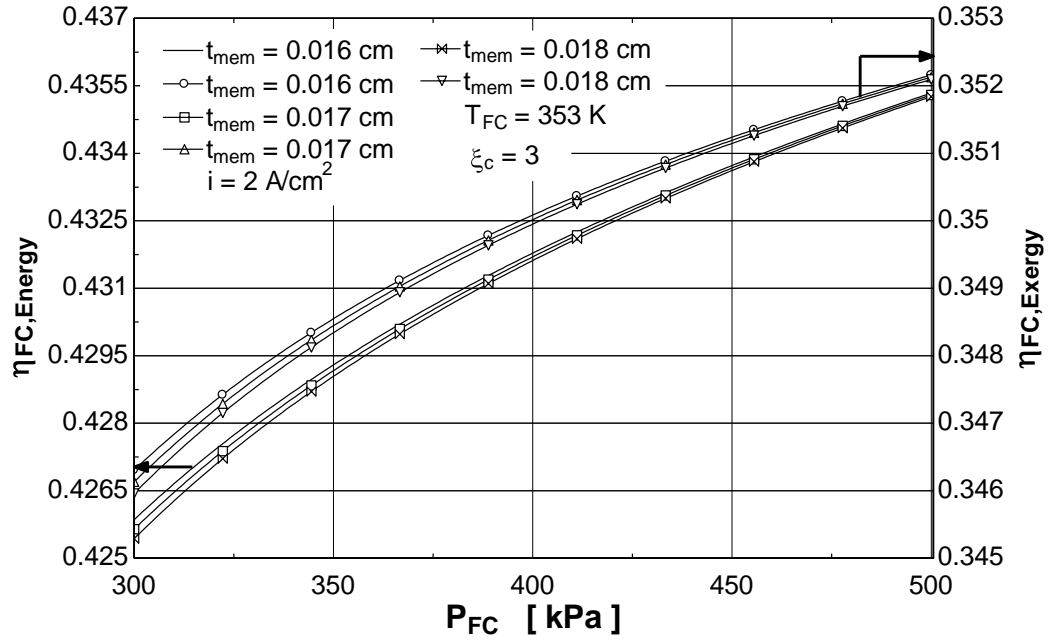


Fig. 4. 6 Effect of pressure of the fuel cell on the energy and exergy efficiencies of the fuel cell

Fig. 4.7 exhibits the variation of both energetic and exergetic COPs with increase in the pressure of the fuel cell. Both the COPs are found to be decreasing from 2.31 to 2.26 and 1 to 0.98, respectively when the pressure of the cell is increased from 300 kPa to 500 kPa for different membrane thicknesses. As the pressure increases, the power produced by the fuel cell increases as explained earlier. This power is then fed into the HTG of the absorption system. Now, as the power increases, there is more energy provided to the absorption system to achieve the desired cooling load than it requires. Therefore, increase in the power required to achieve the desired cooling load results in the degrading of the system and this degrading is noticed in terms of the decrease in the COPs of the system, which are the performance-measuring parameters for any refrigeration system.

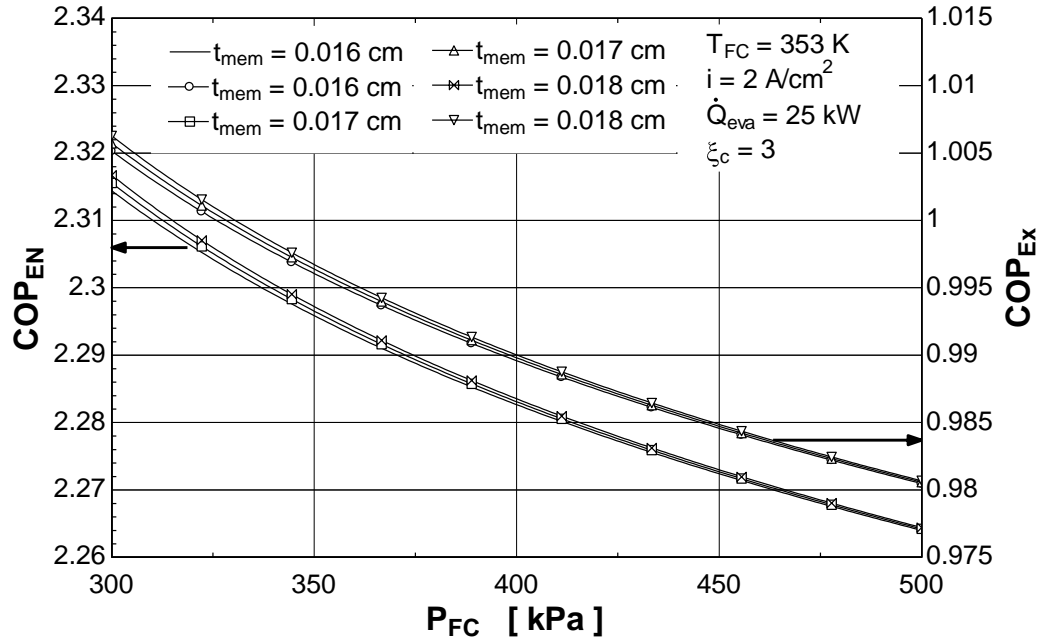


Fig. 4. 7 Effect of pressure of the fuel cell on the energetic and exergetic COP of the absorption system

Fig. 4.8 reveals the effect of increase in current density on the power and irreversibility rate of the fuel cell. As the current density increases from 1 A cm^{-2} to 2 A cm^{-2} , the power and the irreversibility rate increase from 4.1 kW to 5.2 kW , and 3.9 kW to 4.0 kW , respectively, for different pressures of the cell. This behaviour is observed because as the current density increases there is more and more current available per unit area to be extracted out from the fuel cell. This increase in the availability of energy to be extracted out increases the output of the fuel cell. This output of the cell also results in the decrease in the efficiency of the cell as the efficiency of the cell is inversely proportional to the current density and as the current density increases the efficiency of the cell decreases. The energy and exergy efficiency are found to be decreasing from 69.7% to 42.5% and 56.4% to 34.6% , respectively, with the increase in the current density of the system for different operating pressures of the fuel cell as shown in Fig. 4.9.

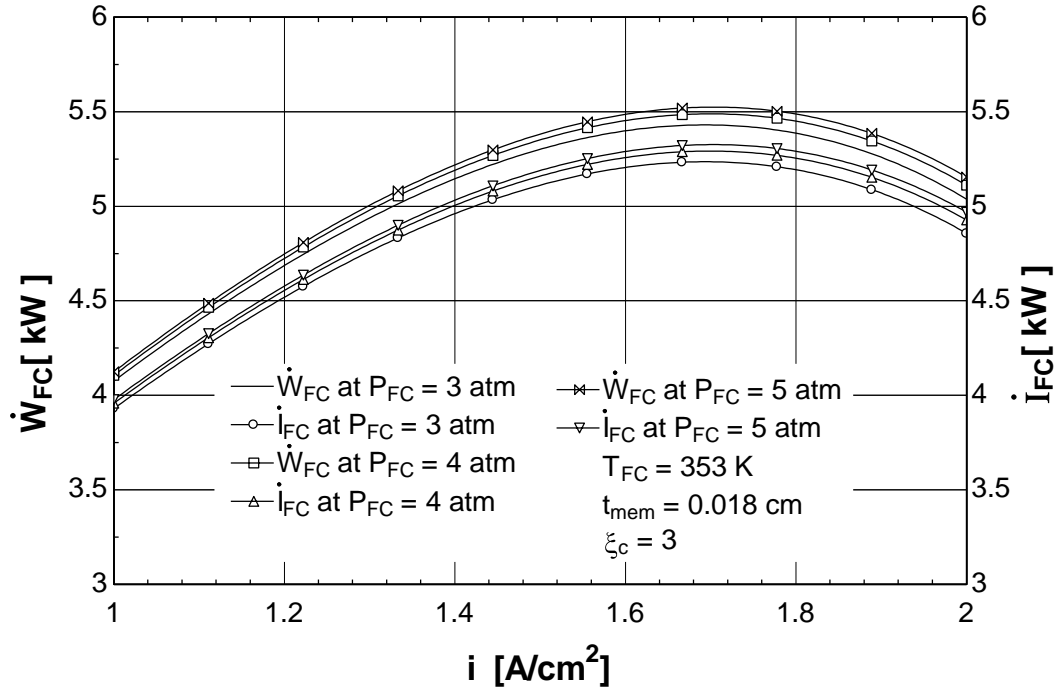


Fig. 4. 8 Effect of current density of the fuel cell on the power and irreversibility rate of fuel cell

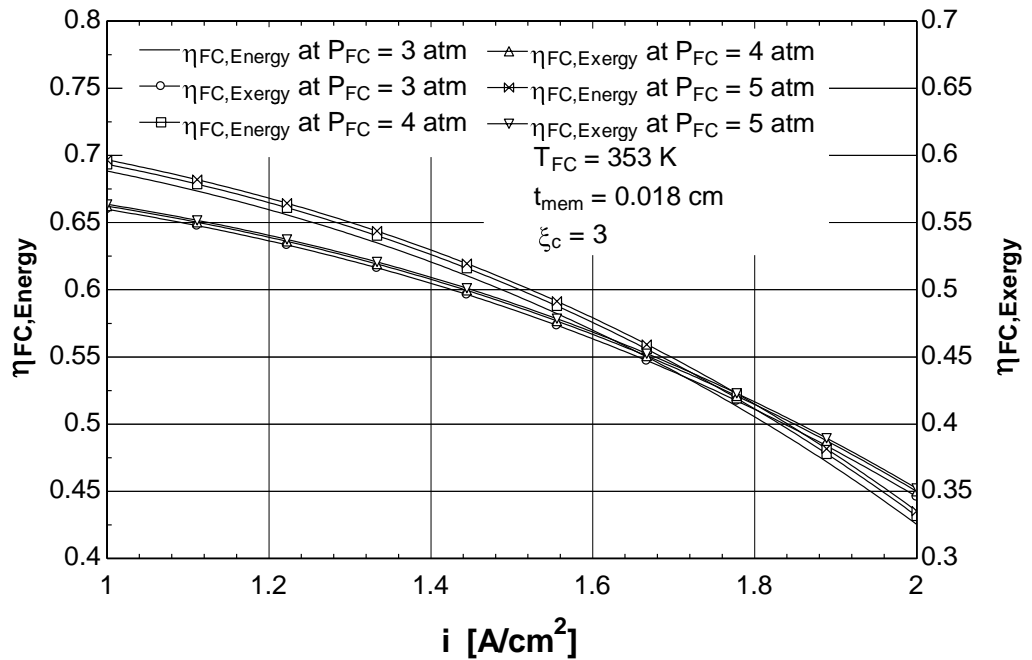


Fig. 4. 9 Effect of current density of the fuel cell on the energy and exergy efficiencies of the fuel cell

When the current density is increased, the energetic and exergetic COP of the system decrease, and it can be seen in Fig. 4.10. The energetic and exergetic COP are found to be decreasing from 2.86 to 2.26 and 1.3 to 0.98, respectively, for increase in current density from 1 A cm^{-2} to 2 A cm^{-2} for different operating

pressures of 3, 4 and 5 atm. The increase in current density increases the output of the fuel cell, which is being used as the energy source to run the absorption system. Hence, as there is more energy being provided to the absorption system to achieve the desired cooling load, the performance of the absorption system drops down because more heat is being dissipated through the condenser. As a result, the COP, which is the evaluation factor of the refrigeration system, decreases.

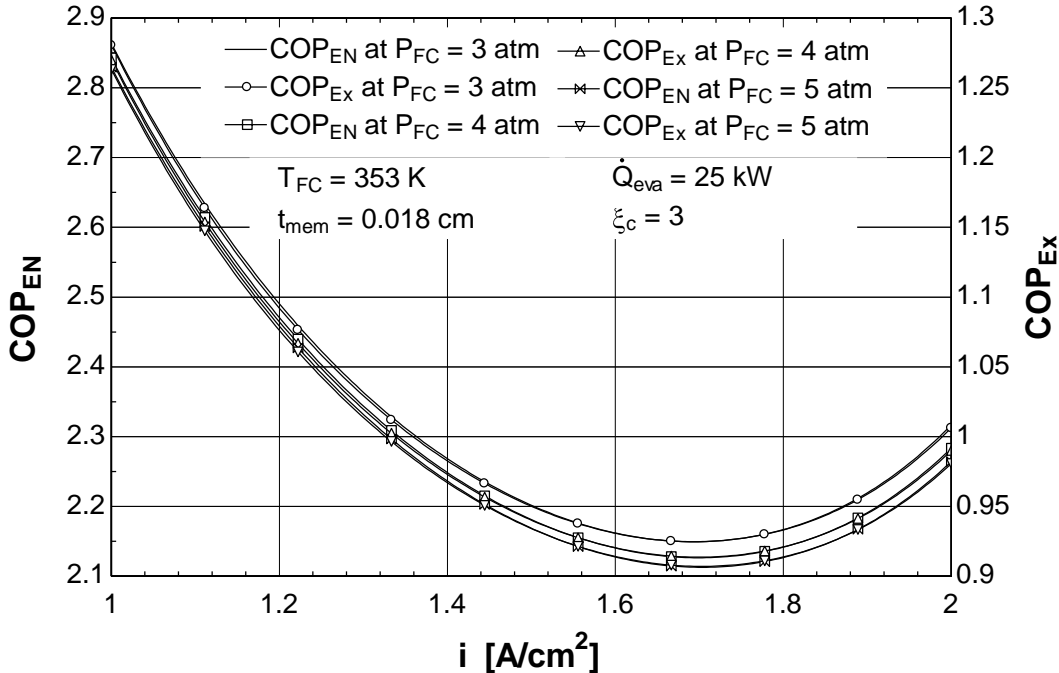


Fig. 4.10 Effect of current density of the fuel cell on the energetic and exergetic COP of the absorption system

Fig. 4.11 depicts the effect of current density of the fuel cell on the energetic and exergetic efficiencies of the integrated system. It can be seen from the figure that both efficiencies decrease as the current density increases. The overall energetic and exergetic efficiencies of the system decrease from 66.9% to 33.4%, and 25.9% to 12.9%, respectively, as the current density increases from 1 A cm⁻² to 2 A cm⁻². However, when fuel cell current density increases from 1 A cm⁻² to 2 A cm⁻²; the overall rate of exergy destruction of the integrated system decreases from 72.96 kW to 47.9 kW. This behavior is observed because increasing the current density means that we are having better output per unit area of the membrane and therefore the rate of exergy destruction decreases as seen in Fig. 4.12.

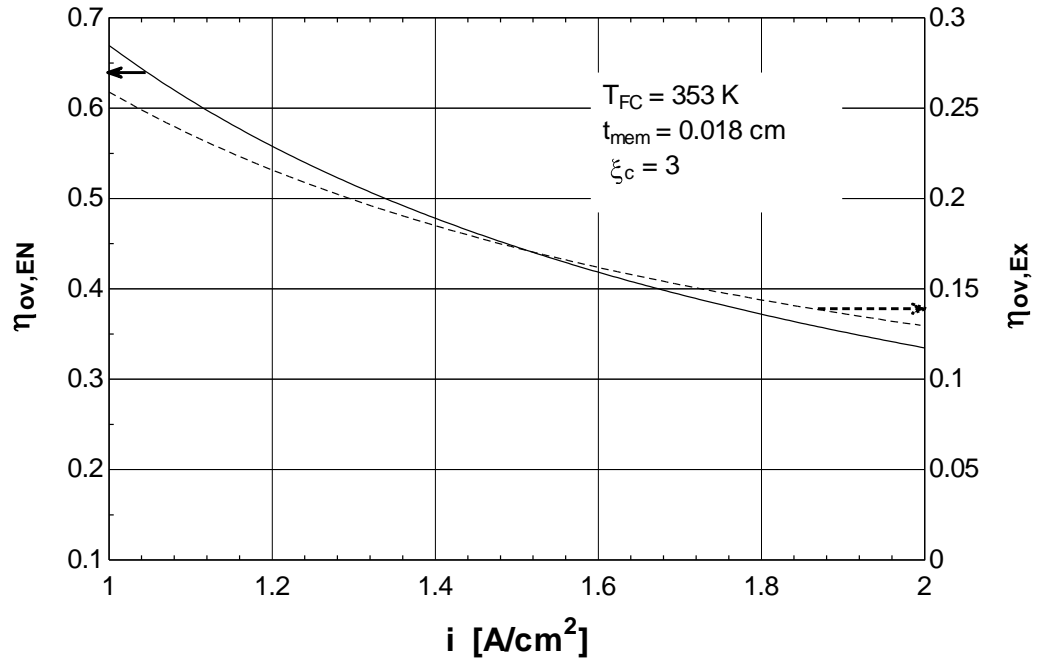


Fig. 4. 11 Effect of current density on the energetic and exergetic efficiencies of the integrated system

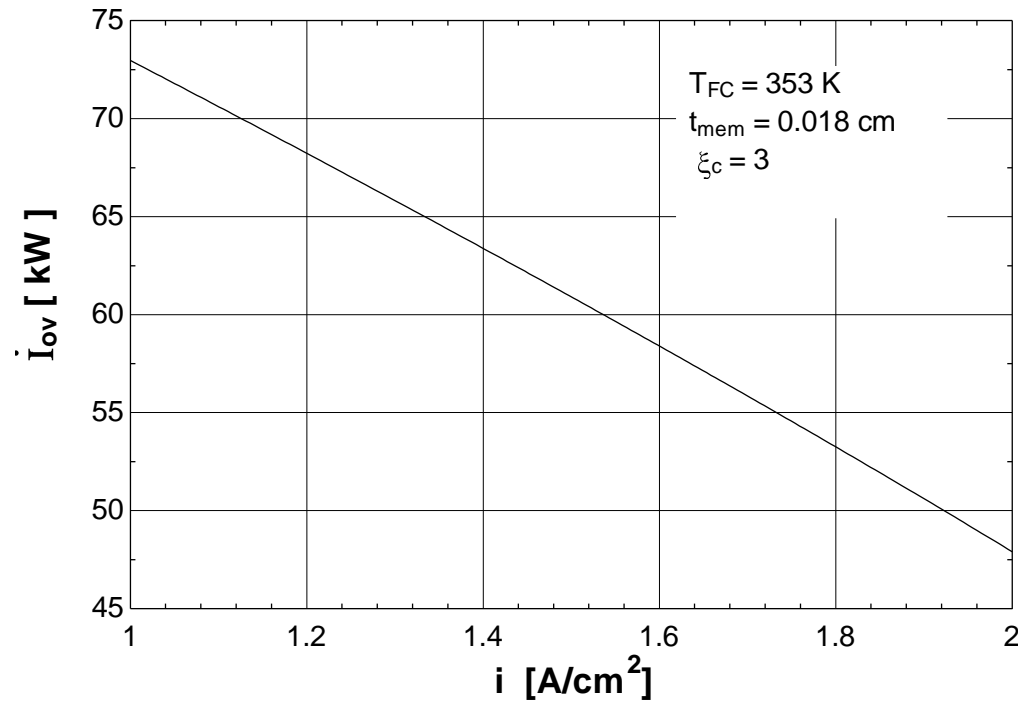


Fig. 4. 12 Effect of current density on the rate of exergy destruction of the integrated system

4.2 Solar PV/T Integrated with TEACS for Cooling and Hydrogen Production

As discussed earlier, it has become very crucial to come up with a system which is eco-friendly and efficient. In this section we study an integrated solar

PV/T cooling system for hydrogen production and cooling. Solar data for Abu Dhabi is considered in order to see the effect of solar radiation on the outputs of the integrated system. Several parameters of solar PV/T systems such as PV area and air inlet temperature are varied to see their effect on the operation of the system. The constants and variable of the Solar PV/T system are listed in table 4.2.

Table 4. 2 Solar PV/T constants

Parameters	Symbols and Values
PV module Area (m ²)	A (10)
Mass flow rate of air (kg/s)	\dot{m}_{air} (0.5)
Cooling load (kW)	\dot{Q}_{eva} (15)
Penalty factor	h_{p1} (0.88)
Packing factor	β_c (0.83)
Solar cell efficiency	η_c (0.12)
Transitivity of glass	τ_g (0.95)
Overall heat transfer coefficient (W m ⁻² K ⁻¹)	U_b (0.62)
Overall heat transfer coefficient (W m ⁻² K ⁻¹)	U_t (2.8)
Absorptivity of cell	α_c (0.90)

In order to run the mathematical model for the PV/T system, weather data for Abu Dhabi is required. The average amount of solar radiation and outside air temperature, which are available every month in Abu Dhabi and are used to analyze the integrated system under different operating conditions are shown in figs. 4.13 and 4.14. These average values are calculated based on the data available in ASHRAE directory for 2009. Moreover, it is seen that when solar radiation increases, the rate of power output of the PV/T increases but when the inlet air temperature is high the rate of heat output of the PV/T system decreases. The highest value of rate of heat output and rate of power output obtained are 14.8 kW and 0.58 kW, respectively for PV/T area of 10 m². This behavior is observed because as the solar radiation increases the power production capacity of solar PV

increases as there is more radiation per area available. Higher the amount of radiation available results in faster breaking of bonds inside the PV and therefore giving more power. However, with the increase in temperature of the air entering the duct of the PV/T, the rate of heat transfer capability of the PV/T system decreases and lesser amount of heat is transferred to the flowing liquid through the duct. This happens because the entering air is at a high temperature and is not capable of taking the amount of heat available. This behavior can be seen in Fig. 4.15.

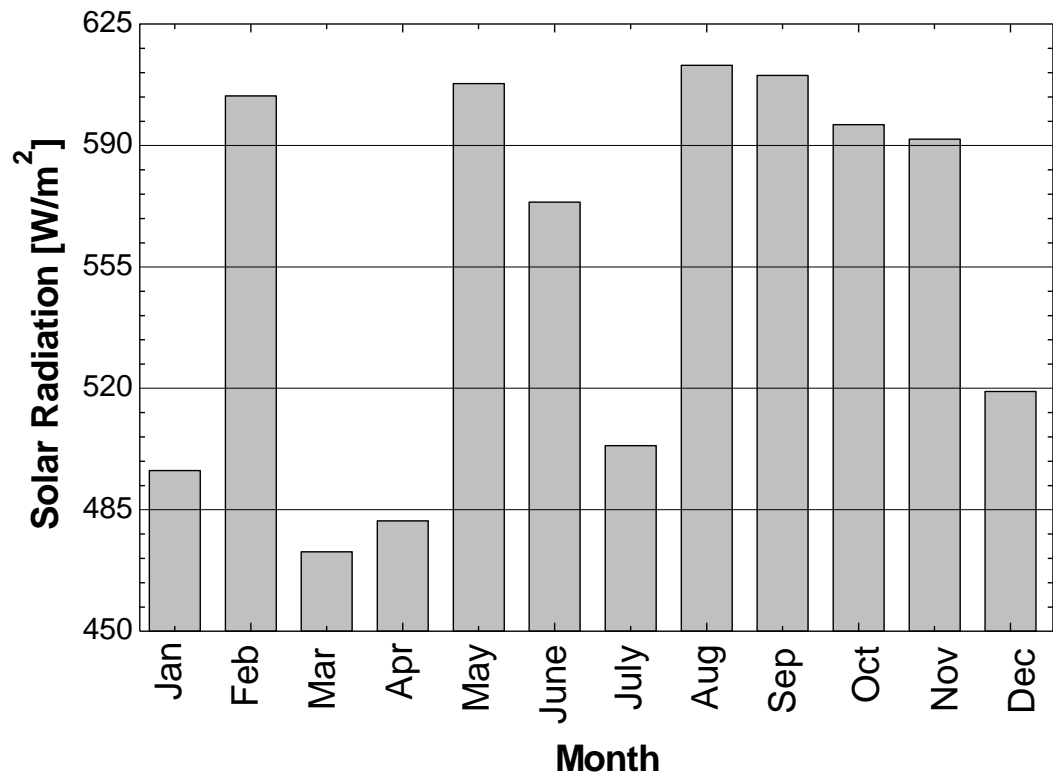


Fig. 4. 13 Monthly average solar radiation of 2009 in U.A.E

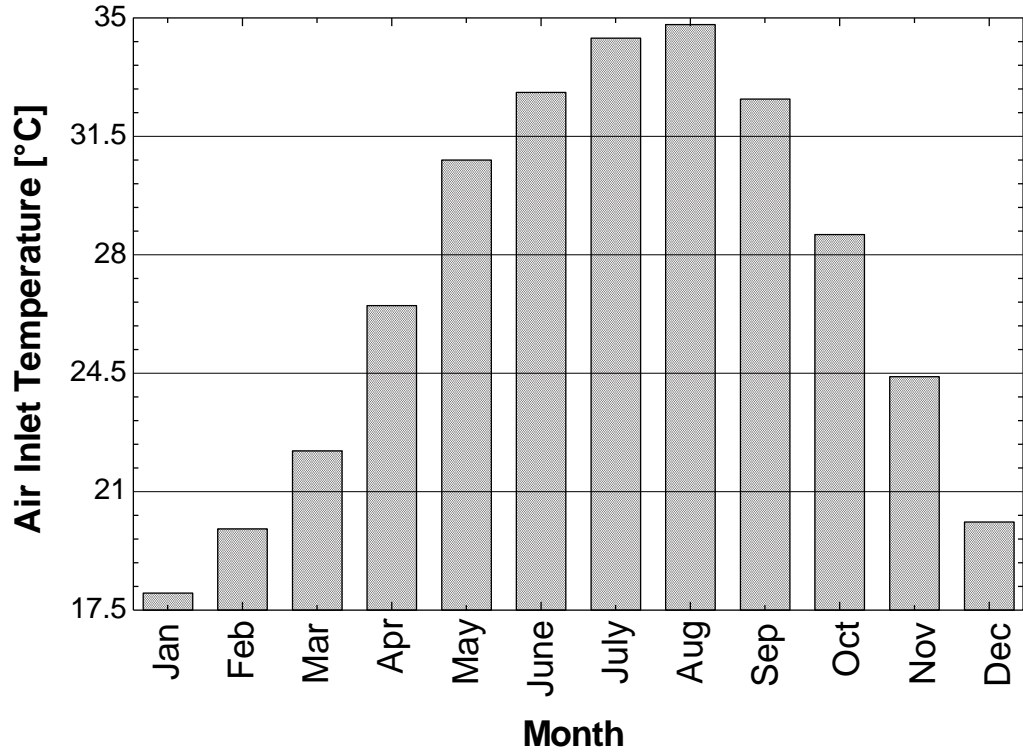


Fig. 4. 14 Monthly average air inlet temperature for 2009 in U.A.E

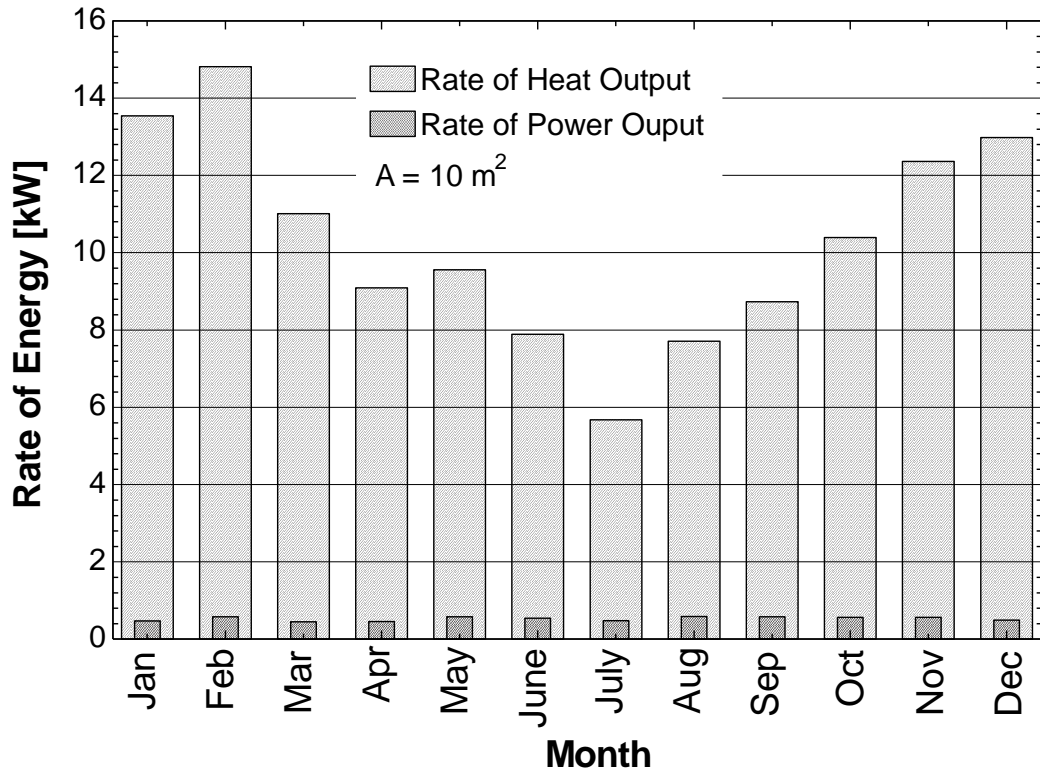


Fig. 4. 15 The rate of monthly energy production of PV/T system

The amount of solar radiation varies from month to month. Fig. 4.16 helps us to understand the effect of change in available solar radiation per unit area on the electrical and thermal efficiency of the system. It is observed that the thermal efficiency decrease and the electrical efficiency increase with the increase in solar radiation. The thermal and electrical efficiencies are found to be varying from 50.54% to 20.86% and 9.2% to 8.31%, respectively. The thermal efficiency is found to be increasing with the decrease in the solar radiation. As the solar radiation decreases the outside air temperature decreases and as a result the air inlet temperature to PV/T decreases. As the air at low temperature is capable of absorbing more amount of heat from the solar panels, higher rate of heat is transferred to the air, hence resulting in higher thermal efficiency. However, when the solar radiation increases the electrical efficiency increases because the vibration of the molecule in the PV module increases which results in higher rate of breaking of the bonds in the module. Hence, more amounts of electrons are available in order to extract power out of them. However, the energetic and exergetic COPs increase as the solar radiation and the outlet air temperature increases. This change in energetic and exergetic COPs vary from 0.95 to 2.28 and 0.90 to 2.14, respectively as seen in Fig. 4.17. This behavior is observed, because as the air inlet temperature increases the heat carrying capacity of the air decreases and the rate of heat transfer from PV module to air decreases. As the amount of heat generated which is later fed into the absorption system decreases the COPs of the system increases for the fixed cooling load. The increase in COPs represents the better performance of the system as the system now takes in less energy to achieve the desired amount of cooling.

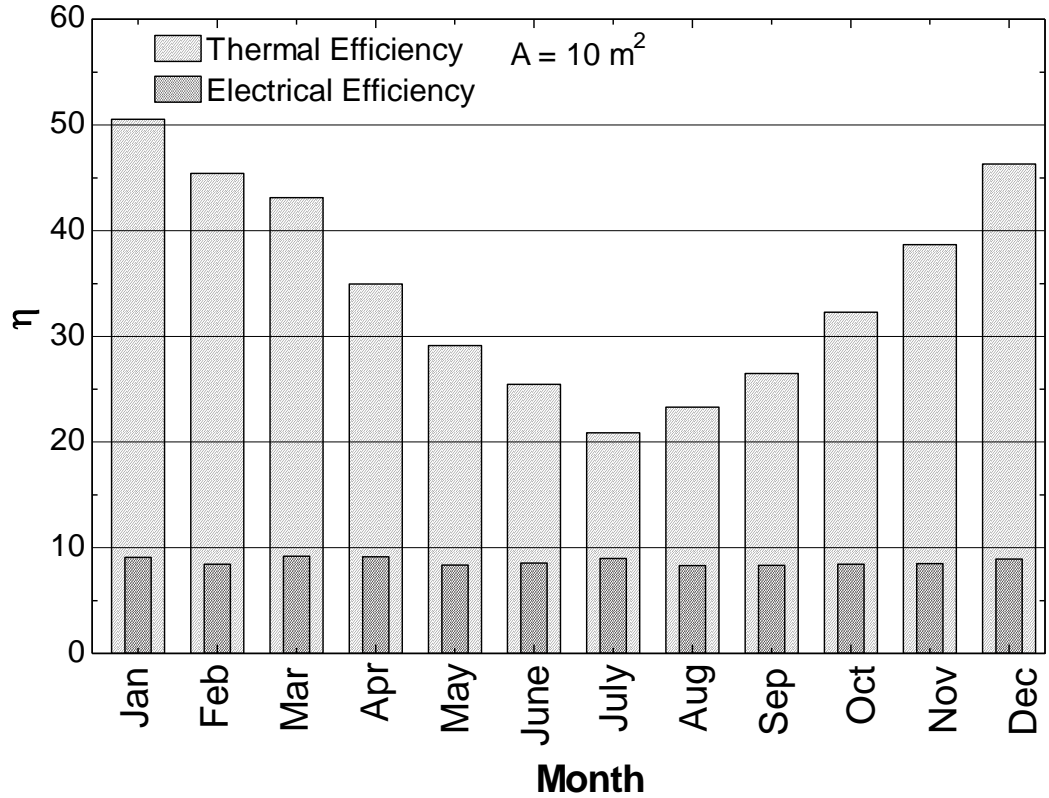


Fig. 4. 16 Monthly thermal and electrical efficiency of PV/T for every month

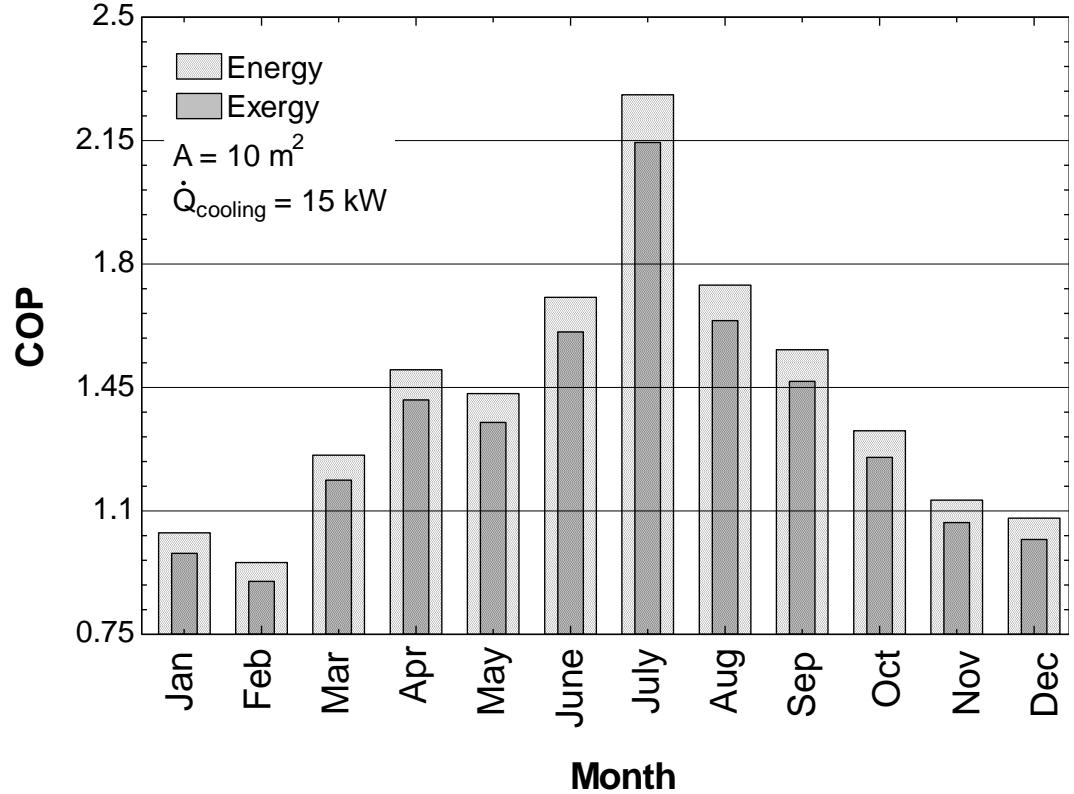


Fig. 4. 17 Monthly COP variation of absorption cooling system

The number of hours for which the solar radiation is available every month affects the hydrogen production in a big manner. The sole energy provider to this integrated system is PV/T. Hence, the amount of solar radiation and its availability over time depicts the performance of the system. The amount of hydrogen produced varies from 7.8 kg to 10.7 kg when the solar radiation and the operating hours are changed. This hydrogen production is calculated for the electrolyzer efficiency of 56%. The highest amount of hydrogen is produced in the month of June when solar radiation is high and the available solar radiation time span is high. As the solar radiation increases the power output of the PV increases which is then fed into the electrolyzer and the pump of the absorption system. As the input power increases there is more energy available for the breaking of hydrogen molecule and hence increasing the production of hydrogen. Moreover, increase in the available time of solar radiation results in power output from PV for the longer time. This increase in time also results in the higher running time of an electrolyzer. When the electrolyzer runs for more time, it processes more water and produces higher amount of hydrogen as it can be seen in Fig. 4.18. In addition, the overall energy and exergy efficiency vary from 15.7% to 14.34% and 7.9% to 7.2%, respectively for different months. This behavior of change in overall efficiencies for every month in Fig. 4.19 is seen because every month, there is a certain amount of solar radiation available at certain amount of time. Therefore, the power, the rate of heat production, and the amount of hydrogen and cooling production differ from month to month. In general, with the increase in the solar radiation, the power output of the PV increases, and with the decrease in the inlet air temperature, the rate of heat output of the system increases. It is hard to make conclusion about the trends of the overall efficiencies because they differ from month to month based on the solar radiation, air inlet temperature, and operating hours.

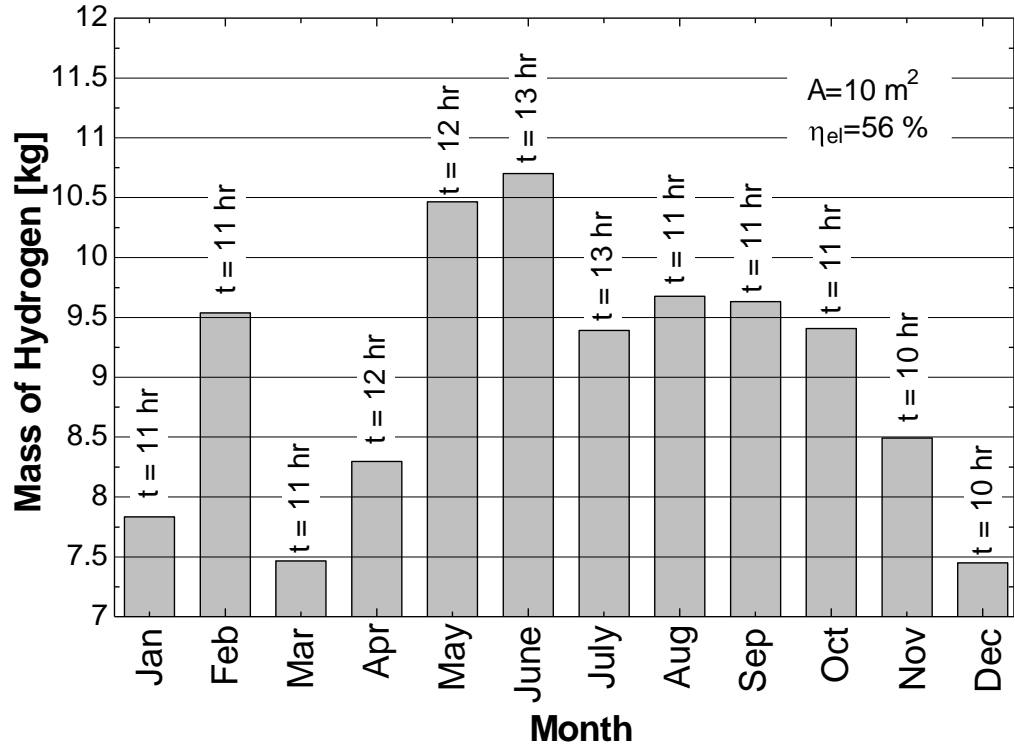


Fig. 4. 18 Amount of monthly hydrogen production

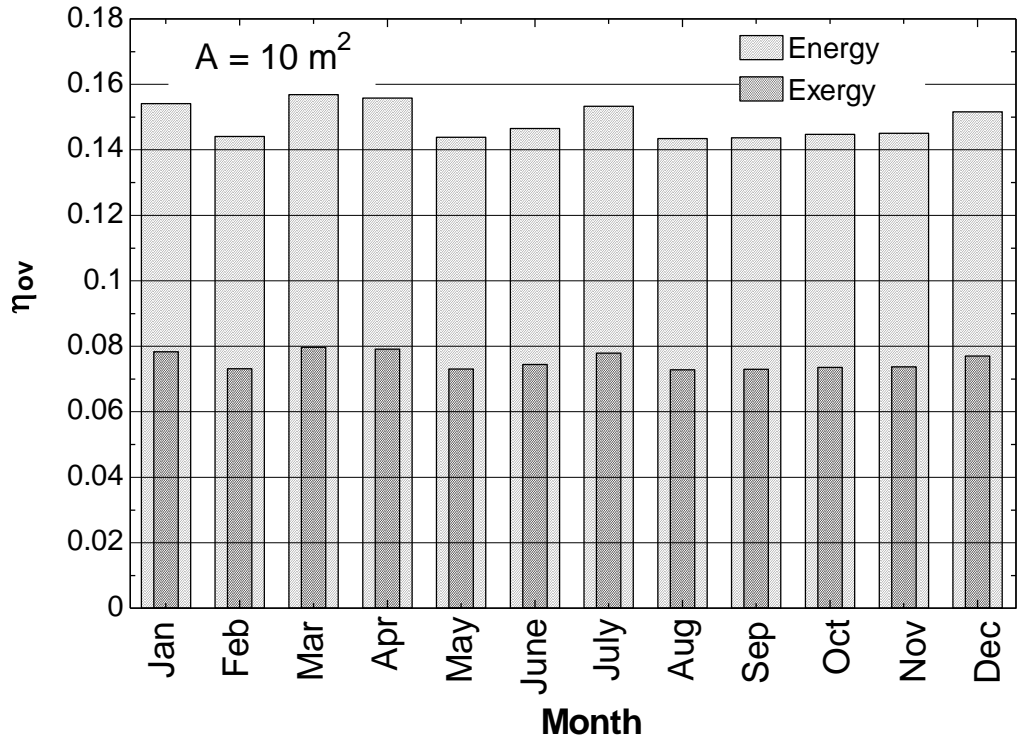


Fig. 4. 19 Overall monthly energy and exergy efficiencies

In Fig. 4.20, the study of effect of solar radiation on the overall energy and exergy efficiencies has been carried out. It is noticed that the overall energy and

exergy efficiencies decrease when the solar radiation is increased while keeping air inlet temperature, area of the PV and time for which solar radiation is available constant at 25 °C, 10 m², and 12 hr, respectively. The energy and exergy efficiencies drop from 15.9% to 14.4% and 8.1% to 7.3% respectively, as the solar radiation increases. As the solar radiation increases the power production capacity of PV module increases and at the same time heat transfer rate also increases. The increase in power means that more water molecules are broken down to give hydrogen. On the other hand, increase in rate of heat results in higher amount of heat given to the absorption system to provide the fixed amount of cooling. This increase in rate of energy fed into the cooling systems results in the degraded performance of the cooling system as cooling system rejects more heat through the condenser to achieve the desired cooling. Thus, the degrading performances of the cooling system results in lower energetic and exergetic COPs of the system. As the performance of the cooling system degrades the overall efficiency of the system decreases because, more energy is being consumed to acquire the required outputs.

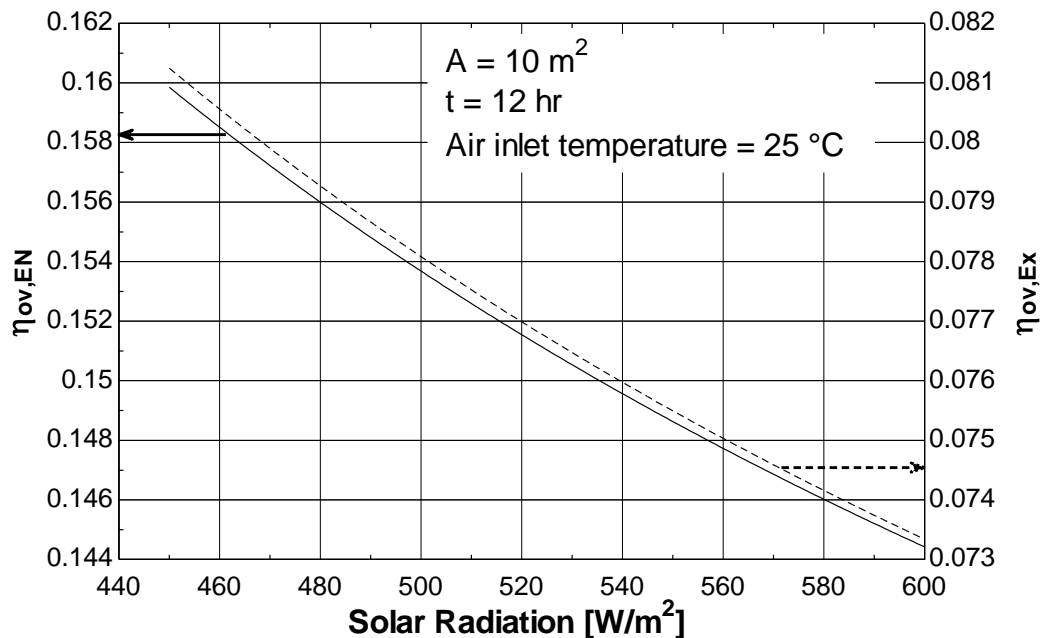


Fig. 4. 20 Overall energy and exergy efficiencies for different solar radiation intensities

The increase in area of the PV module results in the increase in power output of the PV module and hydrogen production. As the area of the PV module increases the amount of area capable of receiving solar radiation also increases, as

a result the power output of the PV system increases. The increase in power production implies that higher amount of hydrogen is produced given constant solar radiation, operating hours, and air inlet temperature. The solar radiation, operating hours, and air inlet temperature are kept constant at 608 W/m^2 , $30.8 \text{ }^\circ\text{C}$, and 12 hr, respectively. The power output and hydrogen production increase from 0.28 kW to 0.86 kW and 5.24 kg to 15.7 kg, respectively as shown in Fig. 4.21. The power output of the PV module is directly related to the solar radiation and the area on which it is concentrated. As the solar radiation increases, the molecules in the PV module vibrate at higher pace and as a result more and more bonds are broken into protons and electron. As the power produced by PV module increases, the hydrogen production increases because more power is being fed into the electrolyzer in order to break the bonds of water molecule at a higher rate to produce hydrogen. When the water molecules are broken into hydrogen and oxygen, higher amount of hydrogen are available which can be taken out and stored in a cylinder for later use as an energy provider by burning or using PEMFC.

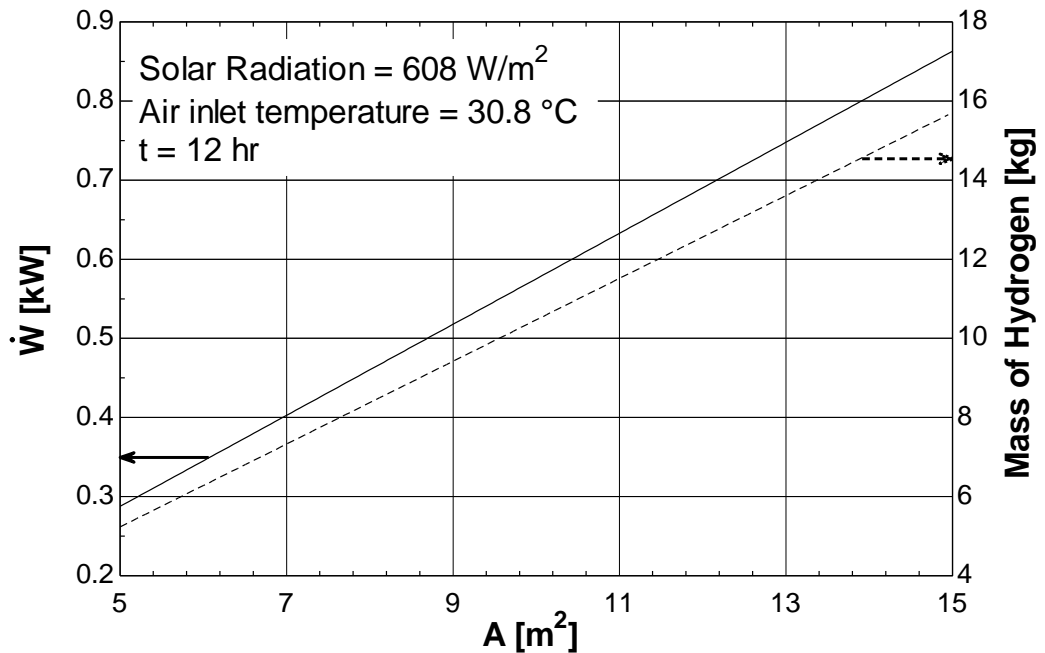


Fig. 4. 21 Power output of PV/T and mass of hydrogen production v/s area of the PV/T

Figs. 4.22 and 4.23 are used to show the relation of rate of heat production, thermal efficiency, and energetic and exergetic COPs with the

increase in air inlet temperature to the PV/T. As the inlet air temperature increases, the rate of heat output and thermal efficiency of the PV/T system decreases from 14.84 kW to 5.06 kW and 45.2% to 15.4%, respectively. This decrease in the rate of heat production and thermal efficiency is observed because, with the increase in the inlet air temperature, the capability of the air to absorb maximum amount of heat from the solar radiation decreases. Thus, the decrease in the absorption of heat results in lesser heat transfer rate from the PV/T and as a result the thermal efficiency of the system decreases. But this decrease in the rate of heat production of the PV/T helps boost the performance of the cooling system. As the air temperature increases, the rate of heat delivered to the cooling system decreases which results in higher energetic and exergetic COPs. The energetic and exergetic COPs are found to be increasing from 0.95 to 2.51 and 0.89 to 2.36, respectively. This increase is seen because, as the rate of heat input to the system decreases till a certain practical limit for achieving certain cooling load, the performance of the system increases and lesser amount of heat is being rejected through the condenser.

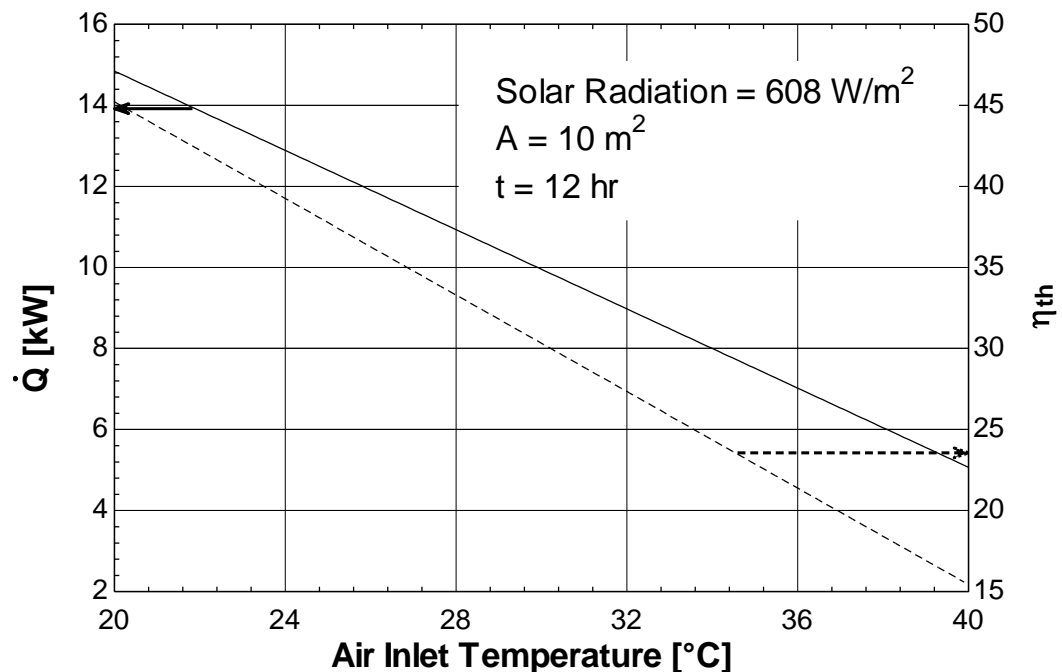


Fig. 4. 22 Rate of heat production and thermal efficiency of the PV/T v/s air inlet temperature

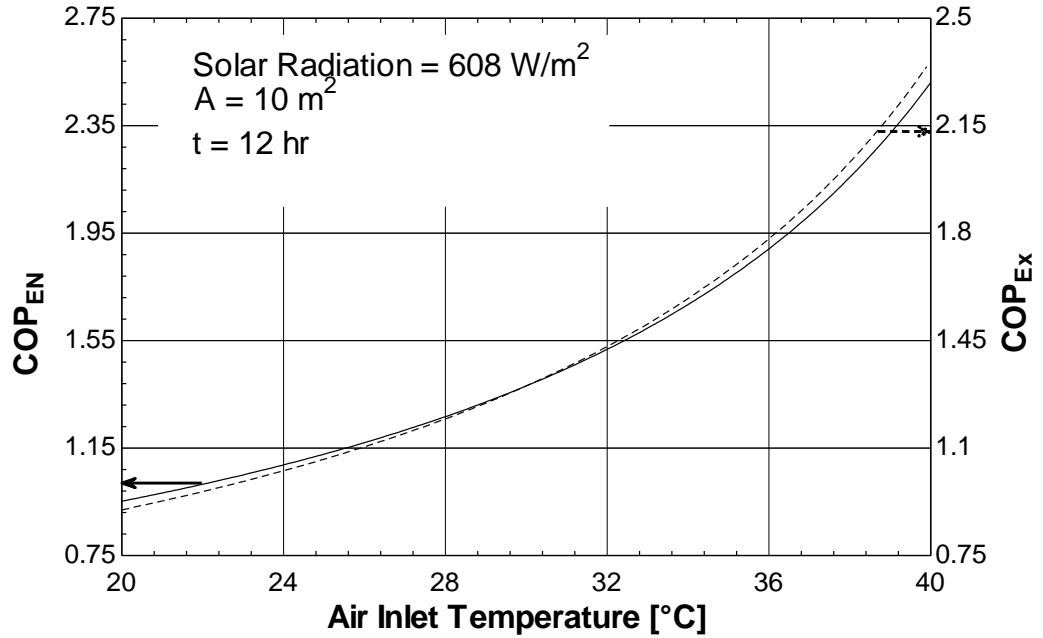


Fig. 4. 23 Energetic and Exergetic COPs of the absorption cooling system v/s air inlet temperature of PV/T

4.3 PEMFC Integrated with QEACS for Cooling Production

Third integrated system studied in this research combines PEMFC and QEACS for more efficient and effective cooling production. After conducting comprehensive parametric studies for different operating and surrounding conditions and plotting these parameters and linkages, different trends for various operating conditions are observed.

It is found that when the temperature of the PEMFC is increased, both energetic and exergetic COPs increase with it. Both the COPs are found to be varying from 1.53 to 2.66, and 0.6 to 1.1, respectively with increase in the T_{FC} from 325 K to 373 K. This parametric study is carried out for condenser loads of 210 kW, 230 kW, and 250 kW. This relationship is seen because increase in the temperature of the PEMFC results in lower energy output from PEMFC. The energy output of the PEMFC decreases because losses associated with the temperature increases with the increase in the T_{FC} . This decrease in energy input to the V.HTG of the absorption system results in the higher cooling load. The decrease in energy input reflects back in terms of lower temperature input to the evaporator for a fixed cooling load. For a fixed exit temperature of the evaporator of 260.25 K, decrease in the inlet temperature of the evaporator results in the

higher cooling load. As the cooling load increases the COPs increase as seen in Fig. 4.24. This increase in the cooling load with increase in the T_{FC} also results in higher overall energetic and exergetic efficiency of the system as seen in Fig. 4.25. Both overall energetic and exergetic efficiencies of the system are found to be varying from 0.17 to 0.23 and 0.06 to 0.01, respectively for increase in T_{FC} from 325 K to 373 K. However, increase in T_{FC} has a negative effect on the performance of the PEMFC. Both energetic and exergetic efficiencies of the PEMFC decrease with the increase in T_{FC} . These efficiencies are found to be decreasing from 0.47 to 0.35 and 0.37 to 0.29, respectively. This behavior can be seen in Fig. 4.26.

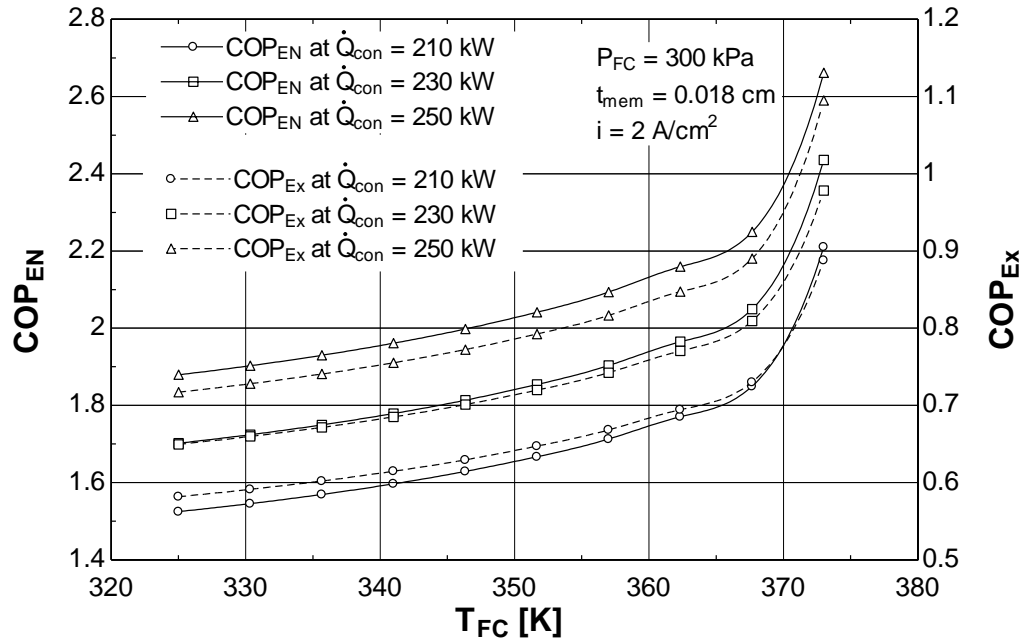


Fig. 4. 24 Variation of both energetic and exergetic COPs with T_{FC}

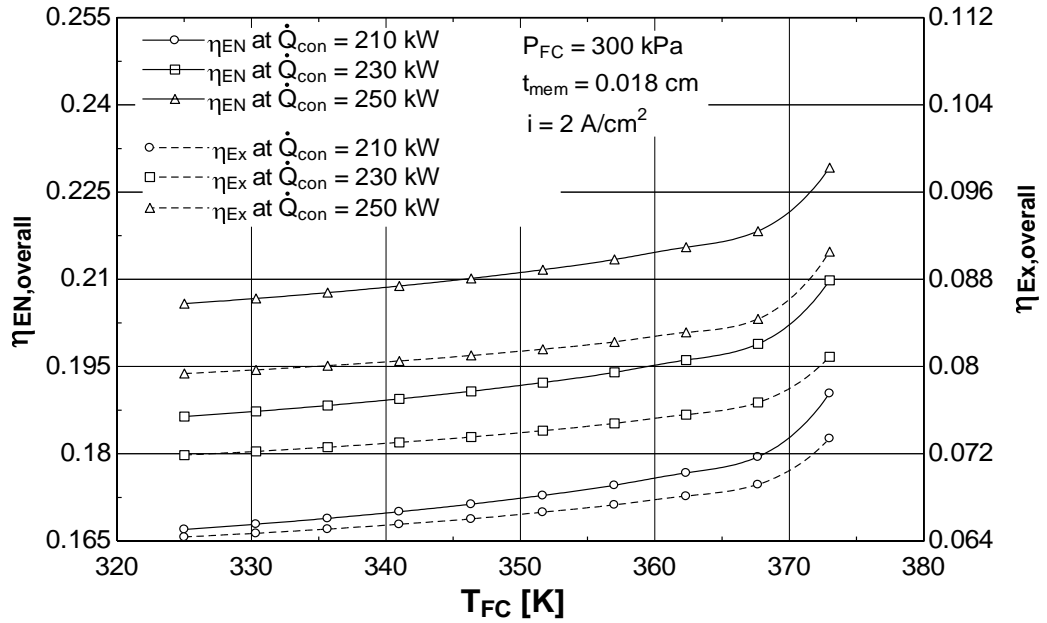


Fig. 4. 25 Variation of both overall energetic and exergetic efficiencies with T_{FC}

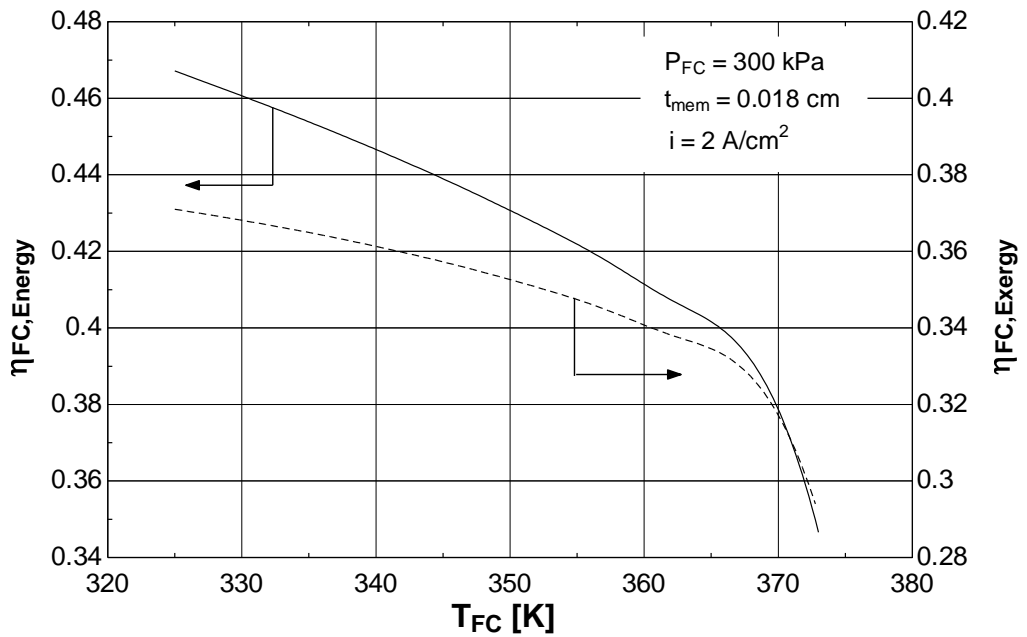


Fig. 4. 26 Variation of both energetic and exergetic efficiencies of PEMFC with T_{FC}

Increase in pressure of the fuel cell has a negative effect on energetic and exergetic COPs of QEACS. Both COPs decrease from 2.2 to 1.6 and 0.9 to 0.6, respectively with increase in P_{FC} from 200 kPa to 500 kPa as shown in Fig. 4.27. This parametric study is conducted for three condenser loads of 210 kW, 230 kW, and 250 kW. Increase in P_{FC} results in higher pressure difference between anode and cathode side of the fuel cell. Higher pressure difference results in higher flow

rate of hydrogen across the membrane. Thus, increase in pressure difference results in higher energy output from the fuel cell. As the energy input to the QEACS increases the performance of the absorption system degrades. Higher energy input for a fixed condenser load results in higher temperature of the stream coming out of the condenser. As temperature of the stream entering the evaporator increases, the cooling capacity of the evaporator decreases for the fixed evaporator temperature. This decrease in the cooling capacity of QEACS for increase in the P_{FC} results in lower COPs. Moreover, the performance of the integrated system also degrades with increase in the P_{FC} . As the purpose of this integrated system is to obtain cooling load, increase in P_{FC} affects this purpose in negative way as seen in Fig. 4.28. Both overall energetic and exergetic efficiencies are found to be decreasing from 0.22 to 0.17 and 0.08 to 0.06, respectively. However, increase in the P_{FC} has a positive effect on the performance of the fuel cell as seen in Fig. 4.29. Increase in P_{FC} results in higher energy output from the fuel cell. This increase in energy output results in higher energetic and exergetic efficiency of the fuel cell. Both the efficiencies increase from 0.40 to 0.44 and 0.34 to 0.36, respectively with increase in P_{FC} .

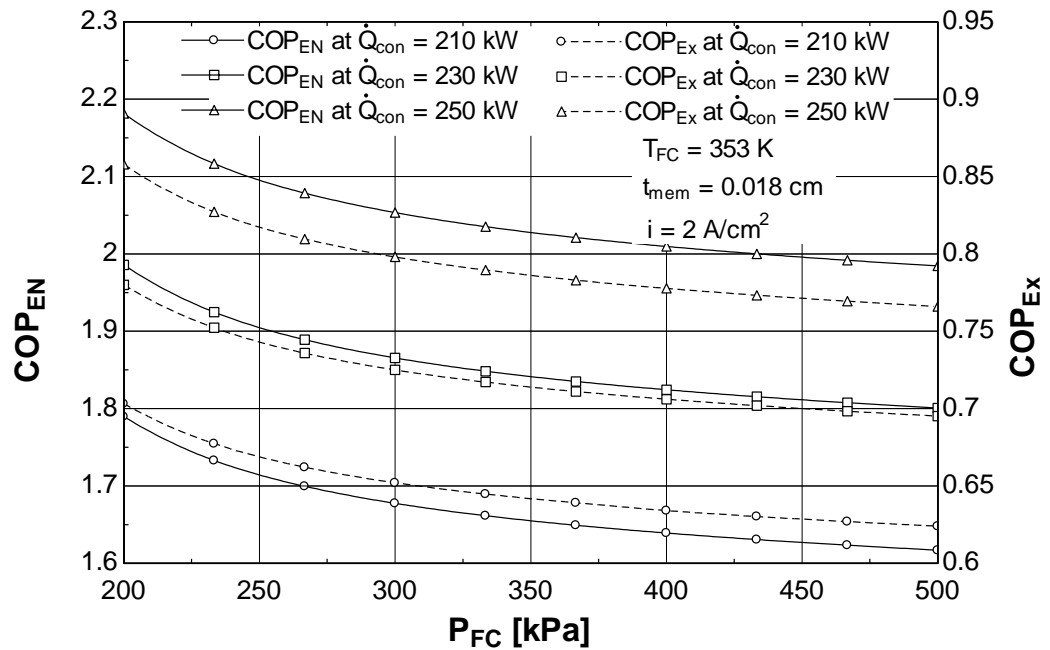


Fig. 4. 27 Variation of both energetic and exergetic COPs with P_{FC}

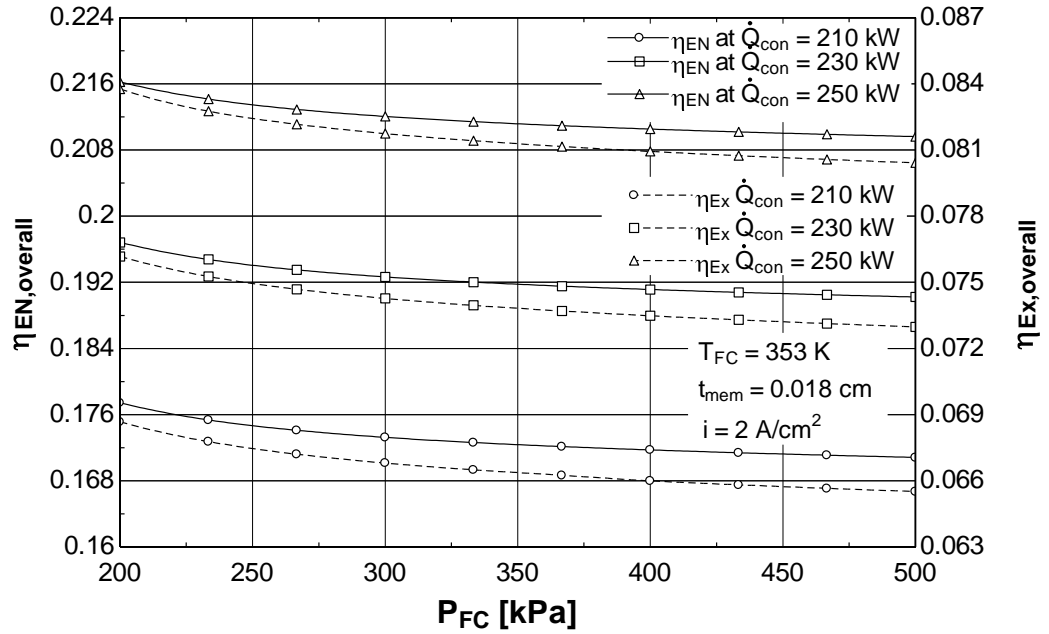


Fig. 4. 28 Variation of both overall energetic and exergetic efficiencies with P_{FC}

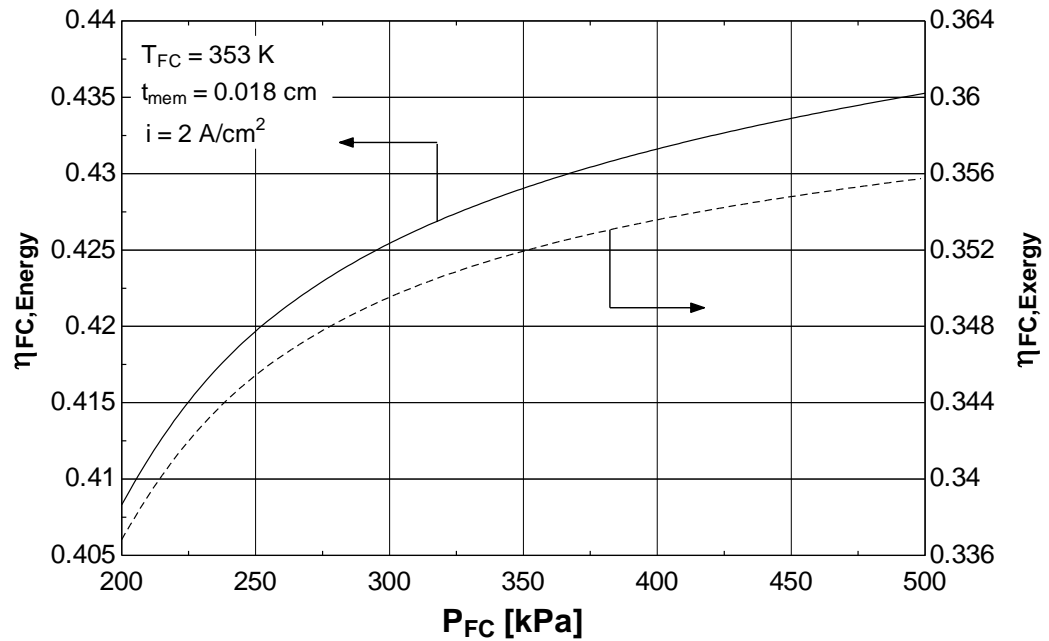


Fig. 4. 29 Variation of both energetic and exergetic efficiencies of PEMFC with P_{FC}

Increase in area of the fuel cell has a positive effect on the energy output of the fuel cell as shown in Fig. 4.30. The power and rate of heat output of the PEMFC are found to increasing from 36 kW to 56 kW and 46 kW to 65 kW, respectively with increase in area from 3.4 to 5 m². This relationship is seen because as the area of the membrane increases the energy production capacity of the fuel cell increases. Increase in membrane area means hydrogen has bigger

area to go through, therefore increasing the energy output. However, increase in an area has a negative effect on the cooling capacity of the QEACS as shown in Fig. 4.30. Increase in energy input to the QEACS for a specific condenser load means higher exit temperature for the stream coming from the condenser. This rise in temperature going into the evaporator for a fixed exit temperature of the evaporator, results in lower cooling capacity of the absorption system due to lower temperature difference across the evaporator. The cooling load decreases from 222 kW to 167 kW with increase in area. This parametric study is carried out for different condenser load of 210 kW, 230 kW, and 250 kW.

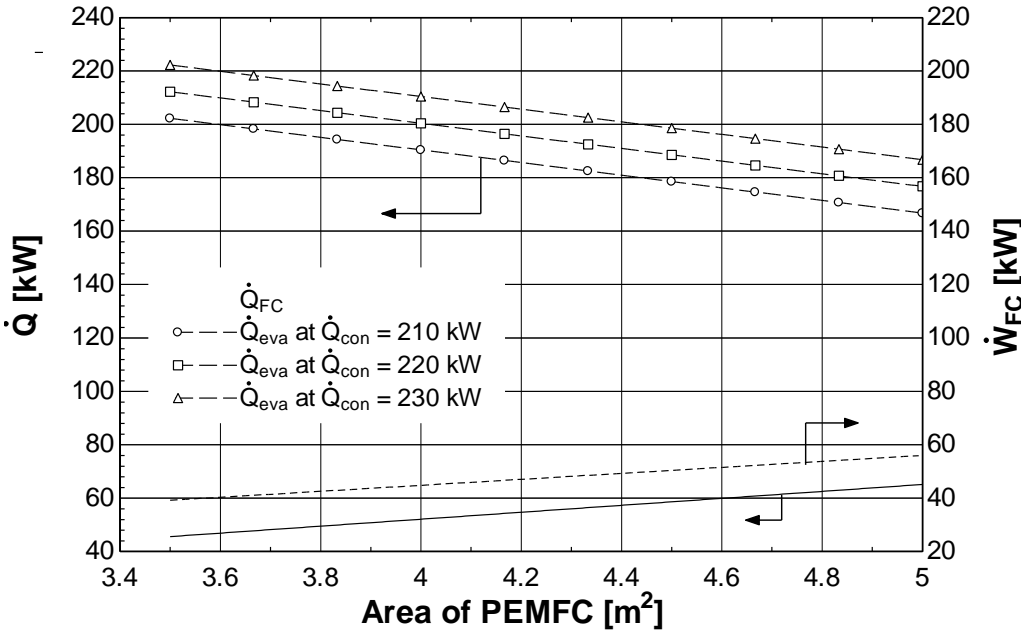


Fig. 4. 30 Variation of power of the fuel cell, rate of heat output of the fuel cell, and cooling load of the QEACS with area of the PEMFC

Chapter 5 Conclusions and Recommendations

The thermodynamic modeling based on energy and exergy analyses of the integrated systems has been carried out in this research. In addition, parametric study is conducted to examine the effect of different operating parameters on the performance of the individual and integrated systems.

5.1 Conclusions

The following conclusions can be drawn from this work:

- The energy and exergy efficiency of the PEMFC is found to be decreasing when temperature, and the current density is increased.
- With the increase in pressure of the PEMFC, the energy and exergy efficiency are found to be increasing
- The increase in temperature of the PEMFC has a positive effect on both energetic and exergetic COP of the system and they are found to be increasing.
- However, when the pressure, and the current density of the PEMFC, are increased the energetic and exergetic COP of the absorption are observed to be decreasing.
- Moreover, increasing current density of the PEMFC resulted in a decrease of overall energy and exergy efficiencies.
- Area of the PEMFC has positive effect on the power and rate of heat output of the PEMFC.
- Cooling capacity of the absorption system is found to be decreasing for increase in area of the PEMFC.
- The rate of heat output decreases with the increase in the air inlet temperature and the rate of power output increases with the increase in the solar radiation.
- The electrical efficiency is found to be highest for the months when solar radiation is high and thermal efficiency is found to be highest for the months where air inlet temperature is low.
- The energetic and exergetic COPs are found to be at most for the month when solar radiation is high and the air inlet temperature is high.
- The maximum amount of hydrogen is produced in the month when high solar radiation is available and that also for the longer time.

- The overall energy and exergy efficiencies decrease with the increase in the solar radiation for the specific air inlet temperature and running time.
- The power output and the electrical efficiency increases with the increase in area of the PV module because, now PV module can harness more amount of radiation.
- Air inlet temperature has an effect on the performance of the PV/T system in a negative way, as the rate of heat output and thermal efficiency of the PV/T decreases with the increase in air inlet temperature. On the contrary, increase in air inlet temperature has positive effect on the performance of the absorption cooling system as it increases the COP.

5.2 Recommendations

Despite getting attractive results by carrying out thermodynamic analysis, it is important to conduct experiments. Experimental results are very important to testify the claim that the system studied is effective and environmental friendly. Moreover, the hydrogen which is obtained through electrolyzer and stored in the cylinder in Solar PV/T integrated with TEACS system can later be used to provide energy to the absorption system by burning it into the HTG to provide higher cooling load. It can also be used as a fuel for power production through PEMFC. In addition, a comprehensive cost analysis is required to assess the feasibility of the systems from economics point of view. Finally, the results obtained in this paper are expected to help researchers, governments, and people in the industry with designing of a sustainable power and cooling production system for buildings.

REFERENCES

- [1] I. Dincer, "Technical, environmental and exergetic aspects of hydrogen energy systems". *International Journal of Hydrogen Energy*, vol. 27, pp.265–285, 2002.
- [2] Wikipedia contributors, "Fuel Cell," in *Wikipedia, the free encyclopedia* (n. d.) [Online]. Available: http://en.wikipedia.org/wiki/Fuel_cell#History [Accessed: December 5, 2010].
- [3] C. Matthew. Refrigeration cycles (n. d.) [Online]. <http://web.me.unr.edu> [Accessed: December 5, 2010].
- [4] *Fuel Cell Basics* (n. d.) [Online]. Available: http://www.fctec.com/fctec_types_sofc.asp (Accessed: December 5, 2010).
- [5] *Fossil Energy* (n. d.) [Online]. Available: http://fossil.energy.gov/programs/powersystems/fuelcells/fuelcells_solidoxide.html (Accessed: December 5, 2010).
- [6] *DIT Energy Inc.* (n. d.) [Online]. Available: <http://www.dtienergy.com/energiedtisa.html> (Accessed: December 5, 2010).
- [7] *Fuel Cell Basics* (n. d.) [Online]. Available: http://www.fctec.com/fctec_types_dmfc.asp (Accessed: December 5, 2010).
- [8] *Fuel Cell Basics* (n. d.) [Online]. Available: http://www.fctec.com/fctec_types_afc.asp (Accessed: December 5, 2010).
- [9] *Tekion* (n. d.) [Online]. Available: <http://www.tekion.com/business/index.htm> (Accessed: December 5, 2010).
- [10] Wikipedia contributors, "Fuel Cell," in *Wikipedia, the free encyclopedia* (n. d.) [Online]. Available: http://en.wikipedia.org/wiki/Formic_acid_fuel_cell (Accessed: December 5, 2010).
- [11] B. Frano, PEM fuel cells: theory and practice. Elsevier Science & Technology Books; 2005.
- [12] J. Larminie, and A. Dicks, *Fuel cell systems explained*. Second ed. John Wiley & Sons Ltd; 2003.
- [13] L. Barelli, G. Bidini, F. Gallorini, and A. Ottaviano, "Analysis of the operating conditions influence on PEM fuel cell performances by means of a

novel semi-empirical model”, *International Journal of Hydrogen Energy*, pp. 1-9, 2010.

[14] M. Ni, M.K.H. Leung, D.Y.C. Leung, and K. Sumathy, “Potential of renewable hydrogen production for energy supply in Hong Kong”, *International Journal of Hydrogen Energy*, vol. 3, pp. 1401–1412, 2006.

[15] M. Ni, M.K.H. Leung, D.Y.C. Leung, and K. Sumathy, “An overview of hydrogen production from biomass”. *Fuel Process Technol*, vol. 87, pp. 461-72, 2006.

[16] M. Ni, M.K.H. Leung, and D.Y.C. Leung, “Parametric study of solid oxide fuel cell performance”, *Energy Conversation Management*, vol. 48, pp. 1525-1535, 2007.

[17] M. Ni, M.K.H. Leung, and D.Y.C. Leung, “A modeling study on concentration overpotentials of a reversible solid oxide fuel cell”, *Journal of Power Sources*, vol. 163, pp. 460-466, 2006.

[18] M. Ni, M.K.H. Leung, and D.Y.C. Leung, “A review and recent developments in photo catalytic water splitting using TiO₂ for hydrogen production”, *Renewable and Sustainable Energy Reviews*, vol. 11, pp. 401-425, 2007.

[19] M. Ni, M.K.H. Leung, and D.Y.C. Leung, “An electrochemical model of a solid oxide steam electrolyzer for hydrogen production”, *Chemical Energy Technol*, vol. 29, pp. 636-642, 2006.

[20] A. Saeed, M. Ali, and S. Mahrokh, “Study of PEM fuel cell performance by electrochemical impedance spectroscopy”, *International Journal of Hydrogen Energy*, vol. 35, pp. 9283-9290, 2010.

[21] D.S. Scott, “Hydrogen in the evolving energy system”, *International Journal of Hydrogen Energy*, vol. 18, pp. 197-204, 1993.

[22] A. Szyszka, “Ten years of solar hydrogen demonstration project at Neunburg Vorm Wald, Germany”, *International Journal of Hydrogen Energy*, vol. 23, pp.849–860, 1998.

[23] J.A. Turner, “Sustainable hydrogen production”, *Science*, vol. 4, pp. 305-972, 2004.

- [24] T. N. Veziroglu and F. Barbir, "Hydrogen: the wonder fuel", *International Journal of Hydrogen Energy*, vol. 17, pp. 391-404, 1992.
- [25] F. Sarhaddi, S. Farahat, H. Ajam, A. Behzadmehr, and M. M. Adeli. "[An improved thermal and electrical model for a solar photovoltaic thermal \(PV/T\) air collector](#)," *Applied Energy*, vol. 87, no. 7, pp. 2328-2339, 2010.
- [26] T.T. Chow, "[A review on photovoltaic/thermal hybrid solar technology](#)," *Applied Energy*, vol. 87, no. 2, pp. 365-379, 2010.
- [27] Research Institute for Sustainable Energy (RISE). Domestic Solar Hot Water Systems [Online]. <http://www.rise.org.au>. [Accessed: December 6, 2010].
- [28] J.S. Coventry, "Performance of a concentrated photovoltaic/thermal solar collector", *Solar Energy*, vol. 78, pp. 211-222, 2005.
- [29] I. Dincer, and S. Dost, "Energy Analysis of an Ammonia-Water Absorption Refrigeration System", *Energy Sources*, vol. 18, 727-733, 1996.
- [30] O.E. Ataer, and Y. Gögüs, "Comparative study of irreversibilities in an aqua-ammonia absorption refrigeration system", *International Journal of Refrigeration*, vol. 14, pp.86-92, 1991.
- [31] F. Ziegler, R. Kahn, F. Summerer, and G. Alefeld, "Multi-effect absorption chillers", *International Journal of Refrigeration*, vol. 16, pp.301-311, 1993.
- [32] R. Tozer, A. Syed, and G. Maidment, "Extended temperature-entropy (T-s) diagrams for aqueous lithium bromide absorption refrigeration cycles", *International Journal of Refrigeration*, vol. 28, pp. 689-697, 2005.
- [33] J.S. Kim, F. Ziegler, and H. Lee, "Simulation of compressor-assisted triple-effect H₂O/LiBr absorption cooling cycles." *Applied Thermal Engineering*, vol. 22, pp. 295-308, Aug. 2001.
- [34] K. Mori, M. Oka, and T. Ohhashi, "Development of triple effect absorption chiller-heater," Japan Gas Association, Japan, Tech. Rep.
- [35] R. Gomri. Thermodynamic evaluation of triple effect absorption chiller. Theta Conf Proc 2008; 245-50.
- [36] K. Kimura and A. Lipeles, "Triple-effect absorption refrigeration system with double condenser coupling," World Intellectual Property Organization 850,364, September 16, 1993.

- [37] M. M. Hussain, J. J. Baschuk, X. Li, and I. Dincer, "Thermodynamic analysis of a PEM fuel cell power system," *International Journal of Thermal Sciences*, vol. 44, pp.903-911, Apr. 2005.
- [38] M. Ay, A. Midilli, and I. Dincer, "Exergetic performance analysis of a PEM fuel cell," *International Journal of Energy*, vol. 30, pp.307-321, Aug. 2005.
- [39] M. Ay, A. Midilli, and I. Dincer, "Thermodynamic modeling of a proton exchange membrane fuel cell". *International Journal of Exergy*, vol. 3 (1), pp. 16-44, 2006.
- [40] G. Karimi, J. J. Baschuk, and X. Li, " Performance analysis and optimization of PEM fuel cell stacks using flow network approach," *Journal of Power Sources*, vol. 147, pp. 162-177, March 2005.
- [41] S.A. Adewusi, and M. Zubair, "Second law based thermodynamic analysis of ammonia-water absorption system." *Energy Conservation and Management*, vol. 45, pp. 2355-2369, Jan. 2004.
- [42] A. Bejan. *Advanced engineering thermodynamics*. New York: John Wiley & Sons, 1988.
- [43] R.A. Gaggioli. "Available energy and exergy." *International Journal of Applied Thermodynamics*, vol. 1, no. 14, pp. 1-8, 1998.
- [44] S.O. Mert, I. Dincer, and Z. Ozcelik, "Exergoeconomic analysis of a vehicular PEM fuel cell system". *Journal of Power Sources*, vol. 165, pp. 244-252, January 2007.
- [45] T. H. Kuehn et al. *Thermal Environmental Engineering*, 3rd ed., Upper Saddle River, NJ: Prentice Hall, 2001, pp. 114-147.
- [46] V. Dorer, R. Weber, and A. Weber, "Performance assessment of fuel cell micro-cogeneration systems for residential buildings", *Energy and Buildings*, vol. 37, pp. 1132-1146, 2005.
- [47] U. Eicker, and D. Pietruschka, "Design and performance of solar powered absorption cooling systems in office buildings", *Energy and Buildings*, vol. 41, pp. 81-91, 2009.

- [48] H. Ren, and W. Gao, "Economic and environmental evaluation of micro CHP systems with different operating modes for residential buildings in Japan", *Energy and Buildings*, 2010.
- [49] E. Cetin, A. Yilanci, Y. Oner, M. Colak, I. Kasikci, and H. K. Ozturk, "Electrical analysis of a hybrid photovoltaic-hydrogen/fuel cell energy system in Denizli, Turkey", *Energy and Buildings*, vol. 41, pp. 975-981, 2009.
- [50] I. Pilatowskya, R.J. Romero, C.A. Isaza, S.A. Gamboa, W. Rivera, P.J. Sebastian, and J. Moreira, "Simulation of an air conditioning absorption refrigeration system in a co-generation process combining a proton exchange membrane fuel cell", *International Journal of Hydrogen Energy*, vo. 32, pp. 3174-3182, 2007.
- [51] A. Ferguson, and V. I. Ugursal, "Fuel cell modelling for building cogeneration applications", *Journal of Power Sources*, vol. 137, pp. 30-42, 2004.
- [52] J.I. San Martín, I. Zamora, J.J. San Martín, V. Aperribay, and P. Eguía, "Trigeneration Systems with Fuel Cells," Dept. Elec. Eng., Univ. of the Basque Country, Spain, Sci. Rep.
- [53] M. A. Darwish, "Building air conditioning system using fuel cell: Case study for Kuwait," *Applied Thermal Engineering*, vol. 27, pp.2869-2876, May 2007.
- [54] J.M. O. Ramí'ez, R.H. Castellanos, A'. M. Jesús, E. B. Arco, and R.C. Pless, "Design and development of a refrigeration system energized with hydrogen produced from scrap aluminum," *International Journal of Hydrogen Energy*, vol. 33, pp.2620-2626, Aug. 2004.
- [55] G. Gigliucci, L. Petruzzi, E. Cerelli, A. Garzisi, and A. L. Mendola, "Demonstration of a residential CHP system based on PEM fuel cells," *Journal of Power Sources*, vol. 131, pp.62-68, 2004.
- [56] R.E. Clarke, S. Giddey, F.T. Ciacchi, S.P.S. Badwal, B. Paul, and J. Andrew, "Direct coupling of an electrolyser to a solar PV system for generating hydrogen", *International Journal of Hydrogen Energy*, vol. 34, pp.2531-2542, 2009.
- [57] M.Y. El-Sharkh, M. Tanrioven, A. Rahman, and M.S. Alam, "Economics of hydrogen production and utilization strategies for the optimal operation of a grid-

parallel PEM fuel cell power plant”, *International Journal of Hydrogen Energy*, vol. 35, pp. 8804 – 8814, 2010.

[58] R.E. Clarke, S. Gidde, and S.P.S. Badwal, “Stand-alone PEM water electrolysis system for fail safe operation with a renewable energy source”, *International Journal of Hydrogen Energy*, vol. 35, pp. 928-935, 2010.

[59] N.S. Isabel, V.A. Lilia, and A.G. Alberto, “H₂ production by PEM electrolysis, assisted by textile effluent treatment and a solar photovoltaic cell”, *International Journal of Hydrogen Energy*, vol. 35, pp. 10833-10844, 2010.

[60] K. McHugh, “Hydrogen production methods”, MPR-WP-0001. Alexandria, Virginia, USA: MPR Associates, Inc.; 2005.

[61] P. Millet, F. Andolfatto, and R. Durand, “Design and performance of a solid polymer electrolyte water electrolyser”, *International Journal of Hydrogen Energy*, vol. 21, pp. 87-93, 1996.

[62] M. Newborough, “A report on electrolysers, future markets and the prospects for ITM Power Ltd’s electrolyser technology”, <http://www.h2fc.com/Newsletter/PDF/ElectrolyserTechnologyReportFINAL.doc>; 2010.

[63] A.S. Joshi, A. Tiwar, G.N. Tiwari, I. Dincer, and B.Y. Reddy, “Performance evaluation of a hybrid photovoltaic thermal (PV/T) (glass-to-glass) system”, *International Journal of Thermal Sciences*, vol. 48, pp.154-164, 2009.

[64] A.S. Joshi, I. Dince, and B.V. Reddy, “Performance analysis of photovoltaic systems: A review”, *Renewable and Sustainable Energy Reviews*, vol. 13, pp.1884-1897, 2009.

[65] C. Koroneos, A. Dompros, G. Roumbas, and N. Moussiopoulos. “Life cycle assessment of hydrogen fuel production processes.” *International Journal of Hydrogen Energy*, vol. 29, no. 14, pp. 1443–50, 2004.

[66] P.A. Lehman, C.E. Chamberlin, and P. Rocheleau, “Operating experience with a photovoltaic-hydrogen energy system”, *International Journal of Hydrogen Energy*, vol. 25, pp. 465-470, 1997.

- [67] A. Yilanci, I. Dincer, and H.K. Ozturk, "A review on solar-hydrogen/fuel cell hybrid energy systems for stationary applications", *Progress in Energy and Combustion Science*, vol. 35, pp.231-244, 2009.
- [68] A. Yilanci, I. Dincer, and H.K. Ozturk, "Performance analysis of a PEM fuel cell unit in a solar-hydrogen system", *International Journal of Hydrogen Energy*, vol. 33, pp.7538-7552, 2008.
- [69] P.C. Ghosh, B. Emont, H. Janben, J. Mergel, and D. Stolten, "Ten years of operational experience with a hydrogen-based renewable energy supply system", *Solar Energy*, vol. 75, pp. 469-78, 2003.
- [70] P. Hollmuller, J.M. Joubert, B. Lachal, and K. Yvon, "Evaluation of a 5 kW photovoltaic hydrogen production and storage installation for a residential home in Switzerland", *International Journal of Hydrogen Energy*, vol. 25, pp. 97-109, 2000.
- [71] N.Z. Muradov, and T.N. Veziroglu. "'Green' path from fossil-based to hydrogen economy: An overview of carbon-neutral technologies". *International Journal of Hydrogen Energy*, vol. 33, pp. 6804-6839, 2008.
- [72] A. Midilli, and I. Dincer. "Development of some exergetic parameters for PEM fuel cells for measuring environmental impact and sustainability". *International Journal of Hydrogen Energy*, vol. 34, pp. 3858-3872, 2009.
- [73] A. Midilli, and I. Dincer. "Hydrogen as a renewable and sustainable solution in reducing global fossil fuel consumption". *International Journal of Hydrogen Energy*, vol. 33, pp. 4209-4222, 2008.
- [74] P. Moriarty, and D. Honnery. "Hydrogen's role in an uncertain energy future". *International Journal of Hydrogen Energy*, vol. 34, pp. 31-39, 2009.
- [75] M.A. Gadalla, "Simulation of Intermittent Thermal Compression Processes Using Adsorption Technology." *Journal of the Franklin Institute*, vol. 344, pp.725-740, 2007.
- [76] A. Zohar, M. Jelinek, A. Levy and I. Borde, "Performance of diffusion absorption refrigeration cycle with organic working fluids", *International Journal of Refrigeration*, vol. 32, pp.1241-1246, 2009.

- [77] S.C. Kaushik and A. Arora, "Energy and exergy analysis of single effect and series flow doubleeffect water–lithium bromide absorption refrigeration systems", *International Journal of Refrigeration*, vol. 32, pp.1247-1258, 2009.
- [78] M. Granovskiyy, I. Dincer, and M.A. Rosen, "Life cycle assessment of hydrogen fuel cell and gasoline vehicles", *International Journal of Hydrogen Energy* 31(3), 337-352, 2006.
- [79] M.A. Gadalla, T.A.H. Ratlamwala, and I. Dincer, "Energy and exergy analysis of an integrated fuel cell and absorption cooling system." *International Journal of Exergy*, vol. 7, pp. 731-754, 2010.
- [80] M.A. Gadalla, T.A.H. Ratlamwala, and I. Dincer, "Evaluation of a triple effect absorption air-conditioning system integrated with PEM fuel cell." *Proceedings of the ASME 2010 Eighth International Fuel Cell Science, Engineering and Technology Conference*, 2010.
- [81] T.A.H. Ratlamwala, M.A. Gadalla, and I. Dincer, "Performance assessment of an Integrated PV/T and triple effect cooling system for hydrogen and cooling production." *International Conference on Hydrogen Production*, 2010.
- [82] T.A.H. Ratlamwala, M.A. Gadalla, and I. Dincer, "Performance assessment of a combined PEM fuel cell and triple effect absorption cooling system for cogeneration applications." *Fuel Cells*, pp. 1-11, accepted for publication, 2011.

VITA

Tahir Abdul Hussain Ratlamwala was born on July 18, 1987, in Karachi, Sindh. He studied in local school and graduated from Commecs Institute of Business and Emerging Sciences in 2005. He then joined The American University of Sharjah to carry out his higher studies in the field of Mechanical Engineering. He was granted financial aid in 2007 and. He was awarded scholarship from 2008-2009 for making in to the Dean's List and Chancellor's List. He graduated from A.U.S in 2009 with Bachelor of Science in Mechanical Engineering.

Mr. Tahir then joined A.U.S for Master of Science in Mechanical Engineering and was awarded full scholarship. He worked in Mechanical Engineering Department as Graduated Teaching Assistant. He was assigned with job of teaching recitations and conducting labs. During his MSc. Mr. Tahir published four papers in reputed journals and 3 other papers are under review. Mr. Tahir also presented four papers in different international conferences and has three more papers accepted for upcoming conferences. Mr. Tahir is being awarded Master of Science in Mechanical Engineering in 2011.